Comparative Trend Analysis of Minimum Temperature using Daily Gridded Data of 72 Years at 1° and 0.5° Resolutions over West Bengal

A thesis submitted towards partial fulfilment of the requirements for the degree of

Master of Engineering
in
Water Resources and Hydraulic Engineering

Submitted by

TIYASA ROY

Examination Roll No - M4WRE24019
Registration No -163872 of 2022-23

Under the guidance of

Dr. SUBHASISH DAS
Associate Professor and Joint Director
School of Water Resources Engineering, Jadavpur University

School of Water Resources Engineering
M.E. (Water Resources & Hydraulic Engineering)
Course affiliated to Faculty Council of Engineering & Technology

Jadavpur University
Kolkata-700032, West Bengal, India
2024

Declaration of Originality and Compliance of Academic Ethics

I hereby declare that this thesis contains literature survey and original research work by the undersigned candidate, as part of my **Master of Engineering** in **Water Resources and Hydraulic Engineering** in the Faculty Council of Interdisciplinary Studies, Law & Management, Jadavpur University during academic session 2023-24.

All information in this document have been obtained and presented in accordance with academic rules and ethical conduct.

I also declare that, as required by these rules and conduct, I have fully cited and referenced all material and results that are not original to this work.

Name	:	**TIYASA ROY**
Exam Roll Number	:	**M4WRE24019**
Thesis Title	:	**Comparative Trend Analysis of Minimum Temperature using Daily Gridded Data of 72 Years at 1° and 0.5° Resolutions over West Bengal**
Signature with Date	:	

M.E. (Water Resources & Hydraulic Engineering) course affiliated to

Faculty of Interdisciplinary Studies, Law & Management

Jadavpur University

Kolkata, India

Certificate of Recommendation

This is to certify that the thesis entitled "**Comparative Trend Analysis of Minimum Temperature using Daily Gridded Data of 72 Years at 1° and 0.5° Resolutions over West Bengal**" is a bonafide work carried out by **Ms. TIYASA ROY** under my supervision and guidance for partial fulfilment of the requirement for the Post Graduate Degree of **Master of Engineering** in **Water Resources and Hydraulic Engineering** during the academic session 2023-24.

THESIS ADVISOR
Dr. Subhasish Das
Associate Professor & Joint Director
School of Water Resources Engineering
Jadavpur University

DIRECTOR
Prof. (Dr.) Asis Mazumdar
School of Water Resources Engineering
Jadavpur University

DEAN
Prof. (Dr.) Joydeep Mukherjee
Faculty Council of Interdisciplinary Studies, Law & Management
Jadavpur University

M.E. (Water Resources & Hydraulic Engg.) course affiliated to
Faculty Council of Engineering & Technology
Jadavpur University
Kolkata, India

CERTIFICATE OF APPROVAL **

This foregoing thesis is hereby approved as a credible study of an engineering subject carried out and presented in a manner satisfactorily to warranty its acceptance as a prerequisite to the degree for which it has been submitted. It is understood that by this approval the undersigned do not endorse or approve any statement made or opinion expressed or conclusion drawn therein but approve the thesis only for purpose for which it has been submitted.

Committee of

Final Examination

for the evaluation

of the thesis

** Only in case the thesis is approved.

ACKNOWLEDGEMENTS

*First and foremost, I express my sincere gratitude to my supervisor, **Dr. Subhasish Das**, Associate Professor and Joint Director of the School of Water Resources Engineering, Jadavpur University, under whose supervision and guidance this work has been carried out. It would have been impossible to carry out this thesis work with confidence without his wholehearted involvement, advice, support and constant encouragement throughout. He has not only helped me in carrying out my thesis but also has given me valuable advice to proceed further in my life.*

*I would also express my sincere gratitude to, **Prof. (Dr.) Asis Mazumdar**, Director, **Prof. (Dr.) Arunabha Majumder**, Emeritus Professor; **Prof. (Dr.) Pankaj Kumar Roy**, **Dr. Rajib Das** and **Dr. Gourab Banerjee**, Faculty members of the School of Water Resources Engineering, Jadavpur University for their continuous encouragement and valuable suggestions, whenever we have met.*

*I also express my sincere thanks to **Mr. Gaurav Patel**, Research Scholar of the School of Water Resources Engineering, Jadavpur University for his constant support and affection throughout my thesis work. Also, thanks to my seniors **Mr. Buddhadev Nandi**, **Mr. Tanmoy Das**, **Mr. Saikat Mondal** and **other** Research Scholars, who have helped me selflessly, during this work. I wish to deliver my gratefulness to all of my friends (classmates), especially my companions cum constant guardians **Mr. Binoy Banik** and **Ms. Shubhashree Laha**, for their persistent mental support and meticulous encouragement throughout my M.E course. Thank you for being my rock and my inspiration.*

*Last, but not least, I would like to extend my special thanks to all the staff of the **School of Water Resources Engineering** for the peaceful atmosphere of the **Application Software Laboratory**, the very pleasant atmosphere of the **Fluvial Hydraulics Laboratory** and the **Regional-cum-Facilitation Centre (RCFC), NMPB, Jadavpur University** for their countless help and support.*

Date : 30 August, 2024

Place : Jadavpur University

Ms. Tiyasa Roy

(Exam Roll No: M4WRE24019)

ABSTRACT

Climate change is expected to significantly increase the frequency of extreme events, with storm events increasing by 21% for every -16.78 °C increase in ocean temperature, leading to severe consequences such as floods, structural damage, and crop loss. Detecting and understanding climate change through trend analysis is an emerging field, though many uncertainties remain. While many studies have focused on warming trends, studies on the coldest years or decades, particularly regarding minimum temperature (T_{min}), are rare. T_{min} is an important variable in climate models, influencing human health, agriculture, and biodiversity. This study aims to analyze and compare the trends of gridded T_{min} data at two resolutions (1° × 1° observed and 0.5° × 0.5° interpolated) over the Indian state of West Bengal (WB) from 1951 to 2022. Using Innovative Polygon Trend Analysis (IPTA), the study examines seasonal, monthly, and decadal trends to understand past and predict future climatic conditions. The findings reveal that the finer 0.5° resolution data gives more detailed results compared to that of 1° resolution, particularly in the central to southern regions of WB. Although the decadal comparison shows minimal differences. Division-wise statistical analysis indicates that trend length (TL) is more consistent than trend slope (TS), with mean TL yielding more stable outputs. IPTA patterns for monthly and seasonal mean T_{min} are identified as nearly identical across divisions, while significant differences are observed in the IPTA of monthly and seasonal standard deviations. This study highlights the persistent T_{min} discrepancies between north and south Bengal, with finer resolutions suggesting more advanced fluctuations. Recent trends show a higher magnitude of slope than historical decades, emphasizing the increasing sensitivity to climate change. This research contributes to understanding the spatiotemporal variations of hydroclimatic variables, offering insights for mitigating the impacts of climate change on natural and human resources. Future studies should focus on the broader implications of these changes on water resources, human health, and overall climate resilience.

CONTENTS

Chapter No.		Content details	Page No.
		Declaration of Originality and Compliance of Academic Ethics	III
		Certificate of Recommendation	V
		CERTIFICATE OF APPROVAL	VII
		ACKNOWLEDGEMENTS	IX
		ABSTRACT	XI
		CONTENTS	XIII-XIV
		LIST OF FIGURES	XV-XVI
		LIST OF TABLES	XVII-XVIII
		LIST OF ABBREVIATIONS	XIX
Chapter-1		**INTRODUCTION**	1-6
	1.1	What is trend analysis?	1-2
	1.2	Classifications of meteorological substances	2-4
		1.2.1 Extreme Weather Events	2
		1.2.2 Hydro-meteorological Events	2
		1.2.3 Seasonal Variability	3
		1.2.4 Morphological Weather Classifications	3
		1.2.5 Temperature and Precipitation Trends	3-4
	1.3	Classification of climatological factors	4-6
		1.3.1 Latitude	5
		1.3.2 Altitude	5
		1.3.3 Distance from the Sea	5
		1.3.4 Nature of the Prevailing Winds	5
		1.3.5 Cloud Cover	5
		1.3.6 Ocean Currents	5
		1.3.7 Mountain Ranges	6
		1.3.8 Nature of Soil and Vegetation Cover	6
		1.3.9 Slope	6
Chapter-2		**OBJECTIVES**	7
Chapter-3		**LITERATURE SURVEY**	8-21
	3.1	Literature Review	8-21
	3.2	Research Gaps	21
Chapter-4		**STUDY AREA AND DATA COLLECTIONS**	22-26
	4.1	Study Area	22
	4.2	Data Collected	23
	4.3	Representation of known and unknown grids	24-26
Chapter-5		**METHODOLOGY**	27-33
	5.1	Development of the new gridded daily minimum temperature (T_{min}) data over West Bengal (WB)	28
	5.2	Inverse Distance Weighted (IDW) method	28-29

	5.3	Trend Methodology	29-30
	5.4	Innovative Polygon Trend Analysis (IPTA)	30-33
		5.4.1 Trend Length (TL)	31
		5.4.2 Trend Slope (TS)	32
Chapter-6		**RESULTS AND DISCUSSION**	34-80
	6.1	Performance of Inverse Distance Weighted (IDW)	34-35
	6.2	Special observation in historical data	35
	6.3	Decade wise spatial analysis	35-40
	6.4	Division wise location details of all (56) grids of WB	40-42
	6.5	Monthly trend analysis	43-55
	6.6	Monthly IPTA for representative boundary grids	55-64
		6.6.1 Monthly Mean	56-58
		6.6.2 Monthly Standard deviation	58-60
	6.7	Monthly spatiotemporal analysis	65-66
	6.8	Seasonal trend analysis	67-72
	6.9	Seasonal IPTA for representative boundary grids	73-79
		6.9.1 Seasonal Mean	73-75
		6.9.2 Seasonal Standard deviation	75-76
	6.10	Seasonal spatiotemporal analysis	79-80
Chapter-7		**CONCLUSIONS AND FUTURE RECOMMENDATIONS**	81-82
	7.1	Conclusions	81-82
	7.2	Future Scopes	82
		REFERENCES	83-87

LIST OF FIGURES

Figure No.	Figure Caption	Page No.
Fig. 4.1	Location of the study area	22
Fig. 4.2	Study area with the gridded position of 21 known (1°×1° from IMD-Pune collected) and 35 unknown (0.5°×0.5° IDW interpolated) grids of West Bengal	23
Fig. 4.3	Divisional representation of West Bengal	26
Fig. 5.1	Flow chart of the methodology	27
Fig. 5.2	Representation of UG30 for IDW determination where D_1, D_2 and D_3 are the radial distances of 0.5,0.707 and 1.118 degrees, respectively	29
Fig. 5.3	IPTA template for monthly T_{min} trends	31
Fig. 5.4	Flowchart illustrating the IPTA applied for the present study	33
Fig. 6.1	T_{min} calculation format of UG30	34
Fig. 6.2	Spatial representation of minimum temperature over West Bengal for Decadal mean of 1951-1960 (a) 0.5° resolution and (b) 1° resolution	36
Fig. 6.3	Spatial representation of minimum temperature over West Bengal for Decadal mean of 1961-1970 (a) 0.5° resolution and (b) 1° resolution	36
Fig. 6.4	Spatial representation of minimum temperature over West Bengal for Decadal mean of 1971-1980 (a) 0.5° resolution and (b) 1° resolution	37
Fig. 6.5	Spatial representation of minimum temperature over West Bengal for Decadal mean of 1981-1990 (a) 0.5° resolution and (b) 1° resolution	37
Fig. 6.6	Spatial representation of minimum temperature over West Bengal for Decadal mean of 1991-2000 (a) 0.5° resolution and (b) 1° resolution	38
Fig. 6.7	Spatial representation of minimum temperature over West Bengal for Decadal mean of 2001-2010 (a) 0.5° resolution and (b) 1° resolution	38
Fig. 6.8	Spatial representation of minimum temperature over West Bengal for Decadal mean of 2011-2022 (a) 0.5° resolution and (b) 1° resolution	39
Fig. 6.9	Division wise all grids and highlighted representative 8 boundary grids of WB	43
Fig. 6.10	Representative eight boundary grids of West Bengal	56
Fig. 6.11	IPTA graphs for the south zone of West Bengal, monthly mean of minimum temperature records from some representative boundary grids (i) UG2, (ii) UG4, (iii) UG15, and (iv) UG30.	57

Fig. 6.12	IPTA graphs for the mid and north zone of West Bengal, monthly mean of minimum temperature records from some representative boundary grids (v) UG17, (vi) UG20, (vii) UG28, and (viii) UG34.	58
Fig. 6.13	IPTA graphs for the south zone of West Bengal, the monthly standard deviation of minimum temperature records from some representative boundary grids (i) UG2, (ii) UG4, (iii) UG15, and (iv) UG30.	59
Fig. 6.14	IPTA graphs for the mid and north zone of West Bengal, the monthly standard deviation of minimum temperature records from some representative boundary grids (v) UG17, (vi) UG20, (vii) UG28, and (viii) UG34.	60
Fig. 6.15	Monthly spatiotemporal variation of average minimum temperature in West Bengal using gridded data at (a) 0.5° and (b) 1° resolutions, based on the 72-year mean (1951-2022)	66
Fig. 6.16	IPTA graphs for the south zone of West Bengal, seasonal mean of minimum temperature records from some representative boundary grids ((i) UG2, (ii) UG4, (iii) UG15, and (iv) UG30.	73
Fig. 6.17	IPTA graphs for the mid and north zone of West Bengal, seasonal mean of minimum temperature records from some representative boundary grids (v) UG17, (vi) UG20, (vii) UG28, and (viii) UG34.	74
Fig. 6.18	IPTA graphs for the south zone of West Bengal, the seasonal standard deviation of minimum temperature records from some representative boundary grids (i) UG2, (ii) UG4, (iii) UG15, and (iv) UG30.	75
Fig. 6.19	IPTA graphs for the mid and north zone of West Bengal, the seasonal standard deviation of minimum temperature records from some representative boundary grids (v) UG17, (vi) UG20, (vii) UG28, and (viii) UG34.	76
Fig. 6.20	Seasonal spatiotemporal variation of average minimum temperature in West Bengal (a) 0.5° and (b) 1° resolutions, based on the 72-year mean (1951-2022)	80

LIST OF TABLES

Table No.	Table Caption	Page No.
Table 4.1	Representation of grids throughout the study area	24
Table 4.2	Grouping of the 23 districts under five divisions	25
Table 6.1	Interpolated data of selective 8 representative boundary grids for 5th January 1955	35
Table 6.2	Division wise location details of 56 grids	40-42
Table 6.3	Representation of trend length (in °C) and trend slope (unitless)for monthly mean across the Medinipur Division	44-45
Table 6.4	Representation of trend length (in °C) and trend slope (unitless)for monthly standard deviation across the Medinipur Division	45-46
Table 6.5	Representation of trend length (in °C) and trend slope (unitless)for monthly mean across the Presidency Division	46-47
Table 6.6	Representation of trend length (in °C) and trend slope (unitless) for monthly standard deviation across the Presidency Division	47-48
Table 6.7	Representation of trend length (in °C) and trend slope (unitless) for monthly mean across the Burdwan Division	48-49
Table 6.8	Representation of trend length (in °C) and trend slope (unitless) for monthly standard deviation across the Burdwan Division	49
Table 6.9	Representation of trend length (in °C) and trend slope (unitless) for monthly mean across the Malda Division	49-50
Table 6.10	Representation of trend length (in °C) and trend slope (unitless) for monthly standard deviation across the Malda Division	50-51
Table 6.11	Representation of trend length (in °C) and trend slope (unitless) for monthly mean across the Jalpaiguri Division	51-52
Table 6.12	Representation of trend length (in °C) and trend slope (unitless) for monthly standard deviation across the Jalpaiguri Division	52-53
Table 6.13	Representation of monthly mean IPTA trend of representative grids	61
Table 6.14	Representation of monthly standard deviation IPTA trend of representative grids	61
Table 6.15	Trend length (in °C) and trend slope (unitless) of eight representative boundary grids for monthly mean data	63
Table 6.16	Trend length (in °C) and trend slope (unitless) of eight representative boundary grids for monthly standard deviation data	63-64

Table 6.17	Representation of trend length (in °C) and trend slope (unitless) for seasonal mean and standard deviation across the Medinipur Division	67-68
Table 6.18	Representation of trend length (in °C) and trend slope (unitless)for seasonal mean and standard deviation across the Presidency Division	68-69
Table 6.19	Representation of trend length (in °C) and trend slope (unitless)for seasonal mean and standard deviation across the Burdwan Division	69-70
Table 6.20	Representation of trend length (in °C) and trend slope (unitless)for seasonal mean and standard deviation across the Malda Division	70
Table 6.21	Representation of trend length (in °C) and trend slope (unitless) for seasonal mean and standard deviation across the Jalpaiguri Division	71
Table 6.22	Representation of seasonal mean and seasonal standard deviation IPTA trend	77
Table 6.23	Trend length (in °C) and trend slope (unitless) of eight representative boundary grids for seasonal mean data	78
Table 6.24	Trend length (in °C) and trend slope (unitless) of eight representative boundary grids for seasonal standard deviation data	78

LIST OF ABBREVIATIONS

The following abbreviations are used in the present study:

Abbreviation		Description
°F	–	Degree Fahrenheit;
°C	–	Degree Celsius;
GIS	–	Geographic Information Systems;
IDE	–	Integrated Development Environment;
IDW	–	Inverse Distance Weighted;
IMD	–	India Meteorological Department;
IPTA	–	Innovative Polygon Trend Analysis;
ITA	–	Innovative Trend Analysis;
KG	–	Known Grid;
MK	–	Mann–Kendall;
NE	–	North-East;
NW	–	North-West;
SE	–	South-East;
std	–	Standard deviation;
SW	–	South-West;
TL	–	Trend Length;
T_{max}	–	Maximum Temperature;
T_{min}	–	Minimum Temperature;
TS	–	Trend Slope;
UG	–	Unknown Grid;
WB	–	West Bengal;

Chapter 1

INTRODUCTION

In sustainable development, changes in weather are considered critical factors, with their impacts visible across various regions around the globe (Dioha and Kumar, 2020). Climate change refers to long-term alterations in temperatures and weather patterns, largely driven by human activities since the 1800s. The burning of fossil fuels such as coal, oil, and gas has been a major contributor, releasing heat-trapping gases into the atmosphere. This has led to more frequent and severe droughts, storms, heat waves, rising sea levels, melting glaciers, and warming oceans. These changes pose significant risks to ecosystems, human livelihoods, and the overall health of the planet. People must come together to find solutions to mitigate climate change for a better future. Researchers worldwide have observed changes in precipitation and air temperature patterns (Sharma and Ghosh, 2022). Recent global warming and its associated climate change impacts are expected to accelerate shifts in the averages of hydro-meteorological variables and increase their variability. To address these challenges effectively, objective methodologies should be employed to manage and control these changes (Sen et al., 2019).

The impact of global warming on climate change has been evident in every region of the world. Some areas are experiencing water scarcity, while others are facing floods, both of which pose significant challenges to society. Consequently, it is crucial to implement measures based on predictive models to address these changes on a regional scale (National Geographic Society, 2023). Numerous researchers have conducted extensive studies worldwide to examine climate change and its effects on key parameters such as temperature, precipitation, water resources, and agriculture (Aktas, 2020). Global warming is a critical issue that the world is currently struggling with, and its effects are particularly severe in India, where it poses significant challenges to the nation's economy. The crucial concern arises from the fact that a large portion of India's economy relies heavily on agriculture, making the country vulnerable to the unpredictable situations created by rising temperatures (Mondal et al., 2012). As global warming intensifies, the type, frequency, and severity of extreme events, such as tropical droughts and heavy rainfall, are expected to increase, even with relatively small rises in average temperature. Given these developments, trend analysis in climatology has become essential.

1.1 What is trend analysis?

A trend is defined as a "long-term change in the mean level," which can occur gradually as a trend or abruptly as a step change (Choudhari, 2016). Trend analysis is a highly effective method for assessing the impacts of climate change on hydro-meteorological variables. Many hydro-climatic variables, including precipitation, temperature, streamflow discharge, wind

speed, relative humidity, evaporation, and evapotranspiration, are inherently complex and stochastic. While analyzing their trends can offer valuable insights into water resources and meteorological sciences, the inherent characteristics of these variables necessitate specialized approaches for trend analysis. These methods must avoid restrictive assumptions, such as normality, independence, and record length. As a result, the use of trend analysis with non-parametric tests has become increasingly common.

Trend detection analysis holds a crucial role in the statistical examination of time series data across various fields, including hydro-meteorology, economics, geophysics, quality control, and similar studies. While temporal trends are often the primary focus, spatial trend analysis is also significant, particularly in regional assessments within geology and engineering. The rise of climate change and global warming has significantly increased the application of trend analysis in hydro-meteorological time series, including variables such as temperature, humidity, precipitation, evaporation, and streamflow (Sen et al., 2019). Notably, trend analysis is particularly critical for temperature records compared to precipitation records when evaluating the impacts of climate change (Hirca et al., 2021).

Since the pioneering works of Mann (1945) and Kendall (1975), which collectively introduced the classical Mann-Kendall (MK) trend test, the number of studies focusing on trend analysis has significantly increased. This traditional method has been widely applied in various research efforts (Jain and Kumar, 2012; Saboohi et al., 2012; Wagholikar et al., 2014; Khan et al., 2015 and 2017; Radhakrishnan et al., 2017; Rangarajan et al., 2017; Datta and Das, 2019; Kundu and Mondal, 2019; Nengzouzam et al., 2019; Esit et al., 2022; Chowdari et al., 2023; Halder et al., 2023; Singh et al., 2023; Patel et al., 2024). Additionally, many studies have applied the MK test with other modified approaches, such as Innovative Trend Analysis (ITA), Inverse Polygon Trend Analysis, and Innovative Polygon Trend Analysis (IPTA). These advanced techniques have been utilized to analyze various meteorological variables across multiple weather events and locations worldwide.

1.2 Classifications of meteorological substances

When conducting trend analysis in meteorology, various classifications of meteorological events are commonly employed. These classifications are essential for identifying patterns, understanding trends, and predicting future events. Some of the key classifications include:

1.2.1 Extreme Weather Events

These include events such as hurricanes, tornadoes, heat waves, and heavy rainfall, which are frequently analyzed to assess their frequency, intensity, and impact over time (Radovic and Iglesias, 2019).

1.2.2 Hydro-meteorological Events

This category encompasses events related to water and weather, including floods, droughts, and storms. Trend analysis in this area is essential for effective water resource management and disaster preparedness (Almazroui and Sen, 2020).

1.2.3 Seasonal Variability

Analyzing seasonal patterns, such as monsoons and dry seasons, is crucial for agricultural planning and water resource management (Thakur et al., 2022).

1.2.4 Morphological Weather Classifications

These classifications are used for general climatic descriptions and have applications in bio-meteorological studies, including climate therapy for spa resorts and agricultural climatology (Piotrowicz and Ciaranak, 2020).

1.2.5 Temperature and Precipitation Trends

Temperature and precipitation are the most fundamental and widely analyzed meteorological variables. Understanding trends in these variables is crucial for climate change research (Shea, 2014). Among various meteorological events, researchers primarily focus on temperature and precipitation trends. In precipitation trend analysis, several types are typically considered, each with distinct characteristics and implications for climate studies. These types include:

- Rain
- Snow
- Hail
- Sleet
- Freezing rain

To analyze these types of precipitation, various statistical methods are employed, such as:

- Linear Regression
- Mann-Kendall (MK) Test
- Sen's Slope Estimator

These methods are essential for understanding how precipitation patterns are evolving over time, which is crucial for climate modeling and forecasting future climate scenarios. Research on precipitation trends is more extensive compared to temperature trends.

Temperature trend analysis generally focuses on two key types:

- **Maximum Temperature**: T_{max} represents the highest temperature recorded at a location during a specific period, typically measured during the day or early afternoon when the sun is at its peak. T_{max} is recorded in degrees Celsius (°C) or degrees Fahrenheit (°F). Factors influencing T_{max} include: Latitude, Altitude, Proximity to water bodies, and Cloud cover.
- **Minimum Temperature:** T_{min} is the lowest temperature recorded at a location during a specific period, typically measured in the early morning or late night when the sun is at its lowest. T_{min} is recorded in degrees Celsius (°C) or Fahrenheit (°F). The factors influencing T_{max} also affect T_{min}. However, T_{min} is particularly relevant to human health, agriculture, and biodiversity. It represents the temperature of the coldest day in a given period, such as a year, season, or month. As part of the Cold Spell and Frost Hazard

categories within the Heat and Cold classification, a lower T_{min} value indicates colder temperatures, which can increase cold stress on both people and the environment (Rao, 2024). Climate change could cause a substantial increase in extreme storms. For every - 16.78 °C (1.8 °F) rise in ocean temperatures, 21% more storms form, the researchers found. More storms mean more flooding, more structural damage, more crop damage and so on unless mitigating measures are implemented (NASA Science Editorial Team, 2024). That is why, T_{min} is a crucial parameter for trend analysis and future climate predictions.

Analyzing trends over large areas requires both collected (measured) and calculated (gridded) data. The difference between measured and gridded temperature data can be substantial, particularly in regions with complex terrain or varying elevations. Key points to consider include:

- **Measured Temperature Data:** This data is gathered directly from weather stations or sensors at specific locations, offering accurate temperature readings for those precise points.
- **Gridded Temperature Data:** This data is generated by averaging measurements over a larger spatial area, resulting in a grid of temperature values. While it is valuable for large-scale climate studies, it may not accurately capture local variations.
- **Differences and Challenges:**
  - **Elevation Effects:** Gridded datasets may not accurately reflect temperature changes with elevation (Tercek et al., 2021).
  - **Heatwave Definitions:** There can be discrepancies in how extreme heat events are represented in different gridded datasets, especially in tropical regions (Coughlan de Perez et al., 2023).
  - **Data Aggregation:** Gridded data aggregates point-level measurements, which can lead to differences in the distribution and behavior of temperature data (Director and Bornn, 2015).

Understanding these differences is crucial for accurate climate modeling and ecological studies.

1.3 Classification of climatological factors

Climatology is the study of climate and its variations, focusing on long-term weather patterns over time and space and the factors that create Earth's diverse climatic conditions. Observed climatic patterns are categorized into regions that form the basis of climate classification. Also known as climate science, climatology examines the Earth's climate, typically defined as weather conditions averaged over at least 30 years. It is a branch of atmospheric sciences and a subfield of physical geography, which falls under Earth sciences.

This field considers various elements such as atmospheric pressure, wind, and precipitation, which interact to shape the weather of a particular place. Consequently, a location's weather and climate influence daily aspects like clothing choices, food, and living conditions. To clarify commonly used terms: Weather refers to the temporary atmospheric conditions at a specific location, resulting from the interaction of factors like temperature,

pressure, and humidity. Climate represents the average weather conditions over a large area across several years. The factors (Manishsiq, 2023) influence by climate include:

1.3.1 Latitude

Places at lower latitudes are generally warmer than those at higher latitudes. This is because the sun's rays strike the equator more directly, while they hit the temperate and polar regions at a more oblique angle.

1.3.2 Altitude

The Earth's atmosphere primarily receives heat from terrestrial radiation. The air near the surface absorbs more heat than the upper layers of the atmosphere. On average, temperature decreases by about 1°C for every vertical rise of 165 meters. Therefore, as altitude increases, temperature generally decreases.

1.3.3 Distance from the Sea

Water has a high specific heat capacity, meaning it heats up and cools down more slowly than land. This results in a moderating effect in coastal areas due to the presence of the sea. As a result, coastal regions experience a reduced daily temperature range and increased humidity compared to inland areas.

1.3.4 Nature of the Prevailing Winds

On-shore winds, which blow from the sea toward the land, carry moisture and can lead to rainfall in the areas they pass over. In contrast, off-shore winds, which blow from the land toward the sea, are typically dry, facilitate evaporation, and do not generally cause precipitation.

1.3.5 Cloud Cover

Cloudless areas receive more direct insolation and experience faster escape of terrestrial heat. As a result, sunny regions often have a high diurnal temperature range, meaning there is a significant difference between daytime and nighttime temperatures. In contrast, cloudy areas tend to have a lower diurnal temperature range due to the cloud cover's insulating effect, which helps retain heat and reduces temperature fluctuations.

1.3.6 Ocean Currents

Warm ocean currents increase coastal temperatures and add moisture to the air, which can lead to precipitation. Conversely, cold ocean currents lower coastal temperatures and reduce the air's moisture-carrying capacity. Onshore winds that pass over the ocean can either raise or lower the temperature of the interior, depending on the temperature of the ocean current they originate from.

1.3.7 Mountain Ranges

Mountain ranges serve as natural windbreaks. Moisture-laden winds ascending along the mountains can lead to significant rainfall on the windward side. However, as the wind descends on the leeward side, it becomes drier and results in much less precipitation. Additionally, mountain ranges help moderate extreme temperatures by blocking very cold or hot winds. When a mountain range runs parallel to the prevailing wind direction, it typically results in minimal rainfall, as seen with the Aravalli Range.

1.3.8 Nature of Soil and Vegetation Cover

Rocky or sandy soils are effective conductors of heat, while black soil absorbs heat more quickly. Bare surfaces of the Earth radiate heat rapidly, resulting in a higher diurnal temperature range compared to areas with vegetative cover. Forests, through the process of transpiration, release moisture into the air, which can contribute to precipitation.

1.3.9 Slope

Heat concentration is higher on gentler slopes, such as in plains, which raises the air temperature in these areas. Conversely, steeper slopes have lower heat concentrations, leading to reduced temperatures.

Climate classifications provide a simplified way to understand the typical conditions a region experiences throughout the year. Instead of describing the full range of conditions observed each month or season, a classification scheme uses just two or three terms to convey the expected climate characteristics.

Climate change is an increasingly serious issue that requires effective understanding and the implementation of appropriate adaptation and mitigation strategies. Accurate assessment of climate change is crucial for selecting the best strategies. There are various trend analysis techniques available for this purpose, but the field is still evolving, and many uncertainties remain in climate change assessment and prediction. Therefore, continued research is essential to achieve more precise and reliable climate change assessments.

Chapter 2

OBJECTIVES

The main objective of this research is to compare and analyze the trend of minimum temperature (T_{min}) data of different resolutions over West Bengal (WB). The results will not only help to understand the past climatic conditions, timing and severity of extreme events, but also support to forecast the future climatic conditions, extreme events and their severity. Stepwise sub-objectives of this thesis are mentioned below:

- To utilize the higher resolution data for trend analysis.
- To compare the trends using different resolutions.
- To determine the patterns using a decade wise analysis.
- To conduct the monthly and seasonal analysis for T_{min}.
- To evaluate the trend statistics to understand the nature of the trend.
- To visualize the spatial variation for T_{min}.

Chapter 3

LITERATURE SURVEY

The primary goal of this chapter is to conduct a thorough literature review of previous climate change trend analysis studies. This review aims to identify the patterns of change in meteorological data, with a particular focus on minimum temperature (T_{min}) trends in West Bengal (WB), in relation to varying resolutions of gridded data. This chapter presents studies from the past 12 years that have focused on modified interpolation methods and updated trend analysis applied to temperature and rainfall data worldwide. Brief descriptions of these studies are given below:

3.1 Literature Review

Jain and Kumar (2012) analyzed trends in rainfall and temperature across India. Their research highlighted the importance of understanding the spatial and temporal distribution, as well as the changing trends in rainfall, across 22 river basins for effective water resource planning and management. Their study showed an increase in the annual rainfall trend in six river basins in India ranging from 0.27 to 10.16 mm, and a decrease in 15 river basins ranging from 0.45 to 4.93 mm.

Further investigations of rainy days revealed a rising trend in four river basins, while fifteen river basins showed a declining trend. Seasonal analysis indicated that rainfall increased in nine river basins during the pre-monsoon season (with four basins experiencing more rainy days), six basins during the monsoon season (with four basins also having more rainy days), 13 basins in the post-monsoon season (with four basins showing an increase in rainy days), and 18 basins during the winter season. According to the study, rainfall decreased in 13 river basins before the monsoon, 16 river basins during the monsoon, and eight river basins after the monsoon, some of which were major and water-deficient basins.

Furthermore, the majority of the basins did not show any significant increasing or decreasing trend in seasonal rainfall and rainy days. The lack of significant change in the number of rainy days indicated no clear evidence of major changes in rainfall intensities. However, the temperature data exhibited nearly consistent rising trends, although the behavior of T_{max} and T_{min} varied across different locations.

Another observation was that most of the data used for trend detection came from stations located in urban areas, which act as heat islands. Therefore, using this data might not accurately reflect reality. Consequently, the study concluded that there is a need for an integrated nationwide program for change detection, impact assessment, and adoption of mitigation strategies.

Saboohi et al. (2012) conducted a trend analysis of long-term annual and monthly trends in mean maximum, mean minimum, and mean temperature at 35 synoptic stations in Iran using the Mann- Kendall (MK) test.

The analysis revealed significant trends in the monthly mean maximum temperature (T_{max}) time series during spring, summer, and autumn at most of the stations in Iran. Additionally, it was found that the mean annual T_{max} exhibited significant positive trends at 34% of the stations. The results of the MK test for the annual and monthly mean T_{min} time series revealed that most of the stations in Iran exhibited an increasing trend. Although the strongest trends were observed in November and December, the most significant trends occurred in summer. Only two stations in the west and northwest regions of Iran exhibited significant negative trends in annual mean minimum temperature, while the 21 stations showed significant positive trends.

The MK test results for mean temperature showed no significant positive trends in March, but widespread significant positive trends in August. Significant positive trends were particularly evident during the summer and autumn months in the northwest and northeast, as well as in some regions in the center, southwest, and southeast. Approximately 46% of the stations in Iran exhibited a significant positive trend in the mean annual temperature time series.

Sen (2012) established the method of Innovative Trend Analysis (ITA). As the MK test, Spearman's Rho (SR) test and Regression methodology were the only methods available for calculating trend magnitude, and it requires assumptions for theoretical validation in real-world applications. This research has introduced a new methodology using subsection time series graphs on a Cartesian coordinate system. In this illustration, trend-free time series subsections appear along a 45° straight line.

The proposed methodology was applied to several yearly runoff and rainfall series from Turkey, as well as annual Danube River flows. The validity of the methodology was illustrated by means of Monte-Carlo simulations applied to the annual runoff, precipitation, and Danube River flows in Turkey. The first quadrant of the Cartesian coordinate system was where the increasing tendencies in the time series place them, according to the results.

Furthermore, the segmentation of the 1:1 line scatter method into three clusters (low, medium, and high) provided insight into the internal trend structure of the time series under consideration. The trend magnitude decreases as the cluster of points approaches the 1:1 line. If a straight line is parallel to the 1:1 line, the time series has a monotonic trend. Otherwise, there are many trends or trend-free parts.

This new approach avoids all of the aforementioned assumptions in the MK and SR tests, and it also allows for the calculation of trend magnitude using square area plots. This methodology was applied to a variety of precipitation and runoff time series from around the world.

Pai et al. (2014) developed a new high spatial resolution (0.25° × 0.25°) dataset of daily gridded rainfall covering a long period of 110 years (1901-2010) over India. This dataset was compared with existing datasets covering the Indian mainland. The study compared the newly developed IMD4 dataset with four other existing daily gridded rainfall datasets that varied in

spatial resolutions and time periods. To prepare the new gridded dataset, daily rainfall records from 6955 rain gauge stations across India were utilized.

The gridded dataset was created after performing quality control of the basic rain gauge stations. The comparison of IMD4 with other datasets indicated that the climatological and variability features of rainfall over India derived from IMD4 were similar to those of the existing gridded daily rainfall datasets. Additionally, the study observed that the spatial distribution of rainfall, such as heavy rainfall areas in the orographic regions of the west coast and over the northeast, as well as low rainfall in the leeward side of the Western Ghats, was more realistic and accurately represented in IMD4.

To prepare the gridded data for each day of the study period, an average of about 3500 stations, ranging from 1450 to 3900, were used. Before interpolating the T_{min} data onto fixed spatial grid points, various standard quality checking tests were applied to the data. For interpolation, the study employed the IDW interpolation method proposed by Shepard (1968), which was also used for the preparation of IMD1, IMD2, and IMD3. For the period 1901-2010, the all India annual and southwest monsoon season mean rainfalls were computed using IMD4 as 3.09 mm/day and 6.99 mm/day, respectively, with standard deviations of 0.27 mm/day and 0.66 mm/day, respectively.

The study compared the interannual variation of all India's southwest monsoon season rainfall derived from various gridded datasets. It was observed that the large-scale climatological features in the mean annual rainfall and the seasonal mean rainfall patterns during each of the four seasons were nearly similar in all the datasets. The zone of higher rainfall areas along the west coast was narrower in the higher resolution datasets compared to that in IMD1 and IMD2. The mean annual cycle of all India rainfall in all the datasets was also identical, with a peak during the middle of the monsoon season and a minimum during the winter season.

The all India mean annual rainfall was highest in IMD1 (3.21 mm/day) and lowest in APHRO (2.68 mm/day) for northern parts of Uttarakhand, northern parts of the east coast, Sikkim, and Arunachal Pradesh, with IMD4 being drier than the former value by about 4% and wetter than the latter value by about 13%. It was also observed that the highest 10 rainfall years and lowest 10 rainfall years in the time series of both IMD4 and IMD_OP (operational time series of all India) were nearly the same except for differences in rank.

The study concluded that updating this IMD dataset in real-time could be used for important operational services such as real-time drought monitoring at various spatial and temporal scales, flood forecasting, stream flow forecasting, etc.

Wagholikar et al. (2014) investigated trends in seasonal temperatures across India using a high-resolution daily gridded dataset prepared by the IMD for the period 1969–2005. The study utilized IMD's high-resolution (1° × 1°) daily gridded data to analyze trends in maximum, minimum, and mean temperatures over the Indian landmass during the winter (January and February), pre-monsoon (March-May), southwest monsoon (June-September), and post-monsoon (October-December) seasons.

The T_{max} over India's west coast has shown an upward trend during the winter, southwest monsoon, and post-monsoon seasons, while there has been no decreasing trend in maximum temperatures across the rest of the region. On the other hand, T_{min} has been rising

in North Indian states throughout the year, as well as on the west coast of India during the winter and southwest monsoon seasons.

It was observed that mean temperatures on India's west coast showed a rising trend during the winter and southwest monsoon seasons. Conversely, the temperature range in North India decreased across all seasons due to an increase in T_{min}. During the pre-monsoon, southwest monsoon, and post-monsoon seasons, certain areas of India's west coast and southern states experienced an increase in temperature range. North and northeast Indian states showed a declining trend in temperature range, with no significant increase in maximum temperature but a substantial increase in minimum temperature.

These observations indicated that rising T_{min} led to a decrease in temperature range. In summary, mean maximum and mean temperatures over the west coast of India and southern Indian states showed an increasing tendency during the winter, southwest monsoon, and post-monsoon seasons. Additionally, it was noted that the average T_{min} in north Indian states was higher than that in south Indian states.

Khan et al. (2015) examined the long-term (1941-2010) variability of temperature trends and changes in surface air temperature at the Kolkata weather observatory in WB, India. The impact of climate change on annual air temperature has been a crucial point for climate scientists globally. Air temperature is a key component of climate parameters and is commonly monitored as an initial step in comprehending climate variability and change.

The MK test is commonly paired with Theil-Sen's robust estimate of linear trends to analyze trends. This approach allows for the identification of general increasing and declining trends with varying degrees of significance. The analysis of monthly and seasonal temperatures indicated a warming tendency in both the annual and seasonal datasets.

The findings showed that the average temperature decreased for four months-January, February, March, and December while increasing for the other eight months. The warming trend for the summer and winter seasons was statistically significant, with rates of increase at 0.034°C and 0.032°C per year, respectively. Overall, both monthly and seasonally efficient time series displayed positive trends.

The study concluded that the Kolkata weather observatory is situated in a rapidly urbanizing area. Temperature trends could significantly impact human existence and urbanization in this region, with climate variability potentially contributing to long-term temperature increases.

Khan et al. (2017) conducted a study on air temperature variability and trend analysis using non-parametric tests at the Kolkata observatory in WB, India. Like their earlier research, this study found a decreasing trend in average temperature for January, February, March, and December, while the other eight months showed an increasing trend. Furthermore, the study highlighted that most trends, both seasonal and monthly, pointed towards rising temperatures during the monsoon and post-monsoon periods.

Over the past 70 years (1941–2010), it has been observed that winter temperatures have increased more than summer temperatures. The most significant temperature rise occurred in December and February, followed by November and October. In Kolkata, the highest increase

in mean temperature during this period was recorded in the post-monsoon or colder months of November and December, with a rise of 0.9°C.

The warming trend has been evident throughout the year but is more pronounced in the post-monsoon and winter months. This trend could lead to a reduction in the amount of solar radiation reaching the Earth's surface, resulting in less warmth during the pre-monsoon or summer months compared to the post-monsoon and winter months.

Radhakrishnan et al. (2017) analyzed the climate trends of annual and seasonal mean rainfall and temperature in India from 1901 to 2014. The study evaluated the long-term trends of rainfall and temperature using linear regression and the MK test, with the magnitude of the trend assessed by Sen's Slope.

Following the analysis, it is evident that 64.5% of the states in India exhibited an increasing trend in mean winter temperatures. Only one state out of 31 showed a statistically significant negative trend. For summer and monsoon seasons, 10 and 16 states, respectively, displayed an increasing trend in mean temperature. During the post-monsoon season, all states showed a rising trend in mean temperature, with 95% of states showing an increase, one state showing a decrease, and no trend observed for Punjab (2.5% state).

Over the last 30 years (1985-2014), both annual and summer rainfall significantly decreased, while seasonal temperature nearly doubled compared to the monsoon season. The annual mean temperature increased by 0.86°C from the first two decades to the last two decades.

Temperature and rainfall are crucial climate variables that impact people's livelihoods, particularly those dependent on agriculture and related fields. This study concludes that India is susceptible to climate variability, and climate change is likely to worsen these conditions.

Rangarajan et al. (2017) conducted a trend analysis of temperature using nonparametric tests in Coimbatore, Tamil Nadu, India. The study applied well-established nonparametric tests such as the MK test, Sen's slope, and Pettitt's test to determine the nature of trends and detect change points in the T_{max} and T_{min} of the city from 1902 to 2002.

The trend analysis using the MK test and Sen's slope revealed a positive trend in both minimum and maximum temperature series between 1902 and 2002. From 1902 to 1950, an insignificant trend was observed, but a significant rising trend was evident from 1941 to 2002. The Sen's slope values further supported the temperature increase after 1940.

Additionally, the analysis confirmed an increasing trend in both T_{max} and T_{min} in all months and seasons post-1950. The study concluded that this temperature increase could alter the hydrological cycle, ultimately impacting crop production and agricultural activities.

Datta and Das (2019) conducted an analysis of the long-term (1901–2002) seasonal and annual temperature trends in North Bengal, India. The study area has experienced substantial changes in its natural landscape over the past century due to factors such as resource exploitation, population growth, and agricultural expansion.

The study focuses on analyzing long-term trends in T_{max} and T_{min} in six northern districts of WB, collectively known as North Bengal. Using the non-parametric MK test and Theil-Sen's slope estimator, the study identified warming trends in both T_{max} and T_{min}. With the

exception of the monsoon season, most districts exhibited a significant warming trend. Specifically, during the post-monsoon and winter seasons, there was significant warming of both T_{max} and T_{min} compared to the monsoon and pre-monsoon seasons. This suggests that the rising temperatures during the post-monsoon and winter months primarily contribute to the overall annual warming trend.

Malda experienced the most significant increase in both T_{max} and T_{min} during the post-monsoon and winter seasons. In the region, T_{min} were increasing at a faster rate than T_{max}, except during the post-monsoon season. Sequential MK tests revealed periodic fluctuations in trends, especially during the pre-monsoon and monsoon seasons.

These findings align with previous broader-scale studies, although differences may arise due to regional variations in the climate system or the use of different trend-detection methods. The results of this study provide important evidence of warming trends over the 20th century, which can inform adaptation and mitigation strategies.

Kundu and Mondal (2019) conducted a study on the long-term (1901-2002) annual and seasonal rainfall trends, as well as change points, in WB, India. They analyzed monthly rainfall data from 18 rainfall stations. The study utilized several methods including the MK test, Theil-Sen's slope estimator, trend-free pre-whitening method, percentage change over mean rainfall, Pettitt-Mann-Whitney test, and standard normal homogeneity test to identify rainfall trends and change points.

In the northern and western parts of WB, all rainfall stations exhibit decreasing trends, with significant decreases noted in Uttar Dinajpur, Malda, and Birbhum for annual rainfall. Conversely, the southern part of the state shows a significant positive Z value of the MK test for annual and monsoon rainfall, with post-monsoon rainfall increasing significantly, except in Jalpaiguri and Darjeeling.

Pre-monsoon rainfall in WB does not significantly decrease, while eight rainfall stations in the western and southern regions of the state demonstrate a significant increase in post-monsoon rainfall. Winter rainfall in West Bengal has not decreased significantly, except for four stations in the south.

However, post-change point, there was a decrease in the south but an increase in the north and west. This research focuses on regional variables such as topographical variances, agricultural land use, urbanization, aerosol emissions, and deforestation to investigate rainfall changes in WB. The results could support further research on intra-regional hydrological modeling for livelihood sustainability and improve agricultural planning, regional crop-water management, and rainwater harvesting strategies.

Malik et al. (2019) examined the spatial-temporal trend analysis of seasonal and annual rainfall (1966–2015) using the ITA method with a significance test at 13 stations located in the central Himalayan region of the Uttarakhand State of India.

The ITA results were compared to the MK test at a significance level of 5%. The comparison's findings showed that ITA (significantly positive in 19 time series and substantially negative in 32 time series) can successfully identify the trend that the MK test (significantly positive in 3 time series and significantly negative in 6 time series) found.

The ITA method discovered significant trends in seasonal and annual rainfall series that the MK method missed. This would help accurately analyze hidden variations in rainfall trends in the research region. The comparison results showed that the ITA approach exceeded the MK method. The ITA approach graphically illustrates data on a Cartesian coordinate system, allowing for additional interpretations through visual inspection (Sen, 2017).

Furthermore, the ITA approach has several benefits, including being easy to understand and calculate, and not relying on distribution assumptions, serial correlation, or seasonal cycles. The study found that the ITA method outperformed the MK test in identifying hidden trends in seasonal and yearly rainfall time series data for the study region.

The spatial maps created will assist citizens and water management in understanding the hazards and vulnerabilities associated with climate change caused by human activity in the region.

Nengzouzam et al. (2019) conducted a detailed analysis of spatial and temporal trends in T_{max} and T_{min} across India using high-resolution gridded temperature data. Covering the period from 1969 to 2005, the study utilized daily data with a spatial resolution of 1° × 1°. They applied the MK non-parametric test at significance levels of 1%, 5%, and 10% to identify trends. Their comparison of gridded data with station data revealed that more than 130 stations exhibited estimations that were nearly perfect for both T_{max} and T_{min}.

This study aims to explain the spatio-temporal variations in daily T_{max} and T_{min}, including their diurnal range, across India. It examines the monthly and annual temporal trends of these temperatures and analyzes the spatial patterns of these trends. The results indicate significant decreasing trends in T_{max} across the entire Indo-Gangetic plains, extending up to the north-eastern region. In contrast, the southern region is experiencing warming trends.

Regionally, the Southern region exhibited consistent increasing trends in all three parameters, while Odisha, Chhattisgarh, and Jammu and Kashmir experienced decreasing trends. On a seasonal scale, the pre-monsoon and monsoon months (April through October, excluding August) primarily showed no clear trends in all three parameters, with occasional patches of slight increases in a few months.

The results also showed that the months from November through March, excluding January, were predominantly experiencing warming trends. Furthermore, the most significant decreasing trends were observed during the drier part of the year (January to May), while the most significant increasing trends were reported during wetter days (June to December).

Moreover, the higher Sen Slope value for the yearly maximum increase in T_{min} indicated a steeper increase in T_{min} compared to T_{max}.

Sen et al. (2019) discussed the basic concepts of Innovative Polygon Trend Analysis (IPTA) and its application. The paper explained a non-parametric approach to simplify the methodology and avoid most difficulties.

This approach not only identifies trends in a given series but also detects trend transitions between successive sections of two equal segments from the original hydro-meteorological time series, resulting in a trend polygon. This polygon serves as a useful basis

for detailed interpretation, including linguistic and numerical interpolations and inferences, from the time series.

In this study, the IPTA method was applied to analyze three hydro-meteorological records from diverse locations worldwide (New Jersey, USA; Danube River, Romania; and Goksu River, Turkey) in terms of precipitation and runoff. The paper provided practical IPTA templates that offer valuable linguistic and numerical information, including trends between successive months, their slopes and lengths, monthly amounts, homogeneities, isotropies, and other relevant data.

Achite et al. (2021) utilized the IPTA technique to discover precipitation trends at seven sites situated in the Wadi Sly basin, Algeria, which was spanning with a half-century (1968–2018) data. The study emphasizes the importance of analyzing future changes in precipitation data due to climate variability and its impact on water resources, agriculture, and ecosystems.

The IPTA method was introduced as a novel approach for detecting trends in precipitation data, offering a simple qualitative method for trend analysis. This study compares the results of the IPTA method with traditional trend analysis methods such as the MK test and Sen's slope estimator, highlighting the effectiveness and agreement between these approaches.

The findings suggest that the IPTA method can be used for preliminary trend analysis of monthly precipitation data, indicating its potential utility in assessing climate change impacts on precipitation patterns.

The study highlighted the importance of paying attention to flood risk management during stormy seasons and drought risk management in transitional seasons based on the observed precipitation trends in the study area of Algeria. There was good agreement across all approaches when comparing the trend analysis results from the IPTA method with the other assessed tests. This demonstrates that monthly precipitation trends can be preliminary analyzed using the IPTA approach.

Ceribasi et al. (2021) analyzed temperature data from the Susurluk Basin, Turkey, using the IPTA and the trend polygon star concept methods. These techniques were applied to monthly average temperature data spanning 22 years (1996–2017). The study generated IPTA and Trend Polygon Star Concept visualizations and calculated trend slopes and lengths of the temperature data.

The study computed monthly average temperature data for each station. The graphs they generated represent the distance between two months, divided into four sections, and were examined for each station. However, the arithmetic means and std of Bandirma Station did not display a regular polygon in IPTA.

The analysis of the arithmetic mean indicated a rising trend in most months. The graph of Bandirma Station's arithmetic average, constructed using the Trend Polygon Star Concept Method, showed a shift between two months in the first and third regions. The standard deviation (std) graph revealed two-month transitions across all four locations.

In conclusion, a more comprehensive trend analysis of a hydro-meteorological parameter (such as precipitation, humidity, or snow) can be achieved by utilizing both the methods employed in this study.

Hirca et al. (2021) investigated the historical variations of hydroclimatic variables and changes in water resources within the water cycle of eight measuring stations in the Eastern Black Sea Basin (EBSB). This basin, situated on the northeast coast of Turkey, receives one of the highest significant amounts of annual precipitation and possesses considerable hydroelectric potential. The study had two main objectives: (1) Investigating potential changes in monthly precipitation and (2) Comparing the outcomes obtained using a traditional trend analysis method, the MK method, with one of the latest trend analysis methods described in the literature, IPTA.

The methods were applied to 56 years of precipitation data. A comparison of the trend analysis results obtained by IPTA and MK revealed a significant discrepancy in the number of months with detected trends. IPTA was found to be relatively more sensitive in identifying trends.

The main reason for this discrepancy was that IPTA is more sensitive than MK in determining trends. Additionally, the polygons formed by the mean IPTA graphs were narrower and relatively smoother compared to the standard deviation graphs. Specifically, IPTA and MK identified trends in approximately 81.25% and 12.5% of all months, respectively. The polygons developed by IPTA for the mean and standard deviation graphs provided a yearly cycle, offering valuable information for water utility sectors and decision-makers in the study area.

The study's findings significantly contributed to the broader research endeavour aimed at understanding spatiotemporal variations of hydroclimatic variables worldwide. This research not only enhances our understanding of changes in the water cycle but also helps assess the impacts of climate change. The IPTA graphics suggest a need to examine the parameters that influence precipitation during relevant periods. This study is crucial for understanding the complexity of precipitation patterns and the reasons behind abrupt transitions between successive months.

San et al. (2021) explained the applications of IPTA for rainfall data in Vietnam. Among the approaches highlighted was the IPTA, derived from the ITA, which stands out for its assumption-free nature. This study seeks to compare the methodologies of IPTA, ITA, Significance Test, and MK test.

They analyzed monthly rainfall trends at 15 stations in Vietnam's Vu Gia-Thu Bon River Basin using data from 1979 to 2016. After verifying the homogeneity of the data, five stations were excluded from the study. Consequently, for the remaining 10 stations, they employed the MK method, ITA with a Significance Test, and IPTA.

This research revealed a significant increase in rainfall in March and a decrease in June at nearly all stations. The IPTA, ITA, and MK tests identified patterns in 88%, 93%, and 26% of all months, respectively. Both IPTA and ITA demonstrated higher sensitivity in detecting trends.

The ITA and IPTA showed increasing trends, except in May, June, and October. Additionally, in most stations, the polygons nesting around the global regression line indicated a natural equilibrium in the mean graph. The IPTA graphics highlighted October as a trend conversion point for all stations. According to IPTA, the lack of a trend slope in the

MK test and the general trends identified by MK and ITA were significant drawbacks. In conclusion, IPTA offers both quantitative and qualitative interpretations of periodicity, sequential behavior, and temporal internal variability.

Acar et al. (2022) explained the application of IPTA with star graphs to analyze rainfall and temperature data from nine selected stations in agricultural regions of Turkey, using 52 years (1969 to 2020) of data provided by the Meteorological Service. The analysis showed no pattern in approximately 96% of the monthly rainfall instances according to the MK test. However, both innovative approaches indicated that almost all stations exhibited a tendency to increase around November (and September). Regarding temperature, the data revealed either an increasing tendency or no trend overall. Except for April, the innovative approaches showed growing patterns throughout the year.

In recent decades, temperatures have experienced significant increases year-round across all locations. Furthermore, utilizing IPTA, it was discerned that all agricultural regions exhibit a persistent and rather complex seasonal internal variability of rainfall over the entire period, including the last 30 years.

The findings indicate that crop productivity was adversely affected at all stations, necessitating additional irrigation due to irregular variations in rainfall and rising temperatures. Rainfall often increases in winter, summer, and autumn, but decreases in the spring. Moreover, the comparison of trend methods revealed that innovative approaches placed a strong emphasis on trend identification and provided further insights through visual analysis of trend behaviors. This study examines the impact of climate change on agricultural crop yield by analyzing meteorological data.

Esit (2022) presented the new graphical method IPTA, MK, and ITA with significance tests on monthly and annual hydrometeorological data for Ankara province in Turkey. The study mainly focused on monitoring hydrometeorological trends, crucial due to climate change. ITA with significance tests and IPTA both are introduced as new methods for trend analysis.

Traditional method like the MK test was compared with ITA and IPTA for monthly and annual hydrometeorological data in the Ankara region. Sequential Mann-Kendall (SQ-MK), CUSUM (or cumulative sum control chart), and Standard Normal Homogeneity Test (SNHT) were also used to detect abrupt changes in the data.

These results showed that IPTA and ITA with significance tests are more sensitive than the MK test, which has the lowest in the evapotranspiration series and the highest in the precipitation series. Furthermore, because of the increased trends, three techniques are useful for identifying patterns in evapotranspiration series. As a result, the MK test is unable to identify time series' hidden trends, particularly in precipitation data. Consequently, the ITA and IPTA graphical approaches successfully capture the underlying trend in precipitation.

Sharma and Ghosh (2022) conducted a temporal trend analysis of monthly climate data, including T_{max}, T_{min}, and rainfall, using the IPTA method for the Hardwar district in the western part of Uttarakhand, India, over a 40-year period from 1981 to 2020.

As a result of this analysis, IPTA graphics were generated for the study area, incorporating TL and TS evaluations for the monthly parameters. It was observed that, on a

monthly scale, no single or regular polygon was formed in the IPTA graphics for average minimum temperature and rainfall, indicating their lack of homogeneous and isotropic behavior.

In the case of average T_{max}, a regular and single polygon appearance was observed in IPTA graphics, indicating homogeneous and isotropic behavior. An increasing trend was noticed in T_{min} data for all monthly points, whereas for T_{max} and rainfall, there was both an increasing and decreasing trend observed for different monthly points. The length and slope of the trend provided insights into the variation during the months. This study suggested that the IPTA method could be applied to other meteorological parameters, which could be beneficial for various applications related to water supply and agricultural activities in the future.

Chowdari et al. (2023) applied ITA on seasonal and annual rainfall derived from monthly datasets spanning 102 years (1901–2002) for 11 districts of the semi-arid of Karnataka, India. The two-step homogeneity test was applied to all time series. Then, lag-1 autocorrelation was applied solely to homogenous time series.

Only 78.18% of time series data were homogeneous, whereas 95.35% had no significant autocorrelation. The ITA approach was used for 43 homogeneous rainfall time series, 41 MK and SR tests, and two modified MK tests. The MK and SR tests showed a significant trend in 14.63% of the data.

The MK and SR experiments found substantial trends in two districts' winter and post-monsoon season precipitation, but only one district's summer and annual rainfall. No trend was found in monsoon season precipitation. The modified MK test demonstrated a positive trend during the post-monsoon season in one area.

The ITA approach revealed significant trends for all seasons in the majority of districts. Out of all the districts studied for obscure trend analysis, the district of Belagavi experienced the highest increasing trend magnitude on an annual basis (20.27 mm/year). This means the district experienced the likelihood of more food occurrences. On the other hand, the district of Haveri experienced almost similar trend magnitude (21.28 mm/year), but a decreasing one. That means the district had likely undergone drought to some extent. The sub-trend analysis showed tendencies that previous approaches failed to discover.

Halder et al. (2023) conducted a long-term trend analysis of annual and seasonal rainfall in West Bengal, India, spanning the period 1901 to 2020. They used a gridded rainfall dataset with a resolution of 0.25° × 0.25° and applied the non-parametric MK test, SQMK test, and Sen's slope estimator to analyze the data.

The findings indicated that, except for the winter season, which showed a non-significant decrease, annual and seasonal rainfall in most districts of Sub-Himalayan West Bengal (SHWB) increased non-significantly. However, there was a slight decrease in annual rainfall. In contrast, there was a significant increase in annual precipitation in the majority of Gangetic West Bengal (GWB) districts, with an increase of 1.8 mm to 2.9 mm per year.

In the Dakshin Dinajpur district of SHWB, monsoon rainfall decreased significantly by 3.2 mm per year, while in GWB, it increased significantly from 1.4 mm to 2.1 mm per year.

Additionally, post-monsoon season rainfall increased significantly across GWB, from 0.5 mm to 0.9 mm per year. There was a negligible decrease in winter rainfall in every district.

The overall conclusion suggests that the decreased annual and seasonal rainfall in the districts has heightened the risk of drought and water scarcity. Agrarian economies and resource-poor farming communities must adapt to these shifting rainfall patterns and climates to sustain their livelihoods. This study aims to enhance understanding of the seasonal water budget, which is crucial for crop planning, water security, and livelihood security for resource-poor farmers in the state.

Karacosta et al. (2023) utilized the non-parametric trend analysis methodology IPTA in a case study on the precipitation of Thessaloniki, Greece, spanning 50 years. In this study, IPTA was proposed as an alternative to classical trend analysis methodologies. Monthly precipitation measurements from Thessaloniki were analyzed for the period 1971–2020, divided into two consecutive equal periods, to identify inherent trends among months and seasons, respectively.

The study provided a detailed interpretation of trends with physical and numerical explanations, leading to the obtained results. Total monthly and seasonal precipitation values, along with their associated standard deviations, trend slopes, and trend lengths, were depicted. It was observed that the second sub-period (1996–2020) showed a significant increase in precipitation compared to the first one.

As a result, the study concluded that the majority of months indicated increasing trends, particularly noting sharp transitions from decreasing to increasing trends from August to September and November to December. Moreover, sharp transitions led to very large values of trend length and trend slopes. These conclusions were further supported by strong increasing trends in monthly precipitation tendencies observed in standard deviation polygons and numerous, stronger transitions towards the increasing trend area shown in the precipitation range polygon. Consequently, significant increasing precipitation trends were identified between the two sub-periods (1971–1995 and 1996–2020) for the winter and autumn seasons, while spring and summer showed almost no trend.

Patel et al. (2023) conducted a case study in Eastern India, comparing extreme temperature trends over the last two decades (2001–2020) with the preceding seven decades (1951–2020). Their main focus was investigating extreme temperatures, crucial for the region's cropland and work cultures, which heavily depend on favourable climatic conditions. Identifying trends in climatic scenarios was considered important for understanding the pattern of extreme temperatures.

They analyzed various decadal periods using the Innovative Trend Analysis Method (ITAM). Subsequently, they selected annual and seasonal extreme temperature variations over 70 years (1951–2020) at 11 grid points in the Kangsabati–Silabati–Keliaghai–Dwarkeswar basins of West Bengal. The outcomes from two different time periods, the historical decade (1951–2020) and the recent decade (2001–2020), revealed some surprising results. During the historical decade, T_{max} exhibited negative sloping patterns in the monsoon and autumn seasons, with approximately 100% positive trends at grids. Conversely, the winter, summer, and annual seasons showed decreasing trends at 80% of the selected grids.

On the other hand, for T_{min}, all seasons showed increasing trends at more than 80% of the grids. In the case of the recent decade, T_{max} exhibited positive slopes in the annual, monsoon, and autumn seasons at around 64% of the grids, while the summer and winter seasons showed negative slopes at around 90% of the grids with very high magnitudes. Finally, T_{min} for the recent decade showed negative slopes in all three seasons at more than 82% of the grids, except for the monsoon season, which showed a positive trend with a very significant magnitude for 100% of the grids.

Singh et al. (2023) explored the spatiotemporal variability and trends in rainfall and temperature in the Damodar Canal region of Eastern India, discussing their implications. The study analyzed long-term trends and variability in these two key climatic variables, using data from 14 weather stations situated in this sub-tropical region. At the 1% level of significance, it was found that the temporal and spatial fluctuations in monthly temperatures (T_{max}, T_{min}, and mean temperature) and annual rainfall are statistically significant.

The analysis of yearly rainfall patterns revealed "no trend" at most meteorological stations, except for Burdwan-I and Mejhia, which showed significant increasing trends of 18.98 mm and 20.61 mm annually, respectively. However, notable declining trends in the T_{max} time series were observed in July, September, October, and November, ranging from -0.022°C to -0.064°C annually. In contrast, the T_{min} time series for May showed substantial increasing trends at most locations, ranging from 0.023°C to 0.03°C each year.

The results of this study can be used to develop climate-resilient and adaptive methods for efficient planning and management of water resources, which will support the region's livelihoods, environment, and agricultural output. This study contributes to a better understanding of climate change on a large scale across the Indian subcontinent. Temperature and rainfall data provide crucial regional and national insights into global warming and climate-induced disasters. This study can help decision-makers and water managers enhance plans for sustainable food production and water resource management in Eastern India and other subtropical regions of India. Additionally, the methodology of this study may be applicable globally.

Patel et al. (2024) investigated the optimal method for analyzing long-term (120 years) annual and seasonal rainfall trends in four East-Indian River basins (Keliaghai, Kangsabati, Silabati, and Dwarkeswer). This study examined rainfall changes between 1901 and 2020 using several tests, including the MK Test, Modified MK Test (MMKT), Spearman Rank Correlation (SRC), Sen Slope Estimator (SSE), and ITAM. The focus was on yearly, monsoon, autumn, summer, and winter patterns, aiming to understand their implications for agricultural production and climate conditions.

The MKT, MMKT, SRC, and SSE did not reveal significant trends in the winter season. However, the ITAM identified a notable trend in 88% of the grid points across the study area. In other seasons, the MKT, MMKT, SRC, and SSE detected trends in 76% of the grid points, albeit with lower significance compared to the ITAM. The ITAM and MMKT approaches were more sensitive in detecting trends compared to other methods.

This study offered a scientific foundation for identifying and managing the consequences of climate change on water resources, thereby reducing the potential impact of

climate change. It emphasizes the importance of selecting appropriate methods and statistical techniques in both research and practical applications. The study suggested the potential for regional-scale seasonal pattern research, as well as the development of water-related project planning and mitigation strategies.

Out of 27 literatures, 15 consisted of some old traditional methods like the MK test, SQMK test, SSE, and MMK test. There are some limitations in the methods used to determine the trends of hydro-meteorological variables (i.e., Rainfall, Minimum and Maximum Temperature, Runoff etc.). For instance, the data are serially independent and normally distributed, and the data is of a certain length. For the ITA method developed by Sen (2012), there is no limitation in the data length, and consequently, it can be applied to any time series. Six literatures considering ITA was also included in this study's literature review. As an improved version of ITA, IPTA was considered in this study and nine literatures were included.

3.2 Research Gaps

There are already many articles that use the MK test, as well as ITA and very few studies on IPTA, have illustrated in literature review. However, the aforementioned researches are lacking and have several limitations, which are mentioned below as research gaps.

- **Limited investigations on climatological changes in T_{min} across WB**
  Despite the significance of understanding climate change impacts on regional scales, there has been a lack of comprehensive studies focusing on the T_{min} changes across the entire region of WB.
- **Lack of integrated high-resolution trend and spatiotemporal analysis**
  Existing studies have typically employed either trend analysis or spatiotemporal analysis independently, often using datasets with limited spatial and temporal resolution. None of the available studies have combined high-resolution datasets to conduct a comparative trend analysis alongside detailed spatiotemporal analysis on a monthly and seasonal basis with decadal comparison. This gap highlights the need for integrated methodologies that can provide a better understanding of climate at finer scales.
- **Insufficient discussion on IPTA in T_{min} research**
  IPTA has shown promise in identifying and characterizing climate trends with greater precision. However, its application in the context of T_{min} analysis remains limited.

The study area and data collections are described in the next chapter keeping the previously mentioned shortcomings in mind.

Chapter 4

STUDY AREA AND DATA COLLECTIONS

4.1 Study Area

West Bengal (WB) is a significant state in India, known for its physical and socio-economic diversity (Kundu and Mondal, 2019). It is one of India's 28 states, located in the eastern part of the country (between 21° 25′ 02″ to 27° 13′ 15″ N latitudes and 85° 49′ 20″ to 89° 53′ 04″ E longitudes), covering an area of about 88,000 km² (Halder et al., 2023). The altitude ranges from 3,636 meters in the north (Sandakphu at Singalila range) to less than 3 meters in the south (at Sagar Island), with an average of 44 meters above sea level. This wide range of altitudes and different landforms gives WB a variety of climates, from tropical wet-dry in the south to humid subtropical in the north (Kundu and Mondal, 2019). The state shares its border with five Indian states (Sikkim, Bihar, Assam, Jharkhand and Odisha) and three countries (Bangladesh, Nepal, and Bhutan). Figure 4.1 shows the location of WB.

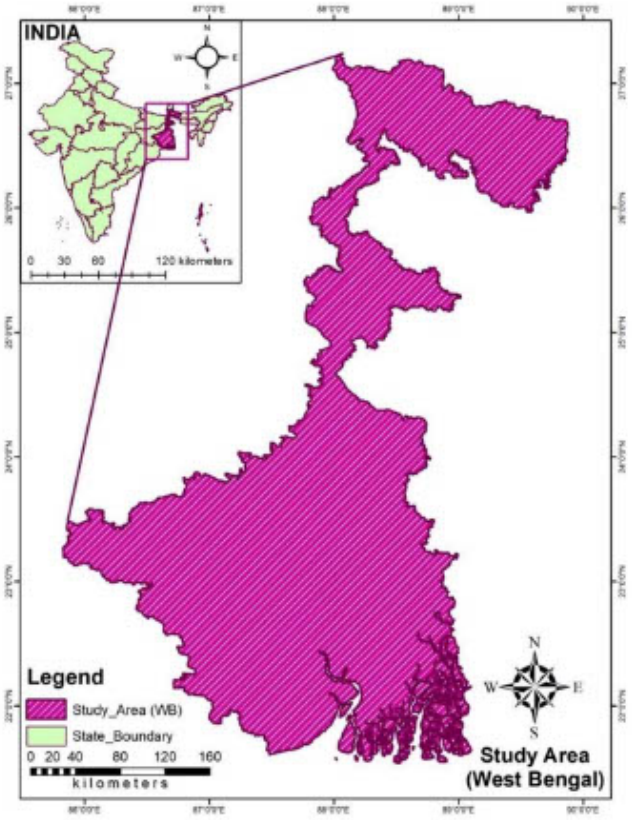


Fig. 4.1 Location of the study area

4.2 Data Collected

The dataset used in this study consists of 72 years of T_{min} gridded data from the IMD, Pune. The data is gridded at a resolution of 1°×1°, as developed by Srivastava et al. (2009). This study analyzes various seasons, including summer (March, April, May - MAM), monsoon (June, July, August, September - JJAS), autumn (October, November - ON), and winter (December, January, February - DJF) (WPCB 2016). The study area, comprising a total of 56 grids, is shown in Fig. 4.2. This figure represents the gridded data positions with resolutions of 1°×1° and 0.5°×0.5°, presented in green and blue colour respectively, across WB.

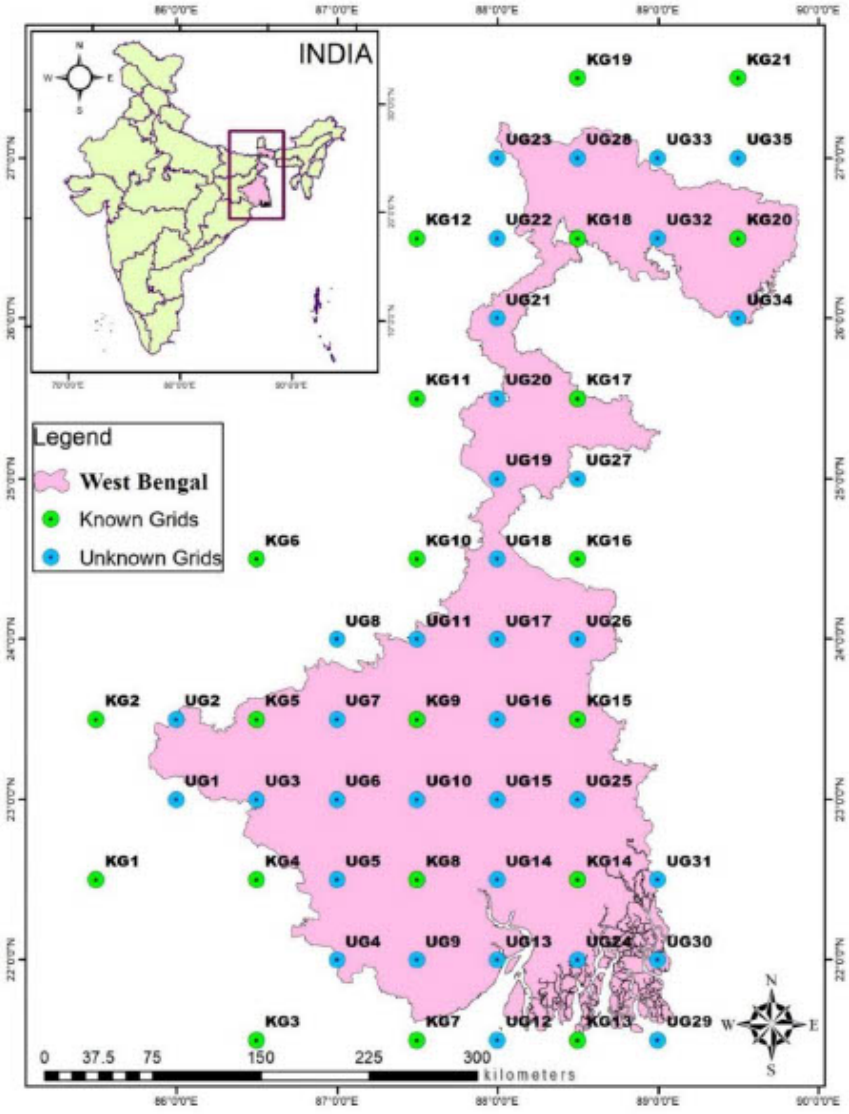


Fig. 4.2 Study area with the gridded position of 21 known (1°×1° from IMD-Pune collected) and 35 unknown (0.5°×0.5° IDW interpolated) grids of West Bengal

4.3 Representation of known and unknown grids

The conversion from 1° to 0.5° resolution is a crucial process in this study for better representation of results. Table 4.1 represents the known grids as KG and interpolated unknown grids as UG which is calculated by using the IDW method for this study.

Table 4.1 Representation of grids throughout the study area

KG	Latitude (in °)	Longitude (in °)	UG	Latitude (in °)	Longitude (in °)
KG1	22.5	85.5	UG1	23	86
KG2	23.5	85.5	UG2	23.5	86
KG3	21.5	86.5	UG3	23	86.5
KG4	22.5	86.5	UG4	22	87
KG5	23.5	86.5	UG5	22.5	87
KG6	24.5	86.5	UG6	23	87
KG7	21.5	87.5	UG7	23.5	87
KG8	22.5	87.5	UG8	24	87
KG9	23.5	87.5	UG9	22	87.5
KG10	24.5	87.5	UG10	23	87.5
KG11	25.5	87.5	UG11	24	87.5
KG12	26.5	87.5	UG12	21.5	88
KG13	21.5	88.5	UG13	22	88
KG14	22.5	88.5	UG14	22.5	88
KG15	23.5	88.5	UG15	23	88
KG16	24.5	88.5	UG16	23.5	88
KG17	25.5	88.5	UG17	24	88
KG18	26.5	88.5	UG18	24.5	88
KG19	27.5	88.5	UG19	25	88
KG20	26.5	89.5	UG20	25.5	88
KG21	27.5	89.5	UG21	26	88
			UG22	26.5	88
			UG23	27	88
			UG24	22	88.5
			UG25	23	88.5
			UG26	24	88.5
			UG27	25	88.5
			UG28	27	88.5
			UG29	21.5	89
			UG30	22	89
			UG31	22.5	89
			UG32	26.5	89
			UG33	27	89
			UG34	26	89.5
			UG35	27	89.5

A group of districts forms a division, which is administered by a "Divisional Commissioner". The Indian state of WB is divided into five administrative divisions. The district-wise divisional combinations along with their respective grids are represented in Table 4.2 (Source: _https://en.wikipedia.org/?title=Administrative _divisions of West Bengal & o l did =1139523251).

Table 4.2 Grouping of the 23 districts under five divisions

Divisions	Districts	Grids
Jalpaiguri	Alipurduar, Cooch Behar, Darjeeling, Jalpaiguri, Kalim pong	KG12, KG18, KG19, KG20, KG21, UG22, UG23, UG28, UG32, UG33, UG34, UG35
Malda	Dakshin Dinajpur, Uttar Dinajpur, Malda, Murshidabad	KG11, KG16, KG17, UG17, UG18, UG19, UG20, UG21, UG26, UG27
Burdwan	Birbhum, Hooghly, Paschim Bardhhaman, Purba Bardhhaman	KG6, KG9, KG10, UG8, UG11, UG15, UG16
Medinipur	Bankura, Jhargram, Paschim Medinipur, Purba Medinipur, Purulia	KG1, KG2, KG3, KG4, KG5, KG7, KG8, UG1, UG2, UG3, UG4, UG5, UG6, UG7, UG9, UG10, UG13
Presidency	Howrah, Kolkata, Nadia, North 24 Parganas, South 24 Parganas	KG13, KG14, KG15, UG12, UG14, UG24, UG25, UG25, UG29, UG30, UG31

Currently, there are 69 subdivisions across 23 districts in WB. Since this analysis already includes 56 grids and adopts a divisional combination approach, there is no need to incorporate the subdivision approach. Therefore, the study area is divided into five divisions, as shown in Fig. 4.3. The arc map representation consists solely of these divisions. There are 12 grids in the Jalpaiguri division, 10 in the Malda division, 7 in the Bardhhaman division, 17 in the Medinipur division, and the remaining 10 grids are in the Presidency division. In this study, several boundary grids were selected for detailed analysis in each division. These grids are represented in Fig. 4.3 as highlighted in green symbols. Figures 4.2 and 4.3 both show that almost 12 grids of the 21 KG are not actually located within WB. It is clear that 57% of known grids (KG1, KG2, KG3, KG4, KG6, KG10, KG11, KG12, KG13, KG16, KG19, and KG21) are located outside of the WB limit. The interpolation of higher resolution grids is required for those outsider grids. The next chapter addresses the detailed methodology applied for this study.

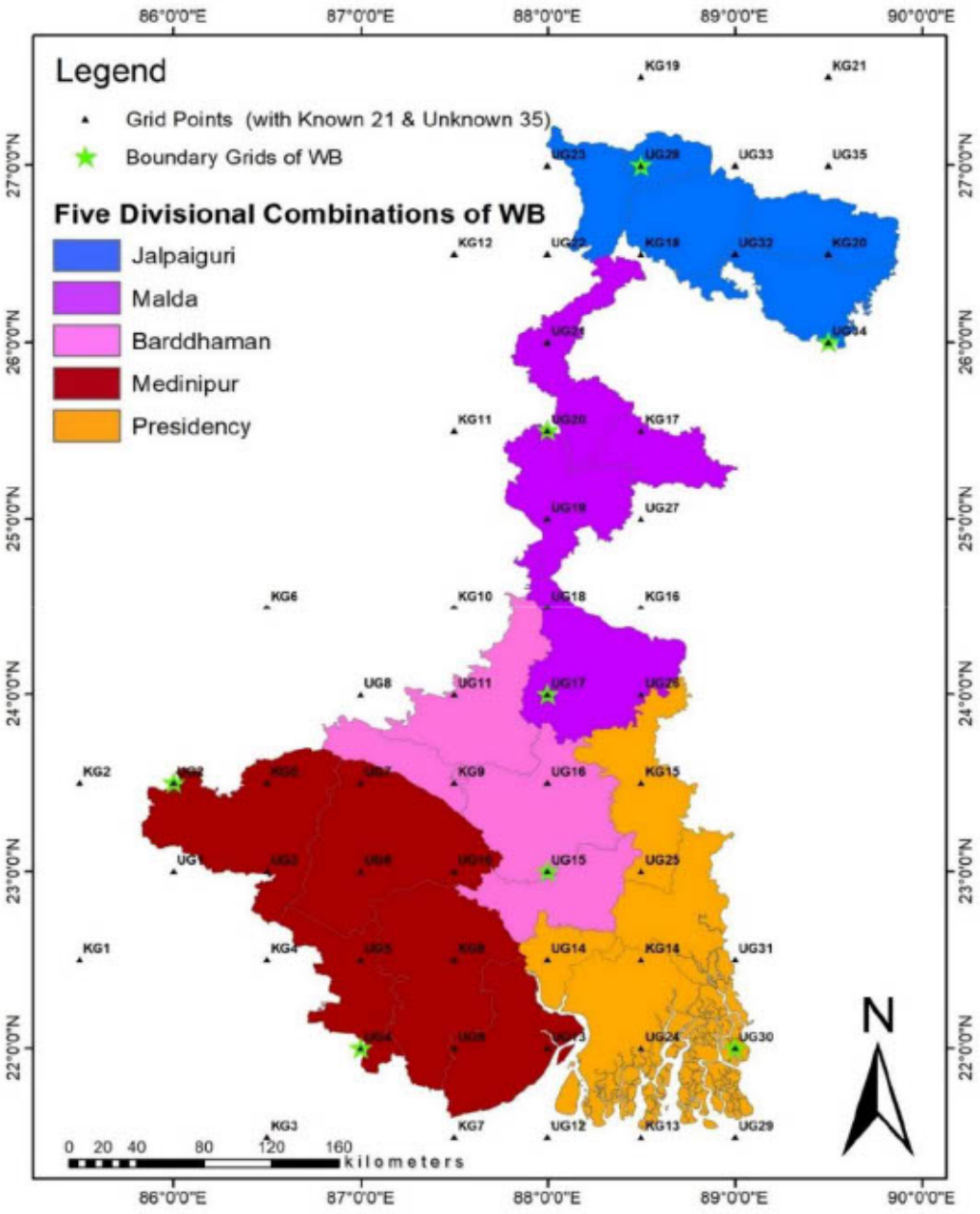


Fig. 4.3 Divisional representation of West Bengal

Chapter 5

METHODOLOGY

In this study, a 72-year trend analysis of minimum temperature (T_{min}) data was conducted using IPTA. Additionally, decadal, monthly, and seasonal temperature variations were investigated with the IPTA method. Daily gridded T_{min} data were utilized for this analysis. Initially, the data were organized and analyzed using ArcGIS. Following this, trends for the period from 1951 to 2022 were examined across 56 grids using different ways. The detailed methodology of this study is depicted in a flowchart (Fig. 5.1).

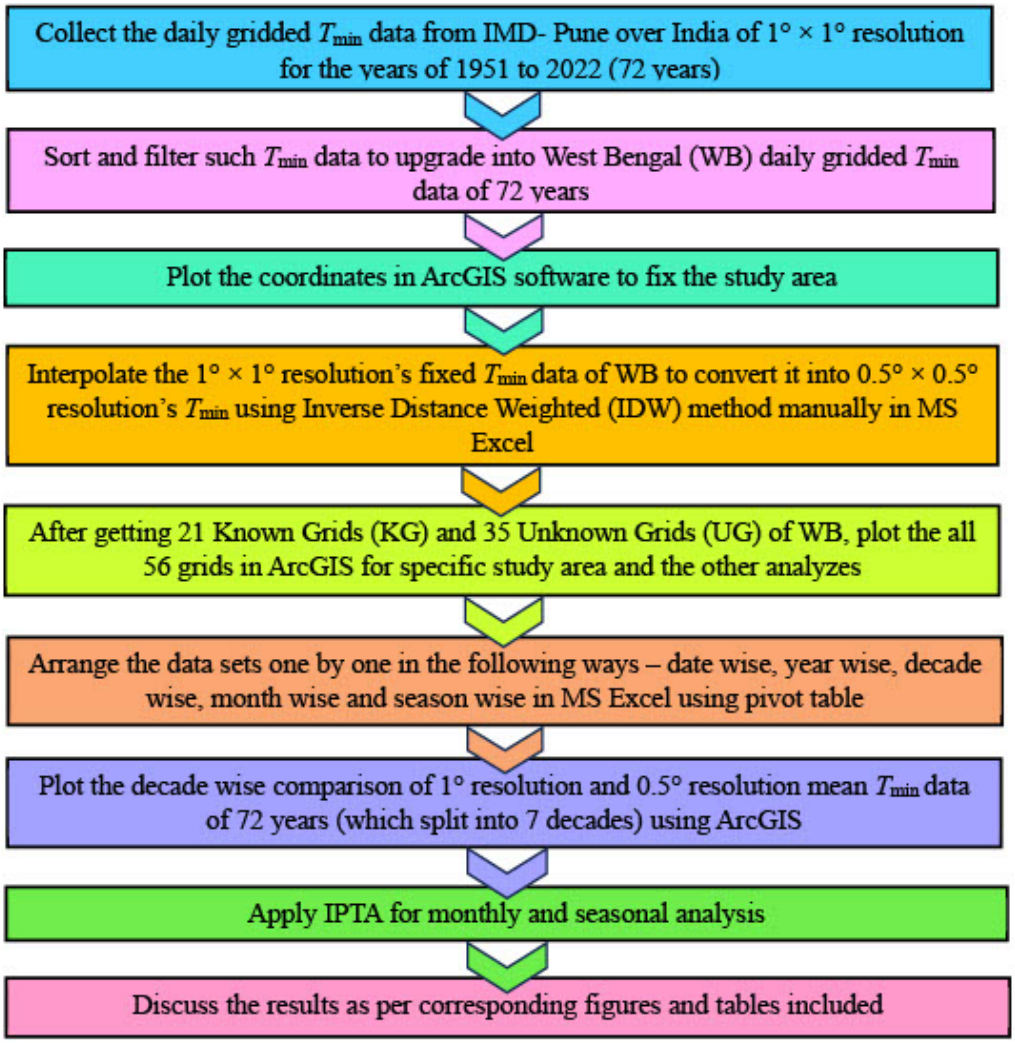


Fig. 5.1 Flow chart of the methodology

5.1 Development of the new gridded daily minimum temperature (T_{min}) data over West Bengal (WB)

The T_{min} for WB, spanning 72 years, were organized after filtering the yearly 1° × 1° resolution data. These data were subsequently divided into seven decades for further analysis. Before interpolating the 1° resolution gridded T_{min} data, the outsider grids were sorted out, and the positional information of the grid points was verified. If any missing data was identified, it was corrected by interpolating between the T_{min} data of the preceding and subsequent dates. Finally, the data was interpolated at fixed spatial grid points of 0.5° × 0.5° resolution.

A common approach for converting the IMD 1° resolution T_{min} data into 0.5° resolution gridded T_{min} data is spatial interpolation. Interpolation methods can be broadly divided into deterministic and geostatistical methods (Pai et al., 2014). Deterministic interpolation methods assign values to grid points based on the measured temperature from surrounding grid points (at IMD grid points) and use specified mathematical formulas to calculate the temperature values. These methods rely either on the degree of similarity (e.g., inverse distance weighting, natural neighbor) or the degree of smoothing in relation to neighboring station data points (e.g., trend analysis, multi-quadratic surface fitting). Geostatistical methods utilize both mathematical and statistical techniques, incorporating autocorrelation (the statistical relationship among gridded temperature data). Due to this capability, geostatistical techniques not only generate an estimation surface of the variable but also provide a measure of certainty or accuracy for the estimations.

5.2 Inverse Distance Weighted (IDW) method

In developing the new dataset, Pai et al. (2014) used the simplest form of the IDW interpolation scheme proposed by Shepard (1968). It is a widely utilized interpolation technique in spatial analysis and Geographic Information System (GIS) to estimate values at unknown grid points based on nearby measured points. IDW interpolation is especially valuable for handling spatially distributed data, such as climate variables and elevations. The fundamental principle of IDW is that the impact of a known data point decreases as the distance from the unknown grid increases. This is accomplished by assigning weights to the known data points based on their distances from the unknown grid (UG) points. IDW is a straightforward and intuitive method for spatial interpolation, and its results can be effectively visualized using contour maps or heat maps (Pai et al., 2014). The general formula of this method is as follows in Eq. 5.1.

$$T_{UG} = \frac{\sum_{i=1}^{n} \frac{T_i}{D_i}}{\sum_{i=1}^{n} \frac{1}{D_i}} \qquad (5.1)$$

where, T_{UG} represents the temperature of unknown grids, T_i denotes the temperature of known grids (KG), D_i signifies the distance from known grids to unknown grids, and n denotes the number of known grids temperature.

Interpolated values are computed as a weighted sum of surrounding observations in the IDW method. This technique operates under the assumption that interpolating locations are primarily influenced by nearby grids and less by more distant ones. For computational efficiency, only T_{min} data from the nearest neighbour grids (ranging from a minimum of 4 points to a maximum of 6 points) within radial distances of 0.5 degrees, 0.707 degrees, and 1.118 degrees around the unknown grid point are used to calculate the weighted average. Figure 5.2 illustrates the detailed calculations of UG30 using IDW interpolation.

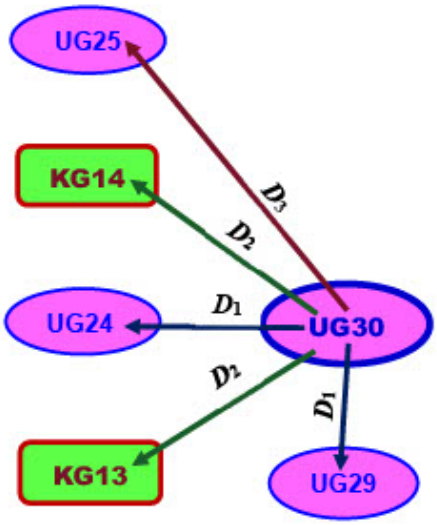


Fig. 5.2 Representation of UG30 for IDW determination where D_1, D_2 and D_3 are the radial distances of 0.5, 0.707 and 1.118 degrees, respectively

5.3 Trend Methodology

In general, trend methods are categorized into two main groups: parametric and nonparametric tests. Classical parametric tests are typically unsuitable for analyzing hydro-climatological time series due to their reliance on assumptions such as normality, linearity, and independence. The MK test (Mann, 1945; Kendall, 1975), a prominent nonparametric method, is widely utilized for trend analysis in time series within climate and water sciences. However, the MK test also has notable limitations (Hirca et al., 2021). Unlike the MK test and other parametric or nonparametric trend methods, graphical methods that do not rely on assumptions have gained popularity in recent years. One such method, Innovative Trend Analysis (ITA), categorically examines trends in hydro-meteorological data by grouping them as low, medium, and high, distinguishing them from all classical trend methods (Sen, 2012). ITA facilitates trend identification from both inductive and deductive perspectives. In its application, ITA does not impose restrictive assumptions, allowing for subjective visual

interpretations that lead to objective linguistic inferences (Sen et al., 2019). Finally, a new approach named Innovative Polygon Trend Analysis (IPTA), an enhanced version of ITA proposed by Sen et al. (2019), has been introduced as a trend analysis method. IPTA methodologies involve distinct procedures for identifying potential trend components in a given time series.

5.4 Innovative Polygon Trend Analysis (IPTA)

IPTA is an innovative and improved method for analyzing trends in recent years without relying on specific mathematical assumptions. It's widely regarded as effective and popular in trend analysis because it avoids the complexities of traditional methods that assume certain data distributions. One of its key strengths is its ability to analyze trends by comparing different sets of time-series data. In a monthly time frame, comparing the first half of the time-series with the second half would involve analyzing 12 sets of respective parameters (Fig. 5.3). In contrast, for seasonal data, there would be four sets (summer, monsoon, autumn, and winter) of respective parameters. Seasonal trend analysis is particularly useful for managing irrigation, agriculture, and water resource systems, where IPTA helps identify trends across specific seasonal sequences. IPTA depicts the trend size and slope between consecutive points, resulting in a trend polygon. This polygon serves as a robust foundation for enhanced linguistic and numerical interpretation and deduction of trends. This method can assess the hydrological balance over a calendar year. IPTA can evaluate the isotropy, homogeneity, and distribution of hydrometeorological data, considering temporal internal variability within the hydrological cycle (Sen et al., 2019). The step-by-step computational methodology of IPTA for both monthly and seasonal cases is illustrated in Fig. 5.4 as a flowchart.

In statistical terms, the IPTA template typically employs the statistical techniques of arithmetic mean and standard deviation. The mean represents the average value in a dataset, while the standard deviation indicates the spread of values relative to the mean. Both parameters are crucial for trend analysis. Figure 5.3 illustrates a schematic view of monthly T_{min}, depicting a hypothetical IPTA template. An ideal line, known as the 1:1 (45 degrees) trendless line or "No trend line", is drawn. The above left portion is the "Increasing Trend Region" and the below right portion of this line is called the "Decreasing Trend Region". Hence, the points plotted above this line indicate an inclining trend, while those below indicates a declining trend. Successive monthly points are connected by straight lines in Fig. 5.3, showing trend information and transitions from one month to the next. The distribution of points across the graph reflects the outcomes of various meteorological activities throughout the seasons. Typically, a regular polygon exhibits a rising limb followed by a declining sequence. For example, in Fig. 5.3, starting from January through points February, March, April, May, and up to June, the monthly values show an upward trend. From June to July, the line remains constant, indicating no rise or fall in values.

Conversely, after a minor rise from July to August, the trend from August through September, October, November, December, and ending in January shows a decreasing trend. In the IPTA template, each of the 12 months is connected by straight lines of varying length and slope. In general, simply a straight-line expression can be obtained after knowing the coordinates of each successive month on the IPTA template, hence each trend line or slope

can be calculated. The length between points is termed "TL", while the slope represents the "TS" between consecutive months.

5.4.1 Trend Length (TL)

It signifies the distance between two consecutive months (or seasons) on the polygons, indicating the presence of a weak or strong trend transition from one month (or season) to the next. A longer trend length indicates greater climatological differences between months (or seasons). Trend length cannot be negative but may be expressed in units such as degrees Celsius (°C) when applied to temperature trends. The general method for determining trend length is shown in Eq. 5.2.

$$TL = \sqrt{(x_2 - x_1)^2 + (y_2 - y_1)^2} \tag{5.2}$$

where, x_1 and x_2 are two consecutive points in the first part in the horizontal axis, on the other hand, y_1 and y_2 are two consecutive points in the second part, respectively.

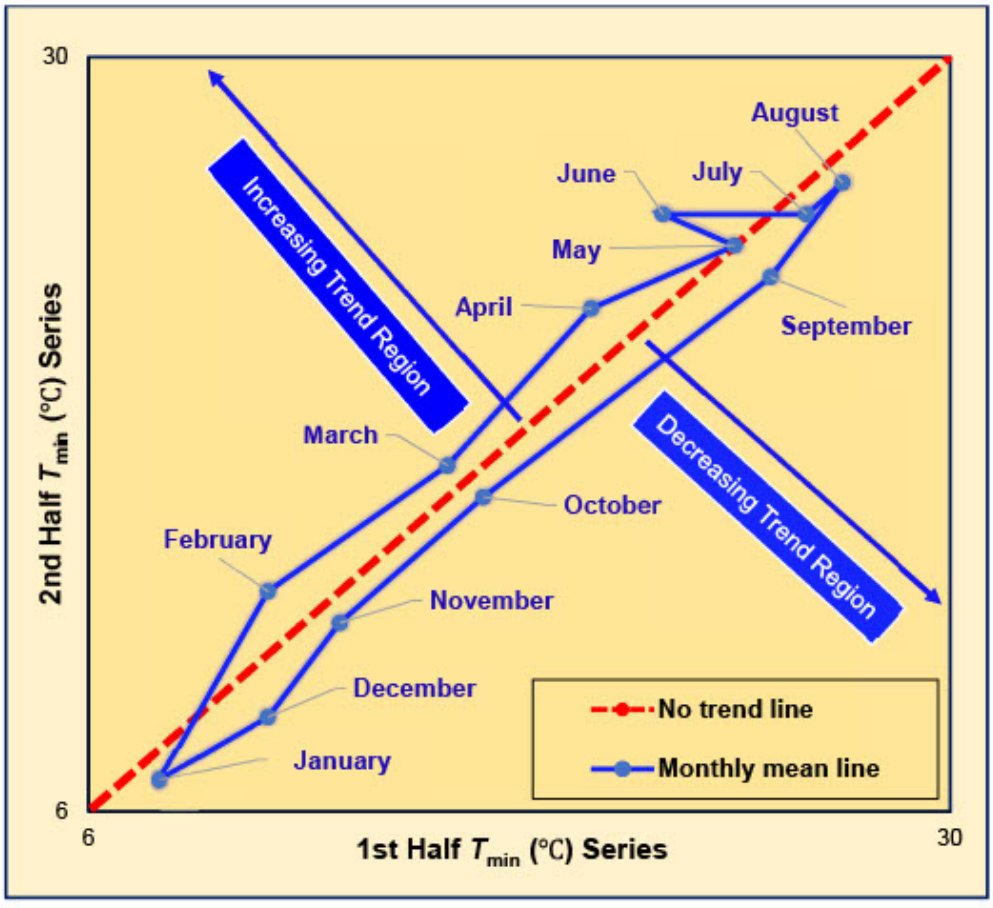


Fig. 5.3 IPTA template for monthly T_{min} trends

5.4.2 Trend Slope (TS)

It illustrates the rate of change from one month (or season) to the next, comparing the first half with the last half of the time series record duration. The trend slope is unitless. The general formula for determining trend slope is as follows (Eq. 5.3):

$$TS = \frac{(y_2 - y_1)}{(x_2 - x_1)} \tag{5.3}$$

Generally, considering two consecutive months (or seasons) leads to the following interpretations:

- If the slope is positive, it indicates that the trend moves from one month (or season) to another in the same direction on both axes of the polygonal pattern. This means there is either an increase or decrease over the two halves of the available hydro-meteorological record.
- If the slope is negative, it means the trend of one month (or season) moves in the opposite direction between the first and second halves of the record duration.
- If the slope is less than 1, it indicates that the variation of the parameter (monthly or seasonal average T_{min}) between the two months (or seasons) in the first half of the time series is wider than in the second half.
- If the slope exceeds 1, it signifies that the variation is greater in the second half compared to the first half of the time series.

In the results and discussion section, the tables present statistical values for all grids, analyzed using the IPTA method, which offers valuable insights for quantitative studies. Overall, an IPTA template for monthly records provides comprehensive information about the hydro-meteorological system, leading to the following key insights.

- A straight line between two consecutive months indicates the change in monthly values. A closed polygon represents the natural balance of the hydro-meteorological variable over the course of one year.
- If the slope of each straight line in the IPTA template is similar in both vertical and horizontal directions, it indicates that the relative monthly rates contribute insignificantly to the overall mean of the hydro-meteorological variation for each consecutive month.
- The smaller the overall slope of the polygon relative to the horizontal axis, the more intensive the occurrence of hydro-meteorological events.
- For any water resources project involving planning, operation, maintenance, and development, the IPTA template offers values that facilitate effective and systematic assessment.

These general characteristics of the polygon diagram reflect many quantitative and qualitative properties of the hydro-meteorological phenomena. In Fig. 5.3, the polygon of the IPTA template is very narrow, which means that the internal change within the hydro-meteorological variable is quite homogeneous, isotropic, and has uniform variation behaviour.

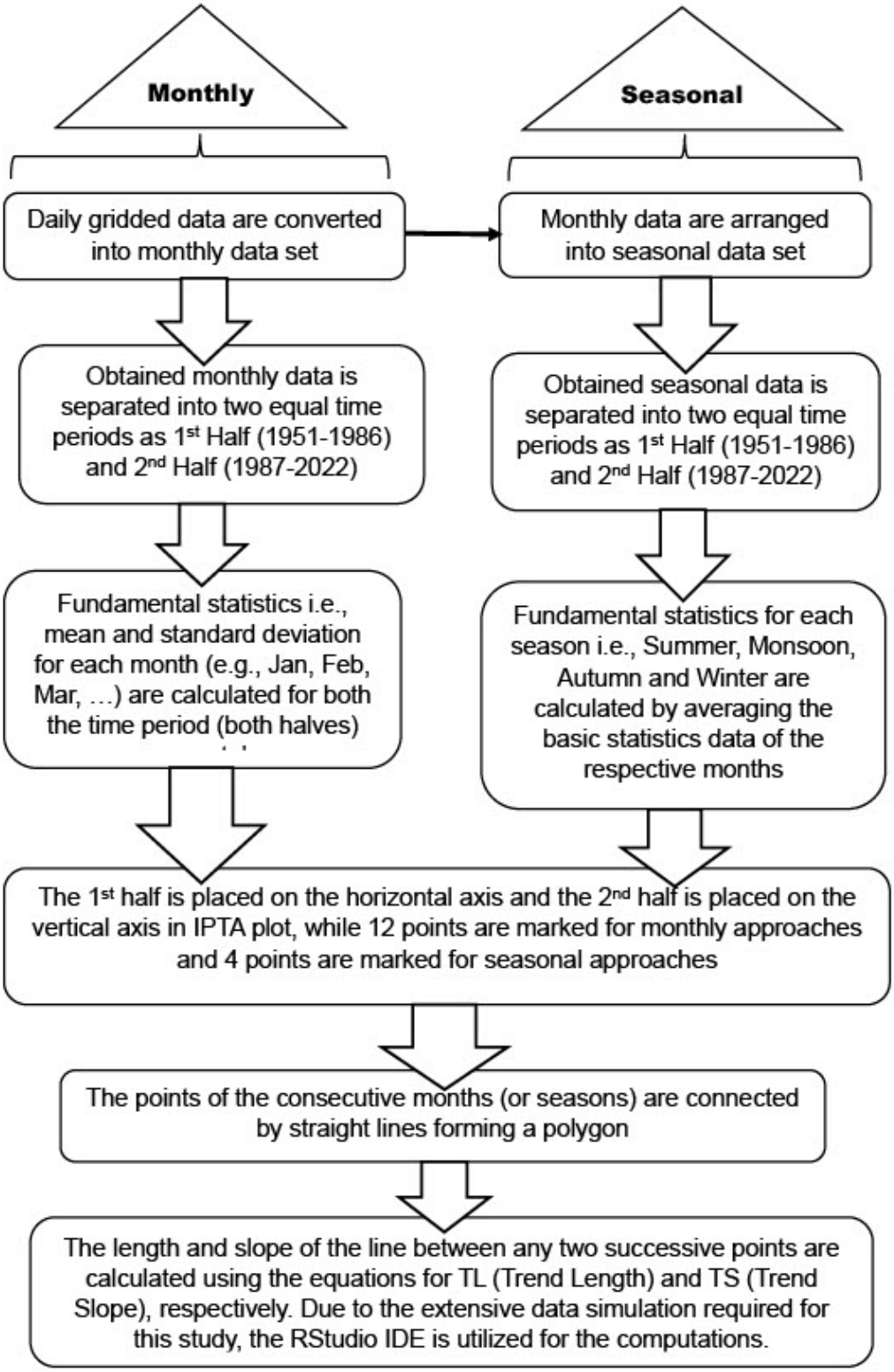


Fig. 5.4 Flowchart illustrating the IPTA applied for the present study

Chapter 6

RESULTS AND DISCUSSION

The outcomes of this study reveal mainly the trend in terms of its length and slope from the monthly (or seasonal) mean and standard deviations (std). Finer resolution is expected to produce better results in trend analyzes. That is why this study compares the variability of gridded minimum temperature (T_{min}) trends in between one degree and 0.5 degrees resolution, primarily in decadal analysis. Furthermore, monthly and seasonal spatiotemporal analyzes have been conducted for the 56 grids in West Bengal (WB), India. ArcGIS has been used to create all types of spatiotemporal maps as well as the interpolation plot. The following results are accomplished one by one applying the methodology discussed in Chapter 5.

6.1 Performance of Inverse Distance Weighted (IDW)

Using a 1° × 1° resolution, there are 21 known grids (KG) that have been interpolated using IDW to obtain 0.5° × 0.5° resolutions for unknown grids across WB. Within the IMD dataset at 1° resolution, this interpolation process results in 35 unknown grids (UG) spanning WB. Over a long period of 72 years, numerous datasets are formed across different decades. We select grid UG30 to illustrate detailed calculations and results, serving as a representative example.

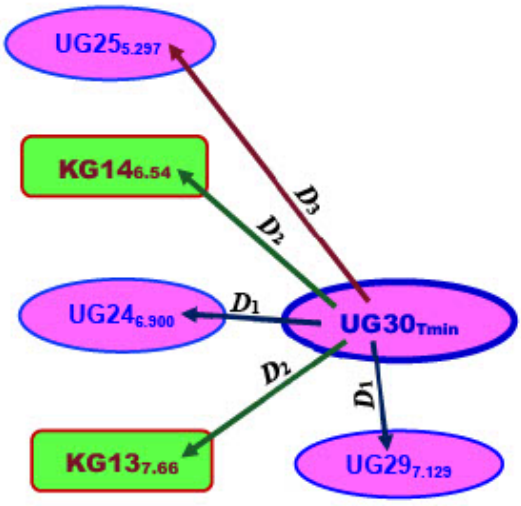


Fig. 6.1 T_{min} calculation format of UG30

where, $D_1 = 0.5$, $D_2 = \sqrt{0.5^2 + 0.5^2} = 0.707$, $D_3 = \sqrt{0.5^2 + 1^2} = 1.118$.

The T_{min} values for UG30 are computed using Eq. 5.1, with radial distances determined as described in the previous section.

$$\text{Now, } T_{min(UG30)} = \frac{\left(\frac{T_{min(UG25)}}{D_3}\right)+\left(\frac{T_{min(KG14)}}{D_2}\right)+\left(\frac{T_{min(UG24)}}{D_1}\right)+\left(\frac{T_{min(KG13)}}{D_2}\right)+\left(\frac{T_{min(UG29)}}{D_1}\right)}{\left(\frac{1}{D_3}\right)+\left(\frac{1}{D_2}\right)+\left(\frac{1}{D_1}\right)+\left(\frac{1}{D_2}\right)+\left(\frac{1}{D_1}\right)}$$

$$= \frac{\left(\frac{5.297}{1.118}\right)+\left(\frac{6.54}{0.707}\right)+\left(\frac{6.900}{0.5}\right)+\left(\frac{7.66}{0.707}\right)+\left(\frac{7.129}{0.5}\right)}{\left(\frac{1}{1.118}\right)+\left(\frac{1}{0.707}\right)+\left(\frac{1}{0.5}\right)+\left(\frac{1}{0.707}\right)+\left(\frac{1}{0.5}\right)} = 6.847\,^{\circ}C$$

where, $T_{min(UG30)}$, $T_{min(UG25)}$, $T_{min(KG14)}$, $T_{min(UG24)}$, $T_{min(KG13)}$, and $T_{min(UG29)}$ represents the minimum temperature of UG30, UG25, KG14, UG24, KG13 and UG25 respectively.

6.2 Special observation in historical data

The selection of boundary grids for different divisional zones is based on specific observations in historical data. Grids were selected based on the date 05/01/1955, when the T_{min} was the lowest among all grid points in WB during the study period (1951-2022). These selections are presented in Table 6.1, including their district-wise positions.

Table 6.1 Interpolated data of selective 8 representative boundary grids for 5th January 1955

Zones	Selected Grids	T_{min} (°C)	District/ State wise positions
South zone	UG2	2.24	Purulia north-west end (Jharkhand state border)
	UG4	6.28	Jhargram west end (Odisha state border)
	UG15	5.19	Purva Bardhhaman south east end (Border of Hooghly mid-north)
	UG30	6.85	South 24 Parganas
Mid and North zones	UG17	3.86	Junction of Birbhum east, Murshidabad south and Purva Bardhhaman north end
	UG20	4.66	Junction of Malda north, Uttar Dinajpur south and Dakshin Dinajpur west end
	UG28	3.76	Mid-west of Kalimpong
	UG34	4.80	Cooch Bihar south east end

6.3 Decade wise spatial analysis

The comparison of T_{min} data resolution between 1° × 1° and 0.5° × 0.5° over WB was represented by seven different decade-wise plots. Establishing the decade-wise mean was the primary task. Due to the vast dataset spanning a long period, pivot table creation in Excel was applied for efficient and accurate determination of decade-wise means. Initially, the daily dataset from the IMD was converted into yearly datasets. From these yearly datasets, decade-wise T_{min} datasets were formed.

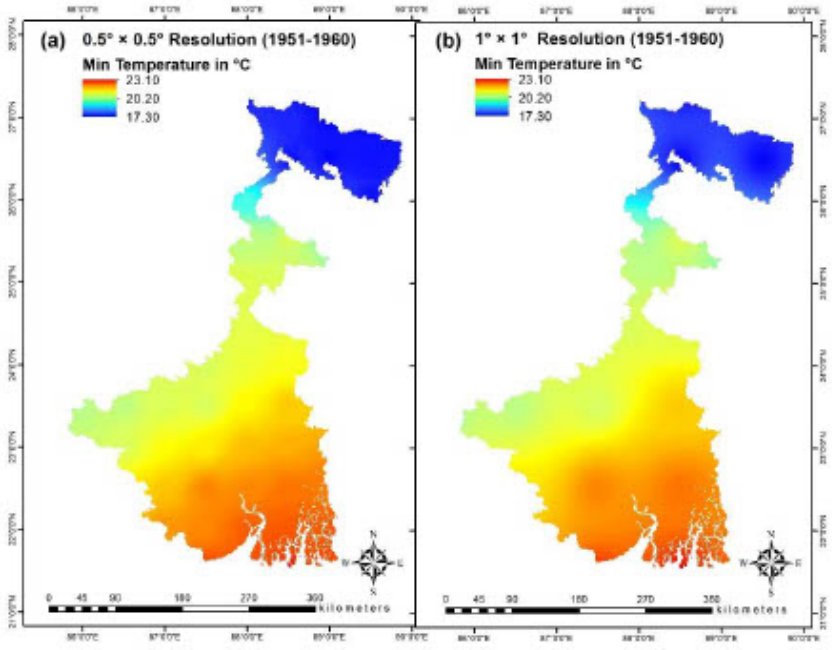


Fig. 6.2 Spatial representation of minimum temperature over West Bengal for Decadal mean of 1951-1960 (a) 0.5° resolution and (b) 1° resolution

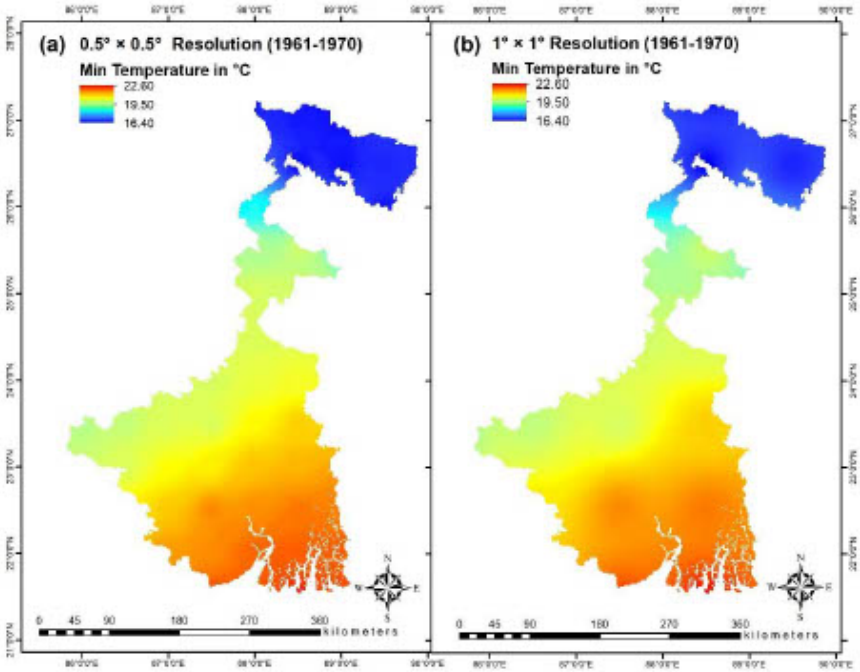


Fig. 6.3 Spatial representation of minimum temperature over West Bengal for Decadal mean of 1961-1970 (a) 0.5° resolution and (b) 1° resolution

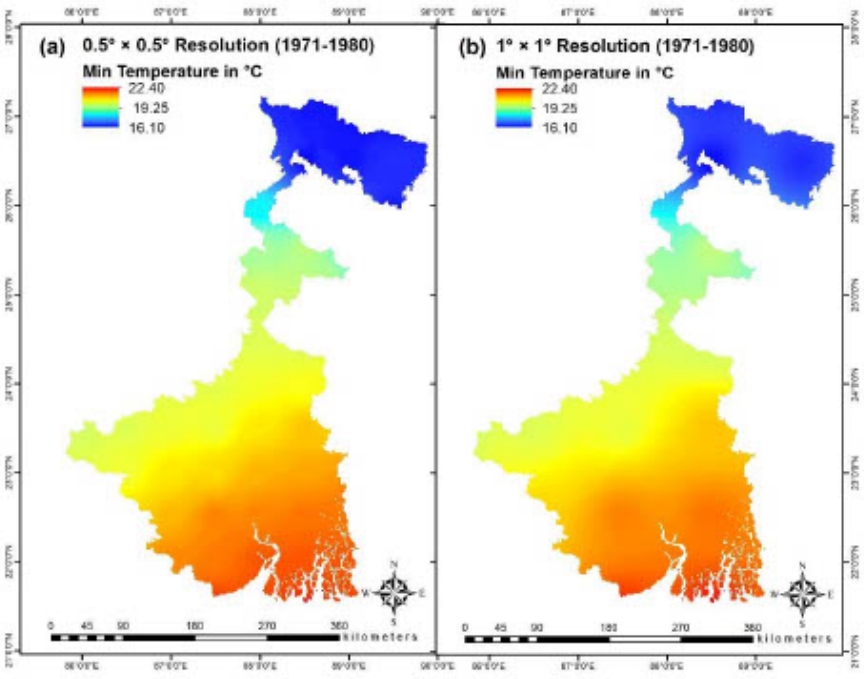


Fig. 6.4 Spatial representation of minimum temperature over West Bengal for Decadal mean of 1971-1980 (a) 0.5° resolution and (b) 1° resolution

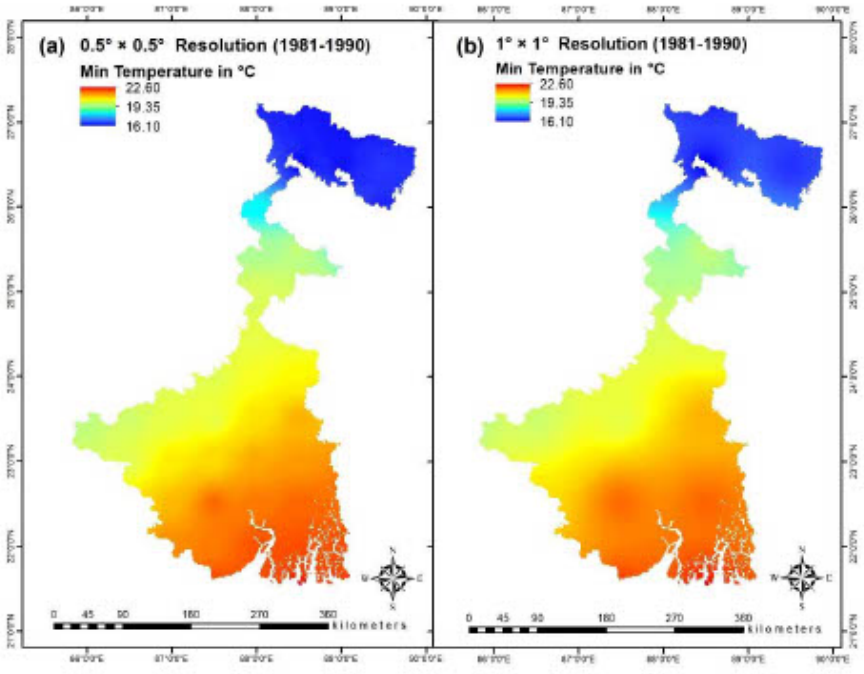


Fig. 6.5 Spatial representation of minimum temperature over West Bengal for Decadal mean of 1981-1990 (a) 0.5° resolution and (b) 1° resolution

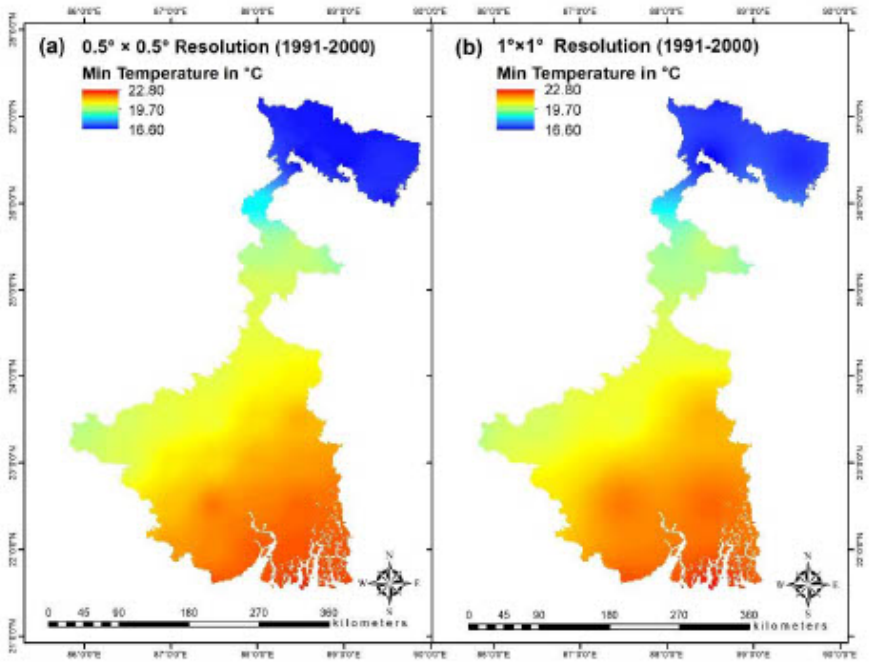


Fig. 6.6 Spatial representation of minimum temperature over West Bengal for Decadal mean of 1991-2000 (a) 0.5° resolution and (b) 1° resolution

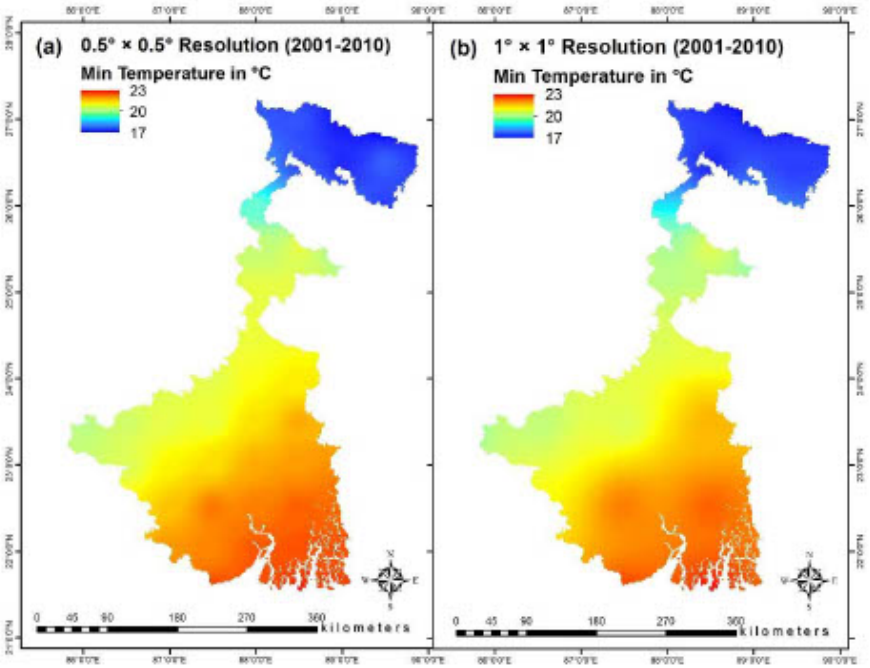


Fig. 6.7 Spatial representation of minimum temperature over West Bengal for Decadal mean of 2001-2010 (a) 0.5° resolution and (b) 1° resolution

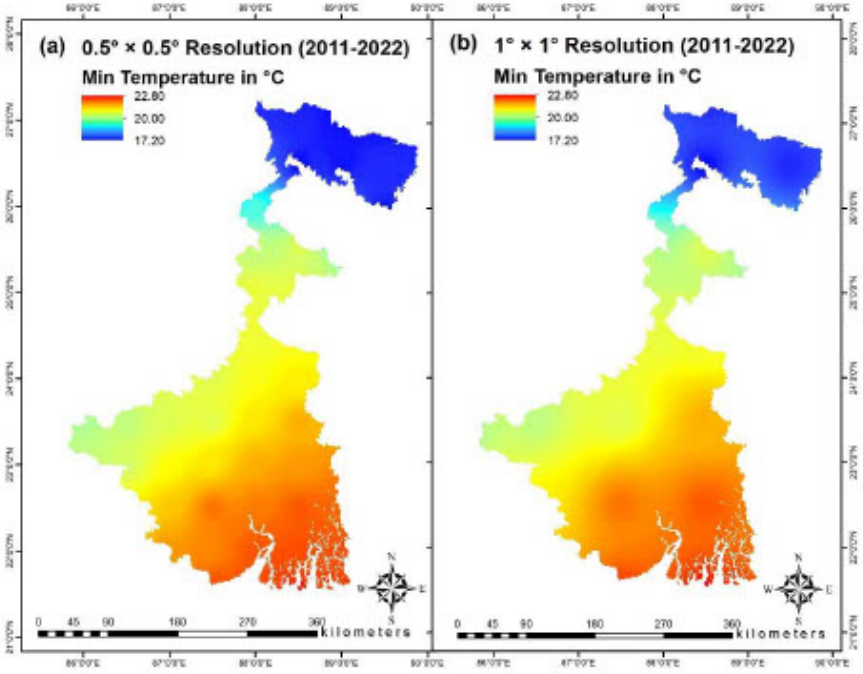


Fig. 6.8 Spatial representation of minimum temperature over West Bengal for Decadal mean of 2011-2022 (a) 0.5° resolution and (b) 1° resolution

Figures 6.2-6.8 show the decade-by-decade mean T_{min} comparison for the two different data resolutions from 1951 to 2022. At a glance, it is difficult to distinguish between these comparisons of decadal mean T_{min}, but the fact is that 0.5° resolution T_{min} data provides more detailed and precise representations than 1° resolution mean T_{min} data. The mean decadal T_{min} in WB demonstrates a gradual decline from the South Bengal to the North Bengal.

The visualization clearly shows that the decadal T_{min} in North Bengal is approximately 17 °C, while the southwest region of WB has a decadal T_{min} of about 23 °C. The middle region of the state has an average decadal T_{min} of around 20 °C. The data reveal a steady decrease in mean T_{min} from the first decade (1951-60) to the third decade (1971-80) across the state. Subsequently, the temperature shows a consistent increase from the third to the sixth decade (2001-10). Finally, in the decade of 2011-22, there has been a slight increase in mean T_{min}, particularly in the northern part of WB.

As a result of each decade-wise comparison (Figs. 6.2-6.8), the most noticeable changes have occurred between the mid-west zone and the southwest zone of West Bengal. This indicates that T_{min} fluctuations consistently ranged between 0.5° and 1° each decade. However, the most accurate comparisons are observed between Figures 6.6(a) and 6.6(b), Figures 6.7(a) and 6.7(b), and Figures 6.8(a) and 6.8(b). It demonstrates that Fig 6.6(a), Fig 6.7(a) and Fig 6.8(a) contain five contours each. On the other side, at 1 degree resolution, three contours are created in the comparison figures [Figs 6.6 (b), 6.7 (b) and 6.8 (b)]. These contours represent the changes in temperature within the state. In the comparative analysis,

notable similarities are observed between the first decade (1951–60) and the second decade (1961–70) as shown in Fig. 6.2 and Fig. 6.3, respectively, as well as between the third decade (1971–80) and the fourth decade (1981–90) as shown in Fig. 6.4 and Fig. 6.5, respectively.

6.4 Division wise location details of all (56) grids of WB

Understanding the location of each grid is crucial before conducting any trend analysis. This knowledge helps in recognizing the significance of nearby towns and villages as landmarks or understanding the rationale behind the selection of certain grids. Table 6.2 provides a comprehensive list of division-wise addresses for all gr62ids. Out of the 56 grids, 20 are situated outside the boundary of West Bengal. These grids are located within neighboring states or countries. Consequently, while West Bengal was the primary focus of this thesis, it became necessary to include data from these neighbouring regions as well.

Table 6.2 Division wise location details of 56 grids

Divisions	Grids	Location Details		
		Villages/Cities	Districts	States (Country)
Medinipur Division	KG1	Buruduya village (Goil Kera Subdivision)	Pashchimi Singhbhum	Jharkhand (India)
	KG2	Jhiri village (Ormanjhi Block)	Ranchi	Jharkhand (India)
	KG3	Mahisasuri village (Sharata tehsil)	Mayurbhanj	Odisha (India)
	KG4	Gohala village under Potka	Purbi Singhbhum	Jharkhand (India)
	KG5	Birkicha village (Para Subdivision)	Purulia	WB (India)
	KG7	Bay of Bengal - south of Digha (SW of Purba Medinipur district, WB, India)		
	KG8	Shata Chak village (Keshpur Subdivision)	Paschim Medinipur	WB (India)
	UG1	Dimuidh village (Chandil Subdivision)	Saraikela Kharsawan	Jharkhand (India)
	UG2	Jogidih village (Pathargama Subdivision)	Godda	Jharkhand (India)
	UG3	Hatnadih village (Barabazar Subdivision)	Purulia	WB (India)
	UG4	Mahulkundia village (Suliapada tehsil)	Mayurbhanj	Odisha (India)
	UG5	Dahijuri village (Binpur I Subdivision)	Paschim Medinipur	WB (India)
	UG6	Kuldiha village (Debra Subdivision)	Paschim Medinipur	WB (India)

	UG7	Patdoha village (Saltora Subdivision)	Bankura	WB (India)
	UG9	Nankar Kadamgerya village (Potashpur I Subdivision)	Purba Medinipur	WB (India)
	UG10	Ashurali village (Jaypur Block)	Bankura	WB (India)
	UG13	Nandigram (Haldia Subdivision)	Purba Medinipur	WB (India)
Presidency Division	KG13	Bay of Bengal (South of Bulcherry Island, South 24 Parganas district, WB, India)		
	KG14	Bhangar I town (Baruipur Subdivision)	South 24 Parganas	WB (India)
	KG15	Dhubulia village (Krishnanagar Sadar Subdivision)	Nadia	WB (India)
	UG12	Bay of Bengal (SW of Sagar Island, South 24 Parganas district, WB, India)		
	UG14	Uluberia city	Howrah	WB (India)
	UG24	Jaynagar II town (Baruipur Subdivision)	South 24 Parganas	WB (India)
	UG25	Madanpur village (Chakdah Subdivision)	Nadia	WB (India)
	UG29	Bay of Bengal (SE of Sundarbans National Park, South 24 Parganas district, WB, India)		
	UG30	Shyamnagar upazila	Satkhira	Khulna division (Bangladesh)
	UG31	Kaliganj upazila	Satkhira	Khulna division (Bangladesh)
Burdwan Division	KG6	Asta village (Dumri Subdivision)	Gumla	Jharkhand (India)
	KG9	Paduma village (Ausgram II tehsil)	Paschim Bardhhaman	WB (India)
	KG10	Madhuban town (Dhanbad Sadar Subdivision)	Dhanbad	Jharkhand (India)
	UG8	Semuldubi village (Fatehpur Block)	Jamtara	Jharkhand (India)
	UG11	Raspur village (Mohammad Bazar Subdivision)	Birbhum	WB (India)
	UG15	Jaragram village (Jamalpur Block)	Purba Bardhhaman	WB (India)
	UG16	Nigan/Negun village (Mangolkote Block)	Purba Bardhhaman	WB (India)

Malda Division	KG11	Sukhasan village (Singheshwar Subdivision)	Madhepura	Bihar (India)
	KG16	Nundapur village	Rajshahi	Rajshahi division (Bangladesh)
	KG17	Lohaganja village (Kushmundi Block)	Dakshin Dinajpur	WB (India)
	UG17	Khargram village (Kandi Subdivision)	Murshidabad	WB (India)
	UG18	Ahiran village (Jangipur Subdivision)	Murshidabad	WB (India)
	UG19	English Bazar city	Malda	WB (India)
	UG20	Chanchal village (Chanchal - I Block)	Malda	WB (India)
	UG21	Saur village (Goalpokhar II Subdivision)	Uttar Dinajpur	WB (India)
	UG26	Garibpur village (Domkal Subdivision)	Murshidabad	WB (India)
	UG27	Porsha town (upazila), NW of Dhaka	Naogaon	Rajshahi division (Bangladesh)
Jalpaiguri Division	KG12	Darbesha village	Morang	Koshi Zone (Nepal)
	KG18	Tetulia Upazila	Panchagarh	Rangpur division (Bangladesh)
	KG19	Barfok village (Mangan Subdivision)	North Sikkkim (Mangan)	Sikkim (India)
	KG20	Chapatali village (Alipurduar-I Block)	Alipurduar	WB (India)
	KG21	Jidekha town	Paro	Paro valley (Bhutan)
	UG22	Jaltha; village	Jhapa	south eastern (Nepal)
	UG23	Pyang village	Ilam	Eastern (Nepal)
	UG28	Singi Khasmahal village (Kalim pong - I Block)	Kalim pong	WB (India)
	UG32	Jnankata Adhikari village (Mekliganj Subdivision)	Cooch Bihar	WB (India)
	UG33	Singyegang village	Samtse Dzongkhag	Tashichhoeling Gewong block (Bhutan)
	UG34	Mogolhat border railway station	Lalmonirhat	Rangpur division (Bangladesh)
	UG35	Gaedu /Gedu town	Chukha	south western (Bhutan)

6.5 Monthly trend analysis

Division-wise monthly trend length (TL) and trend slope (TS) for all 56 grids are presented in the section. Figure 6.9 illustrates the distribution of grids across divisions. Despite being the same as Fig. 4.3 in the study area section, this image is utilized once more to enhance the trend analysis visualization.

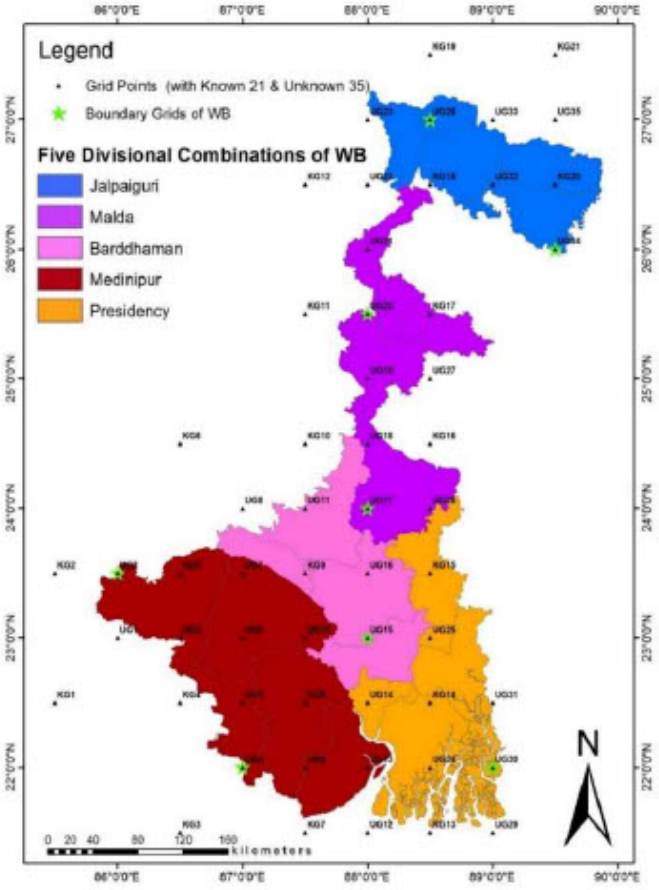


Fig. 6.9 Division wise all grids and highlighted representative 8 boundary grids of WB

The representation of IPTA statistics for mean and std both across all divisions is shown in Tables 6.3-6.12. These tables display the monthly TL (in °C) and TS (unitless) for each grid. The values have been compared across months as well as yearly for a better understanding of trends.

Table 6.3 Representation of trend length (in °C) and trend slope (unitless) for monthly mean across the Medinipur Division

Grids	IPTA Statistics	Jan	Feb	Mar	Apr	May	Jun	Jul	Aug	Sep	Oct	Nov	Dec
KG1	TL	4.119	6.334	6.323	3.083	0.259	1.252	0.309	0.767	4.164	**7.354**	5.781	0.567
	TS	1.242	1.018	0.916	0.908	2.539	0.745	1.200	0.875	1.015	0.937	1.093	**6.041**
KG2	TL	4.120	6.450	6.625	3.243	0.579	1.186	0.278	0.845	4.406	**7.700**	5.929	0.765
	TS	1.289	0.994	0.916	0.909	1.622	0.686	1.045	0.883	1.038	0.944	1.060	**4.681**
KG3	TL	4.468	5.981	4.710	2.051	0.295	0.943	0.079	0.440	3.053	**6.866**	5.722	0.522
	TS	1.185	1.044	0.897	0.863	4.147	0.762	6.315	1.022	1.007	0.933	1.064	**-40.841**
KG4	TL	4.440	6.312	5.697	2.609	0.381	0.890	0.182	0.628	3.771	**7.224**	6.048	0.776
	TS	1.252	1.005	0.936	0.882	2.572	0.728	1.395	0.896	1.018	0.940	1.076	**4.647**
KG5	TL	4.273	6.494	6.325	2.762	0.662	0.824	0.259	0.704	3.972	**7.512**	6.144	1.172
	TS	1.355	0.991	0.918	0.886	1.838	0.621	1.129	0.912	1.022	0.952	1.057	**3.110**
KG7	TL	4.608	6.026	4.218	1.809	0.321	0.748	0.087	0.317	2.649	**6.604**	5.655	0.979
	TS	1.202	1.030	0.901	0.809	**5.285**	0.741	22.253	1.010	0.996	0.934	1.038	3.211
KG8	TL	4.936	6.555	4.869	1.927	0.540	0.649	0.076	0.448	3.046	**7.216**	6.364	1.128
	TS	1.250	1.001	0.920	0.830	1.925	0.665	**41.739**	0.941	0.995	0.936	1.045	3.206
UG1	TL	4.237	6.398	6.243	2.924	0.469	1.037	0.257	0.736	4.078	**7.448**	5.976	0.819
	TS	1.284	1.002	0.921	0.897	1.958	0.699	1.168	0.890	1.024	0.943	1.071	**4.108**
UG2	TL	4.214	6.474	6.397	2.939	0.626	0.969	0.251	0.764	4.121	**7.580**	6.063	0.978
	TS	1.316	0.996	0.915	0.896	1.699	0.657	1.149	0.896	1.026	0.947	1.061	**3.350**
UG3	TL	4.297	6.415	6.147	2.798	0.526	0.927	0.236	0.703	3.975	**7.430**	6.057	0.932
	TS	1.299	0.999	0.922	0.890	1.945	0.678	1.195	0.899	1.023	0.945	1.066	**3.648**
UG4	TL	4.613	6.218	4.873	2.099	0.382	0.807	0.102	0.458	3.130	**6.978**	5.947	0.845
	TS	1.222	1.019	0.915	0.849	2.785	0.728	3.133	0.955	1.005	0.936	1.056	**4.235**
UG5	TL	4.593	6.372	5.337	2.323	0.451	0.810	0.138	0.548	3.441	**7.195**	6.107	0.919
	TS	1.251	1.006	0.924	0.864	2.222	0.703	1.827	0.919	1.010	0.939	1.060	**3.796**
UG6	TL	4.455	6.457	5.748	2.466	0.564	0.788	0.165	0.612	3.615	**7.336**	6.174	1.072
	TS	1.291	0.999	0.921	0.871	1.916	0.671	1.446	0.918	1.012	0.941	1.059	**3.153**

UG7	TL	4.273	6.532	6.137	2.594	0.789	0.709	0.169	0.684	3.757	**7.527**	6.241	1.299
	TS	1.340	0.997	0.911	0.873	1.607	0.609	1.394	0.923	1.009	0.945	1.053	**2.571**
UG9	TL	4.670	6.254	4.776	2.021	0.405	0.770	0.094	0.435	3.039	**6.970**	5.980	0.920
	TS	1.225	1.017	0.913	0.840	2.624	0.718	**4.268**	0.960	1.002	0.936	1.051	3.768
UG10	TL	4.500	6.520	5.629	2.303	0.650	0.696	0.123	0.580	3.435	**7.345**	6.269	1.223
	TS	1.298	0.998	0.916	0.859	1.770	0.650	1.795	0.933	1.003	0.939	1.053	**2.771**
UG13	TL	4.747	6.354	4.559	1.823	0.457	0.667	0.076	0.383	2.769	**6.896**	6.033	1.188
	TS	1.227	1.010	0.911	0.829	2.342	0.699	**-98.690**	0.984	0.995	0.935	1.040	2.642

Note: Bold represents the highest values along the row

Table 6.4 Representation of trend length (in °C) and trend slope (unitless) for monthly standard deviation across the Medinipur Division

Grids	IPTA Statistics	Jan	Feb	Mar	Apr	May	Jun	Jul	Aug	Sep	Oct	Nov	Dec
KG1	TL	0.372	0.225	0.248	0.365	0.334	0.453	0.014	0.065	0.504	**0.740**	0.347	0.149
	TS	0.607	-1.120	-2.098	-1.623	-0.347	1.344	0.109	-3.602	0.857	0.642	0.875	**-3.234**
KG2	TL	0.290	0.114	0.142	0.247	0.298	0.447	0.053	0.055	0.586	**0.595**	0.427	0.260
	TS	1.302	0.087	-0.383	-1.756	-0.292	1.369	0.895	0.730	0.929	0.610	1.019	**-13.147**
KG3	TL	0.344	0.238	0.292	0.388	0.269	0.288	0.043	0.046	0.345	**0.715**	0.249	0.162
	TS	0.094	-5.342	-2.209	-2.415	0.009	1.221	-0.352	-1.087	0.712	0.655	1.639	**3.505**
KG4	TL	0.263	0.096	0.232	0.358	0.362	0.295	0.046	0.062	0.404	**0.670**	0.360	0.244
	TS	0.472	-1.293	-2.003	-1.656	0.238	0.953	2.146	-4.265	0.854	0.647	1.842	**-166.957**
KG5	TL	0.181	0.091	0.203	0.358	0.300	0.305	0.096	0.056	0.506	**0.526**	0.406	0.347
	TS	1.767	-0.590	-0.808	-2.085	0.045	1.093	1.247	0.914	0.972	0.786	1.691	**-11.062**
KG7	TL	0.195	0.096	0.242	0.357	0.252	0.255	0.032	0.074	0.314	**0.683**	0.337	0.310
	TS	0.404	-1.128	-0.735	-3.122	0.400	1.018	1.299	-1.684	0.831	0.673	2.546	**-24.607**
KG8	TL	0.164	0.089	0.266	0.405	0.296	0.237	0.066	0.095	0.337	**0.675**	0.330	0.253
	TS	0.637	-0.300	-0.692	-2.384	0.344	0.827	3.410	-2.191	1.228	0.644	3.272	**-5.249**
UG1	TL	0.280	0.125	0.201	0.334	0.320	0.380	0.057	0.064	0.509	**0.627**	0.387	0.258
	TS	0.886	-0.537	-1.189	-1.761	-0.095	1.283	1.325	7.344	0.892	0.640	1.241	**-10.924**

UG2	TL	0.251	0.107	0.170	0.313	0.314	0.353	0.077	0.061	0.530	**0.543**	0.390	0.303
	TS	1.546	-0.095	-0.629	-1.859	-0.126	1.250	1.251	1.390	0.941	0.674	1.351	**-8.990**
UG3	TL	0.239	0.104	0.202	0.344	0.324	0.333	0.071	0.060	0.487	**0.594**	0.387	0.286
	TS	0.956	-0.493	-1.124	-1.819	0.029	1.172	1.378	3.654	0.912	0.675	1.493	**-12.482**
UG4	TL	0.247	0.123	0.257	0.380	0.297	0.268	0.044	0.078	0.349	**0.693**	0.324	0.245
	TS	0.341	-1.454	-1.232	-2.336	0.233	1.067	1.325	-2.159	0.892	0.648	2.230	**-100.718**
UG5	TL	0.229	0.102	0.242	0.373	0.319	0.280	0.057	0.077	0.385	**0.670**	0.349	0.255
	TS	0.526	-0.820	-1.159	-2.038	0.221	1.024	1.941	-3.300	0.954	0.648	2.088	**-14.469**
UG6	TL	0.208	0.099	0.226	0.377	0.324	0.277	0.075	0.061	0.431	**0.602**	0.366	0.286
	TS	0.816	-0.446	-0.998	-2.010	0.138	1.077	1.620	**-77.974**	0.995	0.686	2.044	-9.890
UG7	TL	0.199	0.093	0.197	0.374	0.327	0.248	0.084	0.040	0.462	**0.483**	0.354	0.329
	TS	2.060	0.033	-0.702	-2.027	0.031	1.043	1.471	1.642	1.022	0.749	2.228	**-6.478**
UG9	TL	0.224	0.111	0.256	0.383	0.288	0.261	0.048	0.082	0.343	**0.688**	0.328	0.257
	TS	0.394	-1.112	-1.017	-2.461	0.264	1.041	1.582	-2.242	0.942	0.650	2.416	**-20.751**
UG10	TL	0.188	0.099	0.232	0.395	0.320	0.244	0.080	0.056	0.414	**0.574**	0.352	0.293
	TS	0.983	-0.203	-0.815	-2.157	0.139	1.034	1.643	**-11.501**	1.076	0.703	2.585	-6.935
UG13	TL	0.178	0.079	0.242	0.412	0.280	0.242	0.054	0.087	0.325	**0.662**	0.327	0.281
	TS	0.425	-0.775	-0.778	-2.654	0.250	1.063	2.298	-2.141	1.075	0.666	3.358	**-7.545**

Note: Bold represents the highest values along the row

Table 6.5 Representation of trend length (in °C) and trend slope (unitless) for monthly mean across the Presidency Division

Grids	IPTA Statistics	Jan	Feb	Mar	Apr	May	Jun	Jul	Aug	Sep	Oct	Nov	Dec
KG13	TL	4.733	6.379	4.241	1.644	0.463	0.630	0.064	0.324	2.436	**6.652**	5.961	1.443
	TS	1.209	1.006	0.917	0.813	2.407	0.704	**-12.827**	0.979	1.000	0.938	1.028	2.100
KG14	TL	4.850	6.655	4.720	1.663	0.616	0.486	0.067	0.394	2.640	**7.103**	6.314	1.601
	TS	1.257	0.992	0.904	0.854	1.763	0.621	-1.568	1.057	0.980	0.927	1.035	**2.103**
KG15	TL	4.497	6.702	5.450	1.977	0.860	0.414	0.063	0.521	2.882	**7.275**	6.665	1.831

UG12	TS	1.322	0.997	0.897	0.873	1.422	0.481	-0.005	0.981	0.977	0.935	1.032	**2.049**
	TL	4.726	6.312	4.477	1.801	0.438	0.674	0.076	0.368	2.714	**6.827**	5.973	1.188
UG14	TS	1.222	1.012	0.911	0.825	2.497	0.706	**-240.235**	0.986	0.996	0.935	1.038	2.600
	TL	4.761	6.478	4.872	1.919	0.534	0.643	0.079	0.440	2.952	**7.099**	6.201	1.228
UG24	TS	1.250	1.003	0.913	0.842	1.983	0.673	15.511	0.973	0.995	0.934	1.044	**2.666**
	TL	4.766	6.441	4.561	1.758	4.201	3.113	1.125	0.352	2.685	**6.909**	6.098	1.345
UG25	TS	1.233	1.004	0.911	0.832	**-19.578**	-6.051	129.430	0.853	0.993	0.934	1.036	2.337
	TL	4.634	6.614	5.195	1.945	0.703	0.527	0.055	0.485	2.945	**7.220**	6.401	1.542
UG29	TS	1.287	0.997	0.905	0.857	1.629	0.599	**-3.015**	0.985	0.987	0.933	1.039	2.234
	TL	4.764	6.439	4.465	1.709	0.499	0.607	0.067	0.361	2.596	**6.841**	6.071	1.399
UG30	TS	1.227	1.003	0.912	0.828	2.158	0.686	**-6.246**	1.000	0.994	0.934	1.034	2.228
	TL	4.760	6.488	4.580	1.728	0.538	0.582	0.065	0.379	2.638	**6.916**	6.141	1.447
UG31	TS	1.237	1.001	0.910	0.835	1.998	0.669	**-4.355**	1.004	0.991	0.933	1.034	2.203
	TL	4.730	6.571	4.826	1.785	0.618	0.533	0.059	0.419	2.732	**7.060**	6.286	1.530
	TS	1.259	0.998	0.906	0.848	1.764	0.630	-2.120	1.008	0.986	0.932	1.036	**2.179**

Note: Bold represents the highest values along the row

Table 6.6 Representation of trend length (in °C) and trend slope (unitless) for monthly standard deviation across the Presidency Division

Grids	IPTA Statistics	Jan	Feb	Mar	Apr	May	Jun	Jul	Aug	Sep	Oct	Nov	Dec
KG13	TL	0.152	0.073	0.211	0.442	0.250	0.255	0.044	0.095	0.312	**0.673**	0.330	0.302
	TS	0.165	-2.073	-0.691	-2.732	0.186	1.115	3.518	-1.544	1.133	0.668	3.765	**-4.718**
KG14	TL	0.142	0.064	0.218	0.459	0.311	0.199	0.063	0.078	0.309	**0.564**	0.307	0.285
	TS	0.647	0.289	-0.661	-2.696	0.103	1.311	3.254	-2.400	1.315	0.716	**11.705**	-4.539
KG15	TL	0.176	0.074	0.198	**0.450**	0.346	0.117	0.080	0.035	0.376	0.421	0.265	0.312
	TS	1.876	0.340	-0.637	-2.505	0.112	1.135	1.793	63.949	1.337	0.816	**-300.785**	-3.864
UG12	TL	0.178	0.080	0.238	0.409	0.273	0.246	0.050	0.086	0.322	**0.668**	0.329	0.287
	TS	0.393	-0.928	-0.769	-2.709	0.260	1.068	2.198	-2.020	1.047	0.666	3.258	**-7.742**
UG14	TL	0.176	0.081	0.244	0.418	0.299	0.235	0.067	0.084	0.344	**0.636**	0.327	0.273

UG24	TS	0.572	-0.377	-0.771	-2.475	0.210	1.047	2.377	-2.667	1.147	0.672	3.555	**-6.500**
	TL	0.162	0.066	0.231	0.433	0.386	0.208	0.406	0.206	0.323	**0.640**	0.323	0.285
UG25	TS	0.426	-0.616	-0.738	-2.657	-0.964	-0.882	**19.898**	5.479	1.159	0.677	4.228	-5.744
	TL	0.164	0.080	0.222	0.442	0.324	0.186	0.081	0.061	0.365	**0.527**	0.308	0.296
UG29	TS	1.036	0.113	-0.690	-2.456	0.122	1.153	1.966	**-4.886**	1.264	0.734	6.362	-4.786
	TL	0.156	0.063	0.225	0.440	0.276	0.238	0.053	0.089	0.319	**0.644**	0.323	0.289
UG30	TS	0.356	-0.822	-0.724	-2.691	0.181	1.146	2.752	-1.935	1.170	0.677	4.390	**-5.259**
	TL	0.154	0.060	0.225	0.445	0.287	0.229	0.058	0.085	0.325	**0.621**	0.320	0.289
UG31	TS	0.452	-0.490	-0.718	-2.659	0.159	1.180	2.574	-2.166	1.212	0.688	**5.043**	-5.036
	TL	0.154	0.065	0.223	0.451	0.309	0.203	0.069	0.075	0.337	**0.569**	0.310	0.290
	TS	0.708	-0.031	-0.703	-2.604	0.132	1.226	2.291	-2.888	1.274	0.713	**6.981**	-4.753

Note: Bold represents the highest values along the row

Table 6.7 Representation of trend length (in °C) and trend slope (unitless) for monthly mean across the Burdwan Division

Grids	IPTA Statistics	Jan	Feb	Mar	Apr	May	Jun	Jul	Aug	Sep	Oct	Nov	Dec
KG6	TL	4.243	6.662	6.383	2.681	1.030	0.661	0.159	0.807	3.914	**7.753**	6.393	1.360
	TS	1.360	1.003	0.893	0.875	1.459	0.502	1.706	0.985	1.011	0.952	1.054	**2.195**
KG9	TL	4.207	6.644	6.115	2.297	0.894	0.561	0.095	0.630	3.411	**7.461**	6.402	1.642
	TS	1.373	0.991	0.907	0.854	1.585	0.590	1.527	0.960	0.992	0.936	1.050	**2.218**
KG10	TL	4.005	6.601	6.368	2.748	1.561	0.328	0.074	0.801	3.860	**8.060**	6.406	1.837
	TS	1.399	1.012	0.881	0.849	1.266	0.247	**-3.794**	0.940	0.981	0.950	1.026	1.904
UG8	TL	4.206	6.581	6.257	2.616	0.966	0.621	0.148	0.717	3.781	**7.653**	6.308	1.454
	TS	1.363	0.998	0.903	0.869	1.476	0.550	1.594	0.928	1.004	0.947	1.047	**2.319**
UG11	TL	4.173	6.600	6.244	2.575	1.065	0.553	0.117	0.717	3.721	**7.694**	6.350	1.558
	TS	1.369	1.000	0.899	0.863	1.425	0.519	2.001	0.935	0.997	0.945	1.044	**2.188**
UG15	TL	4.625	6.581	5.273	2.026	0.670	0.586	0.070	0.503	3.077	**7.246**	6.353	1.414
	TS	1.286	0.997	0.910	0.852	1.704	0.627	**10.207**	0.967	0.992	0.935	1.044	2.411
UG16	TL	4.408	6.616	5.716	2.209	0.823	0.553	0.070	0.583	3.269	**7.389**	6.421	1.552

	TS	1.327	0.996	0.906	0.860	1.551	0.580	3.985	0.956	0.992	0.938	1.044	**2.260**

Note: Bold represents the highest values along the row

Table 6.8 Representation of trend length (in °C) and trend slope (unitless) for monthly standard deviation across the Burdwan Division

Grids	IPTA Statistics	Jan	Feb	Mar	Apr	May	Jun	Jul	Aug	Sep	Oct	Nov	Dec
KG6	TL	0.324	0.139	0.160	0.327	0.354	0.231	0.094	0.137	**0.457**	0.308	0.278	0.361
	TS	**-8.900**	1.196	0.187	-1.730	-0.043	0.989	1.342	1.483	1.115	0.974	3.733	-3.959
KG9	TL	0.175	0.108	0.208	0.409	0.329	0.172	0.088	0.011	**0.429**	0.428	0.348	0.343
	TS	2.414	0.230	-0.639	-2.235	0.021	1.050	**1.339**	0.074	1.114	0.844	3.482	-5.765
KG10	TL	0.257	0.102	0.155	0.372	0.311	0.165	0.042	0.013	**0.392**	0.256	0.231	0.365
	TS	-3.089	3.138	-0.256	-2.196	0.078	0.369	**24.732**	-0.438	1.076	0.855	9.332	-3.688
UG8	TL	0.213	0.092	0.181	0.368	0.330	0.217	0.079	0.035	**0.455**	0.403	0.324	0.350
	TS	**6.635**	0.410	-0.483	-2.013	0.000	0.919	1.500	0.658	1.045	0.798	2.698	-5.139
UG11	TL	0.215	0.096	0.181	0.376	0.331	0.194	0.073	0.025	**0.440**	0.375	0.308	0.351
	TS	**12.722**	0.624	-0.449	-2.048	0.011	0.833	1.668	0.512	1.063	0.812	3.317	-4.664
UG15	TL	0.168	0.087	0.232	0.428	0.318	0.208	0.081	0.063	0.376	**0.558**	0.325	0.292
	TS	0.944	-0.044	-0.718	-2.375	0.144	1.074	1.868	-4.798	1.208	0.717	4.198	**-5.382**
UG16	TL	0.177	0.093	0.212	**0.418**	0.331	0.182	0.086	0.035	0.408	0.472	0.320	0.319
	TS	1.730	0.182	-0.653	-2.269	0.084	1.042	1.621	9.921	1.175	0.771	4.276	**-5.067**

Note: Bold represents the highest values along the row

Table 6.9 Representation of trend length (in °C) and trend slope (unitless) for monthly mean across the Malda Division

Grids	IPTA Statistics	Jan	Feb	Mar	Apr	May	Jun	Jul	Aug	Sep	Oct	Nov	Dec
KG11	TL	3.675	6.222	6.349	3.031	2.072	0.316	0.155	0.924	3.959	**8.251**	6.639	1.985
	TS	1.329	1.036	0.915	0.948	1.184	3.312	0.410	1.178	1.008	0.984	1.036	**1.490**
KG16	TL	3.925	6.403	6.148	2.551	1.592	0.122	0.136	0.719	3.480	**7.905**	6.566	2.069
	TS	1.348	1.017	0.901	0.917	1.241	-0.940	0.382	1.098	1.000	0.963	1.021	**1.634**

KG17	TL	3.526	6.174	6.288	3.058	2.224	0.507	0.247	1.020	4.074	**8.210**	6.584	2.096
	TS	1.318	1.040	0.914	0.964	1.151	**1.600**	0.585	1.107	1.017	0.988	1.033	1.377
UG17	TL	4.213	6.596	6.004	2.392	1.109	0.425	0.051	0.660	3.444	**7.620**	6.458	1.723
	TS	1.354	1.002	0.899	0.868	1.384	0.460	**-5.832**	0.973	0.991	0.944	1.037	2.022
UG18	TL	4.029	6.511	6.204	2.615	1.429	0.270	0.053	0.746	3.655	**7.875**	6.473	1.831
	TS	1.364	1.011	0.897	0.883	1.285	0.197	-0.663	1.011	0.993	0.955	1.032	**1.828**
UG19	TL	3.847	6.392	6.266	2.786	1.749	0.145	0.107	0.834	3.794	**8.046**	6.529	1.951
	TS	1.353	1.022	0.901	0.911	1.220	-1.575	0.212	1.065	1.000	0.967	1.030	**1.633**
UG20	TL	3.644	6.222	6.218	2.949	1.997	0.275	0.148	0.919	3.941	**8.064**	6.471	1.996
	TS	1.344	1.031	0.907	0.932	1.184	3.612	0.362	1.102	1.004	0.976	1.034	**1.508**
UG21	TL	3.373	5.954	5.988	3.017	2.190	0.462	0.188	0.997	3.995	**7.844**	6.227	2.062
	TS	1.332	1.035	0.912	0.953	1.161	**1.750**	0.436	1.127	1.006	0.983	1.035	1.394
UG26	TL	4.214	6.566	5.897	2.340	1.167	0.332	0.052	0.643	3.331	**7.610**	6.526	1.814
	TS	1.342	1.004	0.900	0.882	1.341	0.369	-0.325	1.009	0.991	0.947	1.032	**1.911**
UG27	TL	3.789	6.337	6.227	2.793	1.809	0.178	0.139	0.849	3.788	**8.027**	6.532	1.997
	TS	1.345	1.024	0.904	0.924	1.206	**-23.443**	0.367	1.081	1.004	0.970	1.029	1.571

Note: Bold represents the highest values along the row

Table 6.10 Representation of trend length (in °C) and trend slope (unitless) for monthly standard deviation across the Malda Division

Grids	IPTA Statistics	Jan	Feb	Mar	Apr	May	Jun	Jul	Aug	Sep	Oct	Nov	Dec
KG11	TL	0.194	0.114	0.099	0.303	**0.367**	0.083	0.026	0.057	0.345	0.082	0.235	0.155
	TS	-0.368	-0.705	0.348	**-5.865**	-0.118	-0.004	5.577	-0.361	1.004	2.830	-0.821	-0.999
KG16	TL	0.177	0.112	0.118	**0.369**	0.380	0.008	0.052	0.023	0.329	0.219	0.280	0.343
	TS	-2.013	-0.870	-0.222	-3.662	0.131	**-5.861**	-4.838	0.578	1.278	1.043	-1.568	-2.355
KG17	TL	0.222	0.112	0.046	0.325	0.301	0.052	0.053	0.046	**0.304**	0.040	0.169	0.164
	TS	-0.055	-0.439	0.422	9.424	0.002	0.088	**11.414**	-0.331	0.890	7.823	-0.536	-0.954
UG17	TL	0.190	0.080	0.180	0.401	0.342	0.138	0.072	0.019	**0.402**	0.366	0.287	0.342
	TS	7.128	0.865	-0.525	-2.338	0.067	0.885	2.139	2.016	1.146	0.832	**10.292**	-3.932

UG18	TL	0.201	0.078	0.142	0.380	0.350	0.106	0.047	0.017	**0.384**	0.267	0.255	0.336
	TS	-4.517	9.172	-0.350	-2.557	0.043	0.536	4.354	0.261	1.123	0.912	**-7.771**	-3.066
UG19	TL	0.188	0.092	0.102	0.364	0.348	0.082	0.012	0.026	**0.358**	0.171	0.227	0.284
	TS	-1.302	-1.724	-0.166	-3.837	0.004	0.160	**-3.524**	-0.341	1.064	1.085	-2.122	-2.221
UG20	TL	0.189	0.105	0.079	0.339	0.347	0.083	0.018	0.045	**0.347**	0.094	0.199	0.212
	TS	-0.549	-1.009	0.163	-6.187	-0.069	0.042	**19.142**	-0.406	0.928	1.626	-1.245	-1.654
UG21	TL	0.188	0.113	0.067	0.309	**0.355**	0.064	0.032	0.066	0.339	0.040	0.182	0.151
	TS	-0.101	-0.525	0.678	-15.782	-0.084	-0.129	-3.305	-0.312	0.823	**-71.693**	-0.776	-1.307
UG26	TL	0.178	0.066	0.166	0.406	0.355	0.100	0.066	0.023	**0.380**	0.340	0.272	0.334
	TS	9.374	1.650	-0.521	-2.582	0.085	0.963	2.764	3.972	1.197	0.854	**-11.435**	-3.276
UG27	TL	0.179	0.098	0.089	**0.362**	0.348	0.063	0.008	0.028	0.346	0.151	0.221	0.269
	TS	-0.943	-1.128	-0.133	**-5.275**	0.014	0.056	-0.741	-0.299	1.042	1.136	-1.666	-2.013

Note: Bold represents the highest values along the row

Table 6.11 Representation of trend length (in °C) and trend slope (unitless) of monthly mean across the Jalpaiguri Division

Grids	IPTA Statistics	Jan	Feb	Mar	Apr	May	Jun	Jul	Aug	Sep	Oct	Nov	Dec
KG12	TL	3.029	5.574	5.510	3.096	2.312	0.578	0.173	0.989	4.009	**7.368**	5.782	2.072
	TS	1.355	1.039	0.912	0.950	1.144	**1.459**	0.310	1.158	0.996	0.977	1.047	1.332
KG18	TL	2.879	5.467	5.481	2.978	2.426	0.738	0.234	1.165	4.014	**7.237**	5.556	2.192
	TS	**1.309**	1.032	0.916	0.980	1.139	1.302	0.469	1.107	1.008	0.996	1.024	1.257
KG19	TL	2.868	5.464	5.362	2.952	2.412	0.740	0.225	1.134	3.990	**7.150**	5.526	2.197
	TS	**1.280**	1.025	0.929	0.997	1.113	1.194	0.492	1.112	1.000	0.991	1.024	1.249
KG20	TL	2.826	5.413	5.217	2.782	2.488	0.793	0.188	1.069	3.870	**6.908**	5.458	2.380
	TS	**1.258**	1.009	0.931	1.043	1.085	1.113	0.445	1.079	1.000	0.994	1.002	1.258
KG21	TL	2.666	5.245	5.365	2.974	2.540	0.798	0.152	1.169	4.106	**6.976**	5.415	2.046
	TS	1.220	1.005	0.913	1.074	1.076	1.202	0.389	1.063	1.007	0.997	0.996	**1.235**
UG22	TL	3.064	5.639	5.621	3.020	2.323	0.611	0.201	1.061	4.004	**7.440**	5.812	2.120
	TS	1.326	1.034	0.915	0.965	1.143	**1.410**	0.422	1.127	1.003	0.986	1.034	1.314

UG23	TL	2.970	5.546	5.506	3.012	2.364	0.661	0.207	1.085	4.004	**7.312**	5.682	2.143
	TS	1.318	1.033	0.918	0.972	1.136	**1.333**	0.429	1.125	1.002	0.987	1.033	1.289
UG28	TL	2.936	5.520	5.482	2.988	2.386	0.693	0.218	1.115	4.003	**7.272**	5.631	2.166
	TS	**1.307**	1.031	0.920	0.979	1.132	1.294	0.457	1.117	1.003	0.990	1.028	1.274
UG32	TL	2.847	5.435	5.379	2.922	2.448	0.752	0.207	1.125	3.980	**7.110**	5.522	2.221
	TS	**1.280**	1.021	0.922	1.010	1.111	1.216	0.456	1.096	1.004	0.994	1.015	1.257
UG33	TL	2.844	5.430	5.387	2.935	2.446	0.749	0.205	1.129	3.993	**7.119**	5.525	2.200
	TS	**1.278**	1.021	0.922	1.011	1.110	1.220	0.455	1.097	1.004	0.993	1.016	1.256
UG34	TL	2.844	5.431	5.336	2.880	2.459	0.765	0.204	1.111	3.946	**7.056**	5.504	2.273
	TS	**1.276**	1.019	0.924	1.017	1.105	1.188	0.454	1.092	1.003	0.994	1.012	1.257
UG35	TL	2.839	5.398	5.355	2.922	2.430	0.756	0.178	1.112	3.997	**7.063**	5.502	2.183
	TS	1.230	1.015	0.921	1.020	1.142	1.241	0.499	1.123	1.000	0.992	1.005	**1.289**

Note: Bold represents the highest value along the row

Table 6.12 Representation of trend length (in °C) and trend slope (unitless) of monthly standard deviation across the Jalpaiguri Division

Grids	IPTA Statistics	Jan	Feb	Mar	Apr	May	Jun	Jul	Aug	Sep	Oct	Nov	Dec
KG12	TL	0.177	0.139	0.104	0.284	**0.398**	0.063	0.025	0.084	0.362	0.059	0.154	0.099
	TS	0.015	-0.728	1.657	-8.069	-0.166	-0.161	**-15.914**	-0.327	0.635	-0.481	-0.781	-1.980
KG18	TL	0.198	0.121	0.051	0.275	**0.339**	0.046	0.048	0.095	0.321	0.041	0.158	0.100
	TS	0.528	0.145	**26.749**	7.879	-0.021	-1.004	-1.112	0.182	0.778	0.448	-0.430	-1.065
KG19	TL	0.230	0.102	0.131	0.245	0.335	0.071	0.059	0.096	**0.347**	0.058	0.141	0.072
	TS	0.707	-0.188	1.513	**64.852**	0.059	-2.925	-1.499	-0.346	0.697	0.229	-0.388	-0.035
KG20	TL	0.290	0.116	0.062	0.254	**0.323**	0.060	0.086	0.121	0.320	0.022	0.047	0.051
	TS	0.882	1.024	**4.251**	2.202	0.278	0.994	-0.495	-0.096	0.914	-0.163	-0.341	0.072
KG21	TL	0.240	0.141	0.102	0.208	0.302	0.034	0.113	0.101	**0.309**	0.063	0.100	0.030
	TS	1.033	0.586	-0.827	1.646	0.287	**1.869**	-0.620	-0.211	0.837	0.033	-0.169	1.450
UG22	TL	0.187	0.117	0.078	0.285	**0.362**	0.053	0.039	0.086	0.343	0.038	0.159	0.106

UG23	TS	0.225	-0.330	1.549	**-41.545**	-0.075	-0.557	-1.591	-0.273	0.722	-0.232	-0.610	-1.223
	TL	0.193	0.117	0.089	0.274	**0.360**	0.053	0.043	0.092	0.344	0.047	0.151	0.089
UG28	TS	0.363	-0.274	1.795	**-108.454**	-0.057	-0.913	-1.466	-0.277	0.700	0.022	-0.541	-1.021
	TL	0.202	0.113	0.086	0.269	**0.348**	0.054	0.049	0.094	0.339	0.047	0.151	0.085
UG32	TS	0.477	-0.140	1.921	**33.131**	-0.020	-1.291	-1.305	-0.263	0.721	0.168	-0.479	-0.800
	TL	0.234	0.113	0.071	0.254	**0.331**	0.046	0.069	0.107	0.326	0.046	0.115	0.060
UG33	TS	0.719	0.283	7.303	4.609	0.098	**-67.633**	-0.778	-0.205	0.804	0.251	-0.367	-0.446
	TL	0.230	0.114	0.075	0.250	**0.330**	0.048	0.070	0.105	0.327	0.050	0.119	0.058
UG34	TS	0.718	0.226	7.537	5.019	0.094	**-13.339**	-0.812	-0.225	0.787	0.228	-0.359	-0.390
	TL	0.249	0.112	0.066	0.257	**0.329**	0.047	0.072	0.111	0.323	0.037	0.095	0.058
UG35	TS	0.764	0.466	**6.850**	3.526	0.140	3.663	-0.671	-0.167	0.844	0.245	-0.365	-0.370
	TL	0.193	0.113	0.071	0.233	**0.579**	0.053	0.101	0.186	0.227	0.041	0.051	0.154
	TS	1.296	-0.417	**25.775**	14.147	0.085	1.745	-0.506	-0.116	2.065	0.219	-0.746	0.050

Note: Bold represents the highest values along the row

According to the analysis, TL (Trend Length) shows consistent patterns in the monthly mean across all five divisions, with the highest integer values typically occurring from October to November. However, TS (Trend Slope) exhibits more variability across divisions. The variations in the monthly mean TS of T_{min} are described as follows:

- **Medinipur Division**: The maximum TS values for the monthly mean (Table 6.3) are found in July at three grids: KG8 (Shata Chak village), UG9 (Nankar Kadamgerya village), and UG13 (Nandigram, WB). Additionally, KG7 (near Baleshwar district, Odisha) show the highest TS in May, while the remaining 13 grids in this division reach their maximum TS in December.
- **Presidency Division**: While the maximum TL values have already been discussed, the TS for the monthly mean (Table 6.5) reaches its peak in July at grids UG12, KG13, and UG29, which are located along the Bay of Bengal, as well as UG25 (Chakdaha town) and UG30 (Shyamnagar upazila). At UG24 (Jaynagar town), the highest TS values are observed in May, while the remaining four grids in the Presidency division show maximum TS in December.
- **Burdwan Division**: The highest TS values (Table 6.7) are found in December for five grids, and in July for two grids: KG10 (Madhuban town) and UG15 (Jaragram village).
- **Malda Division**: The maximum TL values for the monthly mean (Table 6.9) consistently occur from October to November across all grids. However, the highest TS values are found in December for 60% of the grids in this division, in June for three grids-KG17 (Lohaganj village), UG21 (Saur Village), and UG27 (Porsha town)-and in July for UG17 (Khargram).
- **Jalpaiguri Division**: In this division (Table 6.11), TS values peak in December for KG2 (Jidekha town) and UG35 (Gaedu town), while KG12 (Darbesha village), UG22 (Jalthal village), and UG23 (Pyang village) show their highest TS values in June. The remaining seven grids in the Jalpaiguri division exhibit their highest TS values in January.

Now, the variations of monthly standard deviation (std) along the divisions are as follows in separate paragraphs with respect to the above tables:

Similarly, all 17 grids in Table 6.4 exhibit the highest integer values for TL (Trend Length) of monthly std in October. Conversely, the maximum TS (Trend Slope) values are observed in December for 15 grids, while the remaining two grids UG6 (Kuldiha village) and UG10 (Ashurali village) in Medinipur division show their highest TS values in August.

In Table 6.6, although nine grids in the Presidency division reach their highest TL values for monthly std in October, one grid namely KG15 (Dhubuliya village)—has its peak trend length in April-May. For TS, the maximum values are observed in November for four grids namely KG14 (Bhangar town), KG15, UG30, and UG31 (Kaliganj upazila). Another four grids namely KG13, UG12, UG14 (Uluberia city), and UG29 show the highest TS values in December. Additionally, the peak TS values for monthly std are found in July at UG24 and in August at UG25 in the Presidency division.

In Table 6.8, the highest TL values for monthly std are observed in September for three grids: UG8, UG11, and three known grids in the Burdwan division. The remaining grids show maximum TL values in October at UG15 (Jaragram village) and in April at UG16 (Negun village). TS values in the Burdwan division are highly variable, with the highest slopes

occurring in January at Asta (KG6), Semuldubi (UG8), and Raspur (UG11) villages, in July at Paduma (KG9) and Madhuban (KG10) villages, and in December at UG15 and UG16.

In Table 6.10, the highest TL values for monthly std in the Malda division are observed in September for six grids located in the Malda, Murshidabad, and Dakshin Dinajpur districts, in April for two external grids in Bangladesh (KG16 and UG27), and in May for the remaining two grids. For the monthly standard deviation of TS, the maximum values are observed in July at KG17 (Lahaganj village), UG19 (English Bazar), and UG20 (Chanchal), while three grids in Murshidabad district show peak TS values in November. Additional peaks occur in April at KG11 (Sukhasan village) and UG27 (Porsha town), in June at KG16 (Nundapur village), and in October at UG21 (Saur village) in Malda division.

In Table 6.12, the highest TL values for monthly std in the Jalpaiguri division are observed in May for 10 grids. Two external grids-KG19 (Barfok village, Sikkim) and KG21 (Jidekha town, Bhutan) reach their highest TL values in September. The maximum TS values are observed in March at KG18 (Tetulia upazila), KG20 (Chapatali village), UG34 (Mogolhat railway station), and UG35 (Gedu town). In April, the peak TS values are found in four grids, including three external grids and one in the Kalimpong district. Additionally, in June, three grids-KG21, UG32, and UG33-show the highest TS values, while the maximum TS in July is observed at the external grid KG12 (Drabesha village).

6.6 Monthly IPTA for representative boundary grids

Due to the large number of grids, representing the data using IPTA poses challenges. Therefore, to facilitate a better understanding, eight grids representing boundary conditions are considered for the analysis. Out of all 56 grids listed throughout West Bengal, these eight have been designated to represent the entire state. They can be approximately divided into two sections: UG28, UG34, UG20, and UG17 are the four grids located in the north and middle of West Bengal, while UG2, UG15, UG4, and UG30 are the four grids selected from the south of the state. The exact location (state/district-wise positions) of the eight representative grids, which are already mentioned in Table 6.1, are mostly found along the boundary of any division to cover the entire T_{min} of West Bengal. These locations are shown in Fig. 6.10.

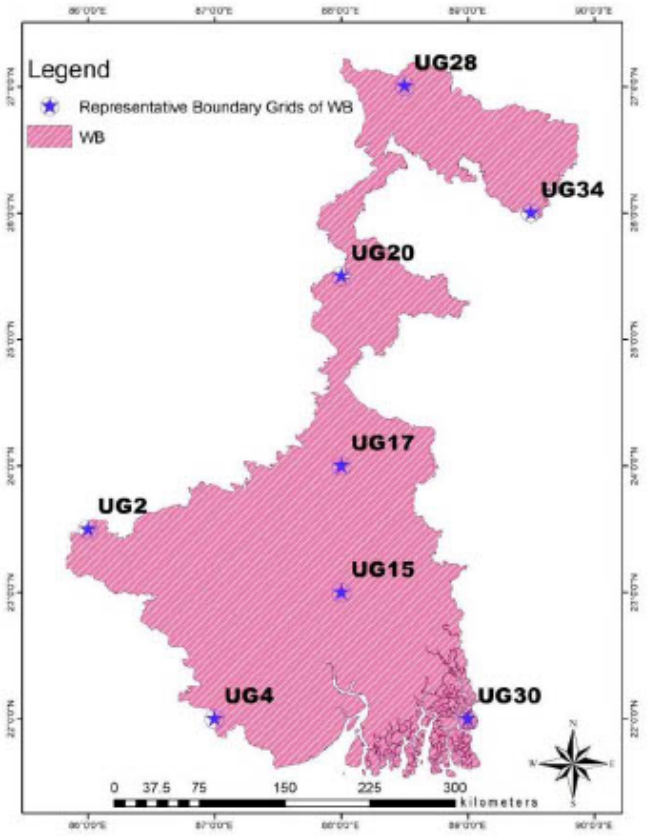


Fig. 6.10 Representative eight boundary grids of West Bengal

6.6.1 Monthly Mean

The T_{min} does not appear in a regular and stable form, and no single polygon is visible in the graph of four different southern district boundary grids in Fig. 6.11. It is observed that almost all months lie near the no-trend line in the four grids. From the figures below, for UG2 (North-West end of Purulia district), it can be concluded that February, March, July, August, September, October, November and December exhibit an increasing trend, while January and May show a decreasing trend. April and June display no noticeable trend. For UG4 (west end of Jhargram), the pattern is similar to UG2, with the exception of April, which shows an increasing trend. Conversely, Fig. 6.11(iii) for UG15 (southeast end of Purba Bardhhaman district) reveals that February, March, April, June, July, August, September, October, November, and December exhibit an increasing trend, while January shows a decreasing trend and May shows no visible trend. In the case of UG30, in the district of South 24 Parganas, the pattern is similar to UG15 (mid-north border of Hooghly district), except for the month of June, which is approximately in the no-trend area.

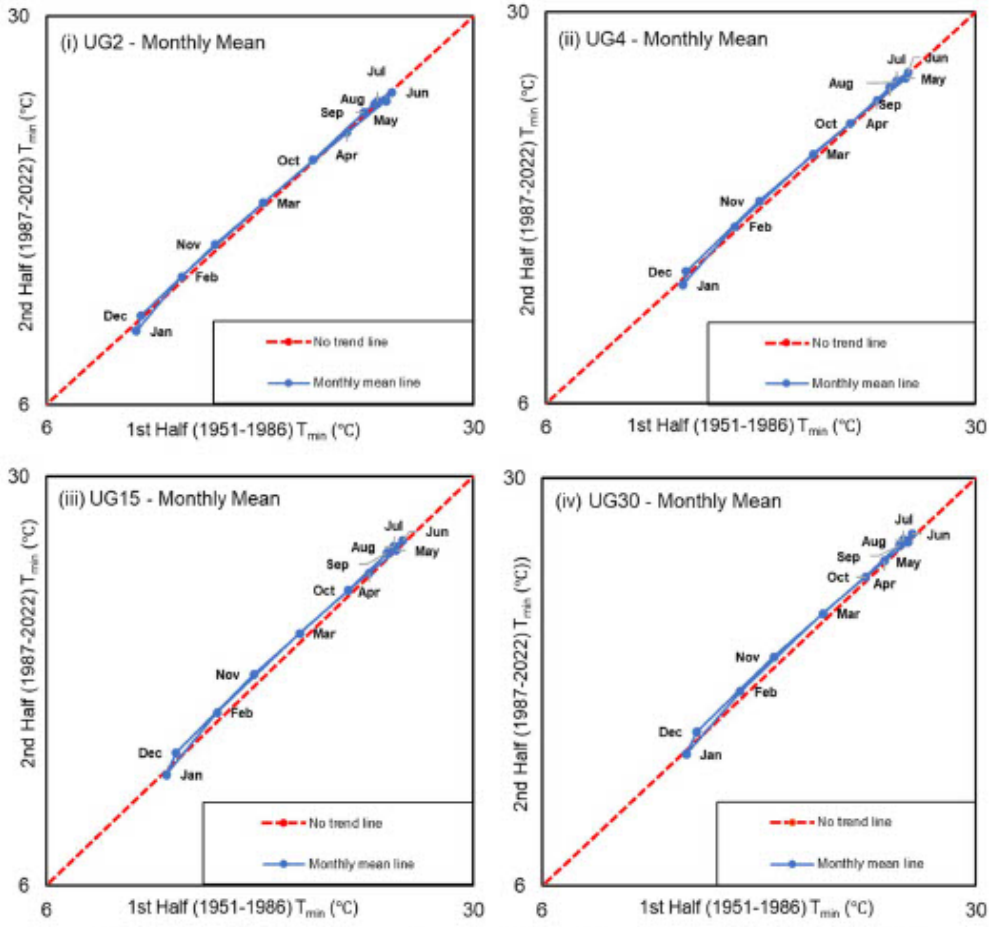


Fig. 6.11 IPTA graphs for the south zone of West Bengal, monthly mean of minimum temperature records from some representative boundary grids (i) UG2, (ii) UG4, (iii) UG15, and (iv) UG30.

Although the four grids in Fig 6.12 are primarily from the north and middle zones of West Bengal, they show similarities to the previously discussed four grids in Fig 6.11. It is evident that the monthly mean T_{min} does not exhibit a regular or stable pattern, and no distinct polygon is visible. It is observed that almost all months are close to the no-trend line. It can be easily noticed that February, March, April, June, July, August, September, October, November, and December show an increasing trend, while January shows a decreasing trend, and May shows no trend in both UG17 (located at the junction of Birbhum, Murshidabad, and Purva Bardhhaman districts) and UG20 (located at the junction of Malda, Uttar Dinajpur, and Dakshin Dinajpur districts). In the mid-west of Kalimpong district (UG28) and the southeast of Cooch Bihar district (UG34), only the month of January shows no trend, while the other 11 months show an increasing trend. Since UG17 and UG20 are located in the mid-zone of West Bengal, they are hotter than the northern grids of UG28 and UG34.

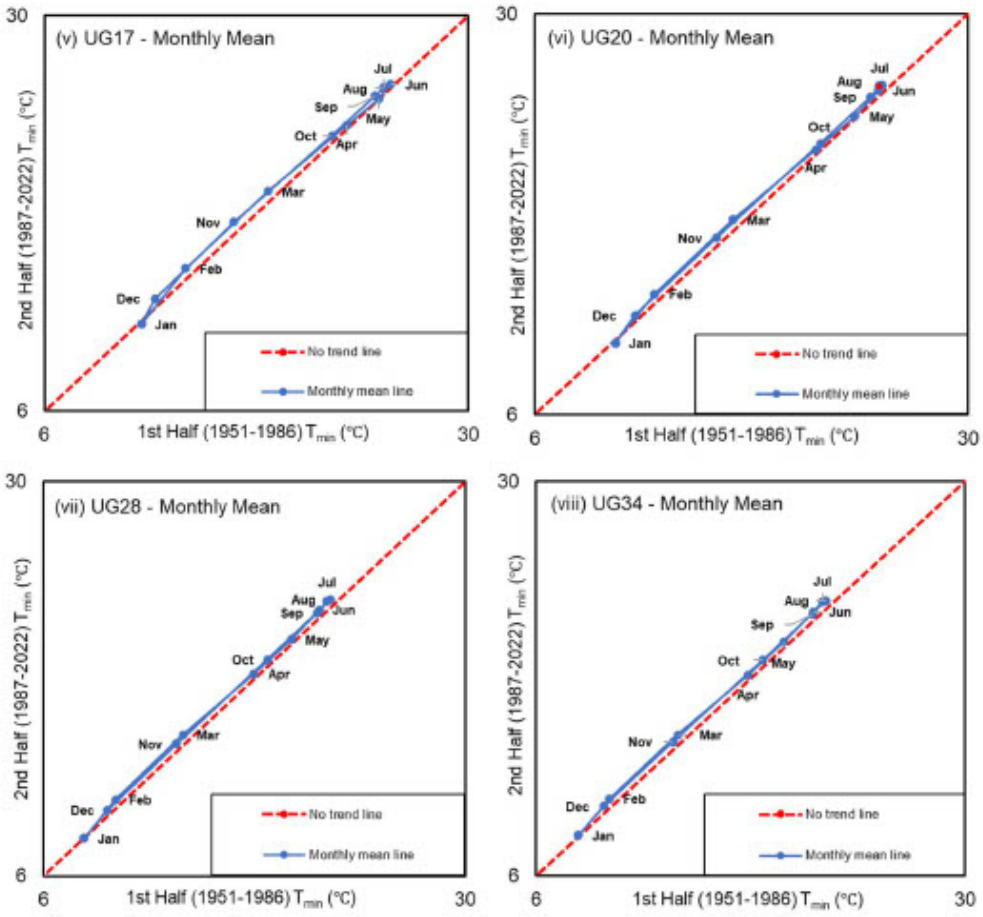


Fig. 6.12 IPTA graphs for the mid and north zone of West Bengal, monthly mean of minimum temperature records from some representative boundary grids (v) UG17, (vi) UG20, (vii) UG28, and (viii) UG34.

6.6.2 Monthly Standard deviation

From Fig 6.13, it is observed that the monthly standard deviation (std) graphs form more complex polygons compared to the monthly mean graphs. In Fig 6.13(i), it is evident that almost all months lie below the trendless line, with April above this 45° line and January showing no trend in the northwest end of Purulia district (UG2). The remaining three grids (UG4 in Jhargram, UG15 in Purba Bardhhaman, and UG30 in South 24 Parganas) exhibit a similar pattern. In these grids, only April lies in the increasing trend area, while all other 11 months are in the decreasing trend zone. Although all of these grids are located in the southern zone of West Bengal, UG2 shows a slightly different trend in the monthly std of IPTA.

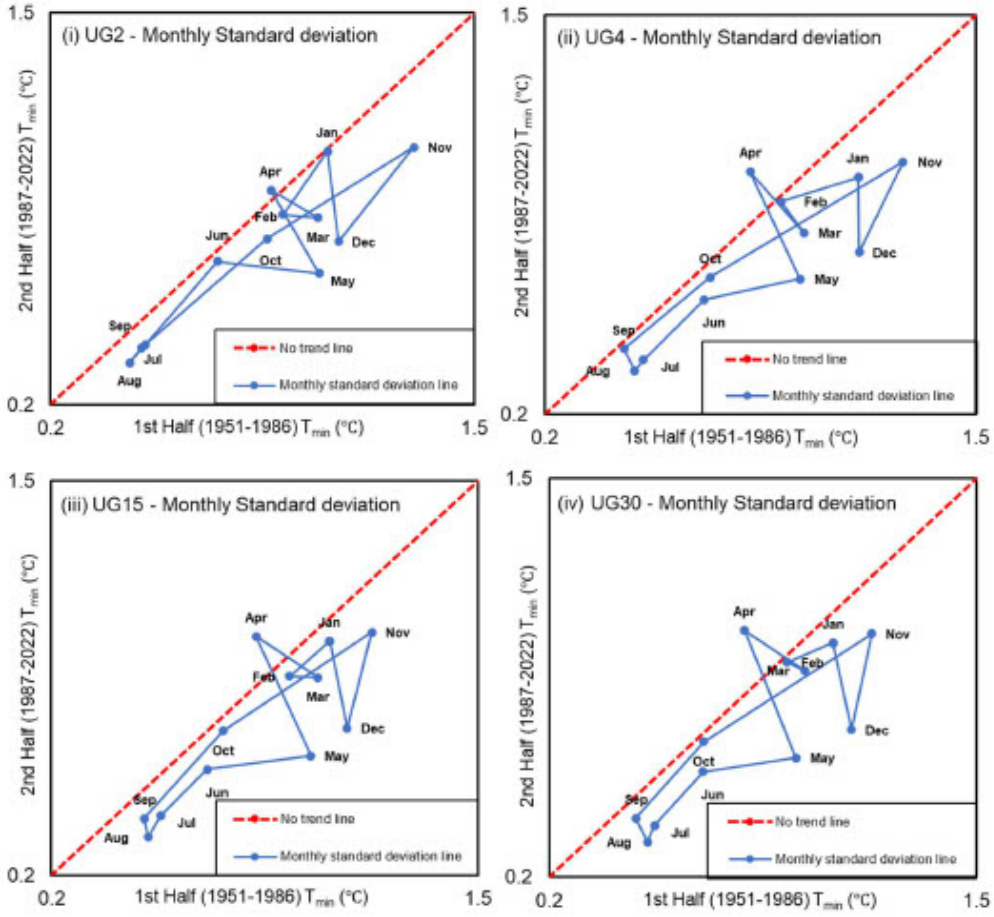


Fig. 6.13 IPTA graphs for the south zone of West Bengal, the monthly standard deviation of minimum temperature records from some representative boundary grids (i) UG2, (ii) UG4, (iii) UG15, and (iv) UG30.

As usual, the monthly std of T_{min} is more complex than the monthly mean. Although the four graphs in Fig 6.14 are mainly from the northern and middle grids of WB, they are similar to those in Fig 6.13. It is observed that the junction of Birbhum, Murshidabad and Purva Bardhhaman districts (UG17) shows an exceptional pattern with an increasing trend in January and April, while the other 10 months are in the decreasing trend area. At the junction of Malda, Uttar Dinajpur and Dakshin Dinajpur districts (UG20), decreasing trends are observed in all the zones for all months except for August which shows no trend. At the mid-west of Kalimpong district (UG28) and at the south-east of Cooch Bihar district (UG34), both have similar patterns, where only July and August are above the no-trend line, September shows no trend, and the remaining months are found to be in decreasing trend zone.

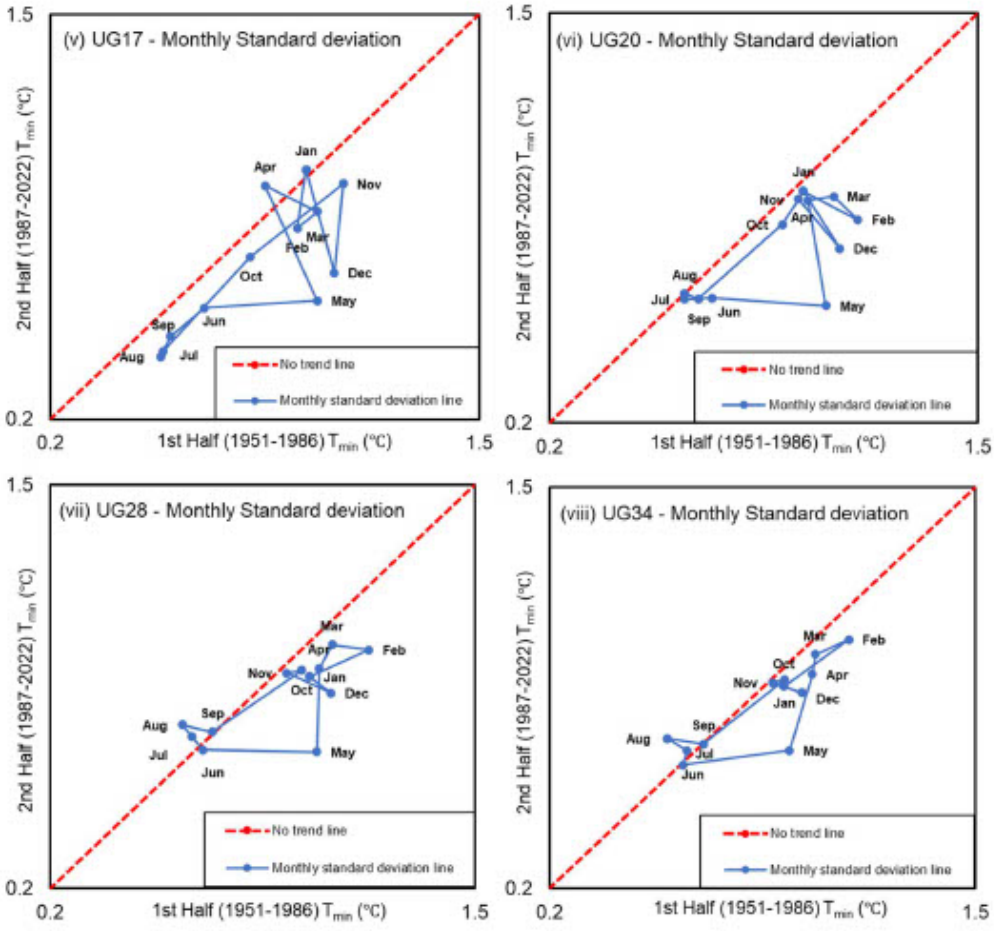


Fig. 6.14 IPTA graphs for the mid and north zone of West Bengal, the monthly standard deviation of minimum temperature records from some representative boundary grids (v) UG17, (vi) UG20, (vii) UG28, and (viii) UG34.

As per the previously plotted T_{min} graphs of IPTA for the representative eight boundary grids of monthly mean and monthly std, the below Tables 6.13 and 6.14 are formed to summarise the no trend, increasing trend and decreasing trend with the help of three different sign conventions. In contrast, it is obvious that maximum trends in monthly means T_{min} are increasing, while maximum trends in monthly standard deviations are decreasing in most of the cases.

Table 6.13 Representation of monthly mean IPTA trend of representative grids

Grids	Jan	Feb	Mar	Apr	May	Jun	Jul	Aug	Sep	Oct	Nov	Dec
UG2	↓	↑	↑	↔	↓	↔	↑	↑	↑	↑	↑	↑
UG4	↓	↑	↑	↓	↓	↔	↑	↑	↑	↑	↑	↑
UG15	↓	↑	↑	↑	↔	↑	↑	↑	↑	↑	↑	↑
UG30	↓	↑	↑	↑	↔	↔	↑	↑	↑	↑	↑	↑
UG17	↓	↑	↑	↑	↔	↑	↑	↑	↑	↑	↑	↑
UG20	↓	↑	↑	↑	↔	↑	↑	↑	↑	↑	↑	↑
UG28	↔	↑	↑	↑	↑	↑	↑	↑	↑	↑	↑	↑
UG34	↔	↑	↑	↑	↑	↑	↑	↑	↑	↑	↑	↑

Note: ↔ represents no trend; ↑represents increasing trend; ↓ represents decreasing trend

Table 6.14 Representation of monthly standard deviation IPTA trend of representative grids

Grids	Jan	Feb	Mar	Apr	May	Jun	Jul	Aug	Sep	Oct	Nov	Dec
UG2	↔	↓	↓	↑	↓	↓	↓	↓	↓	↓	↓	↓
UG4	↓	↓	↓	↑	↓	↓	↓	↓	↓	↓	↓	↓
UG15	↓	↓	↓	↑	↓	↓	↓	↓	↓	↓	↓	↓
UG30	↓	↓	↓	↑	↓	↓	↓	↓	↓	↓	↓	↓
UG17	↑	↓	↓	↑	↓	↓	↓	↓	↓	↓	↓	↓
UG20	↓	↓	↓	↓	↓	↓	↓	↔	↓	↓	↓	↓
UG28	↓	↓	↓	↓	↓	↓	↑	↑	↔	↓	↓	↓
UG34	↓	↓	↓	↓	↓	↓	↑	↑	↔	↓	↓	↓

Note: ↔ represents no trend; ↑represents increasing trend; ↓ represents decreasing trend

With the exception of January and May, Table 6.13 displays a generally positive trend for each month. Except for North Bengal (UG28 and UG34), every grid shows a decreasing trend in January. For UG28 and UG34, there is no trend in January. On the northern side of West Bengal, the typical increasing monthly mean T_{min} pattern is maintained in May. However, in the months of May and April, a declining tendency is also noticed in the western districts of West Bengal (UG2 and UG4), although no trend is seen at UG2 in April. In May, neither an upward nor a downward trend is observed from the middle districts (UG17, UG20) to the southern districts (UG15, UG30) of West Bengal. In June, no trend is seen in the districts of Jhargram (UG4), Purulia (UG2), and South 24 Parganas (UG30). As these are the representative grids of all over WB, the conclusion may suspect that the average T_{min} of more

or less all grids has increased in last 36 years (1987-2022) comparing by the year of 1951 to 1986 of T_{min} data. There will be a probability of T_{min} increasing (month wise) yearly.

Table 6.14 indicates a mostly negative trend, with the exception of April. From the top of the WB to Malda district, there are three representative boundary grids UG28, UG34, and UG20 where the monthly std decreases in April. However, the remaining five grid points UG2, UG4, UG15, UG30, and UG17 of South Bengal show a positive trend in that month. There are only two grids in the Jalpaiguri division (UG28 and UG34) that indicate an increasing tendency in July and August, but no trend in September. There is additionally no trend developing at UG2 in January and UG20 in August. UG17 (within Purva Bardhhaman districts) in the month of January displays an inclining tendency.

The TS and TL of eight representative boundary grids of the south and mid-north zones for monthly mean are shown in Table 6.15. Though the highest TL of all grids occurs in the month of October that represents the rapid change in T_{min} are happened in October-November, the lowest integer values of TL of all the above eight representative grids are observed in July which means, the T_{min} are almost the same in the month of July and August. The unique aspect of this table is the month of July, when the maximum or minimum values of all grids for TL and TS are obtained, except for the TS of the western grids (UG2 and UG4). As the trend slope has no systematic approach, the lowest TS integer values are observed in June, except for the northern three grids, which have the lowest slopes in July that represent the rate of change of mean T_{min} is the smallest in July-August. However, the highest integer values of TS are observed in December for the western grids (UG2 and UG4) and at the southeast of Cooch Bihar district (UG34). The highest TS is recorded in June near the intersection of the districts of Malda, Uttar Dinajpur, and Dakshin Dinajpur (i.e., UG20), while the largest slope is observed in January at the Kalimpong district (UG28).

Table 6.15 Trend length (in °C) and trend slope (unitless) of eight representative boundary grids for monthly mean data

	South Zone								Mid and North Zone							
Grids	**UG2**		**UG4**		**UG15**		**UG30**		**UG17**		**UG20**		**UG28**		**UG34**	
Month	**TL**	**TS**	**TL**	**TS**	**TL**	**TS**	**TL**	**TS**	**TL**	**TS**	**TL**	**TS**	**TL**	**TS**	**TL**	**TS**
Jan	4.214	1.316	4.613	1.222	4.625	1.286	4.760	1.237	4.213	1.354	3.644	1.344	2.936	**1.307**	2.844	1.276
Feb	6.474	0.996	6.218	1.019	6.581	0.997	6.488	1.001	6.596	1.002	6.222	1.031	5.520	1.031	5.431	1.019
Mar	6.397	0.915	4.873	0.915	5.273	0.910	4.580	0.910	6.004	0.899	6.218	0.907	5.482	0.920	5.336	0.924
Apr	2.939	0.896	2.099	0.849	2.026	0.852	1.728	0.835	2.392	0.868	2.949	0.932	2.988	0.979	2.880	1.017
May	0.626	1.699	0.382	2.785	0.670	1.704	0.538	1.998	1.109	1.384	1.997	1.184	2.386	1.132	2.459	1.105
Jun	0.969	**0.657**	0.807	**0.728**	0.586	**0.627**	0.582	**0.669**	0.425	**0.460**	0.275	**3.612**	0.693	1.294	0.765	1.188
Jul	**0.251**	1.149	**0.102**	3.133	**0.070**	**10.207**	**0.065**	**-4.355**	**0.051**	**-5.832**	**0.148**	**0.362**	**0.218**	**0.457**	**0.204**	**0.454**
Aug	0.764	0.896	0.458	0.955	0.503	0.967	0.379	1.004	0.660	0.973	0.919	1.102	1.115	1.117	1.111	1.092
Sep	4.121	1.026	3.130	1.005	3.077	0.992	2.638	0.991	3.444	0.991	3.941	1.004	4.003	1.003	3.946	1.003
Oct	**7.580**	0.947	**6.978**	0.936	**7.246**	0.935	**6.916**	0.933	**7.620**	0.944	**8.064**	0.976	**7.272**	0.990	**7.056**	0.994
Nov	6.063	1.061	5.947	1.056	6.353	1.044	6.141	1.034	6.458	1.037	6.471	1.034	5.631	1.028	5.504	1.012
Dec	0.978	**3.350**	0.845	**4.235**	1.414	2.411	1.447	2.203	1.723	2.022	1.996	1.508	2.166	1.274	2.273	**1.257**

Note: Bolds represent column wise highest and lowest values.

Table 6.16 Trend length (in °C) and trend slope (unitless) of eight representative boundary grids for monthly standard deviation data

	South Zone								Mid and North Zone							
Grids	**UG2**		**UG4**		**UG15**		**UG30**		**UG17**		**UG20**		**UG28**		**UG34**	
Month	**TL**	**TS**	**TL**	**TS**	**TL**	**TS**	**TL**	**TS**	**TL**	**TS**	**TL**	**TS**	**TL**	**TS**	**TL**	**TS**
Jan	0.251	1.546	0.247	0.341	0.168	0.944	0.154	0.452	0.190	7.128	0.189	-0.549	0.202	0.477	0.249	0.764
Feb	0.107	**-0.095**	0.123	-1.454	0.087	**-0.044**	0.060	-0.490	0.080	0.865	0.105	-1.009	0.113	-0.140	0.112	0.466
Mar	0.170	-0.629	0.257	-1.232	0.232	-0.718	0.225	-0.718	0.180	-0.525	0.079	0.163	0.086	1.921	0.066	**6.850**
Apr	0.313	-1.859	0.380	-2.336	0.428	-2.375	0.445	-2.659	0.401	-2.338	0.339	-6.187	0.269	**33.131**	0.257	3.526
May	0.314	-0.126	0.297	**0.233**	0.318	0.144	0.287	**0.159**	0.342	**0.067**	**0.347**	-0.069	**0.348**	**-0.020**	**0.329**	**0.140**
Jun	0.353	1.250	0.268	1.067	0.208	1.074	0.229	1.180	0.138	0.885	0.083	**0.042**	0.054	-1.291	0.047	3.663
Jul	0.077	1.251	**0.044**	1.325	0.081	1.868	**0.058**	2.574	0.072	2.139	**0.018**	**19.142**	0.049	-1.305	0.072	-0.671

Aug	**0.061**	1.390	0.078	-2.159	**0.063**	-4.798	0.085	-2.166	**0.019**	2.016	0.045	-0.406	0.094	-0.263	0.111	-0.167
Sep	0.530	0.941	0.349	0.892	0.376	1.208	0.325	1.212	**0.402**	1.146	0.347	0.928	0.339	0.721	0.323	0.844
Oct	**0.543**	0.674	**0.693**	0.648	**0.558**	0.717	**0.621**	0.688	0.366	0.832	0.094	1.626	**0.047**	0.168	**0.037**	0.245
Nov	0.390	1.351	0.324	2.230	0.325	4.198	0.320	**5.043**	0.287	**10.292**	0.199	-1.245	0.151	-0.479	0.095	-0.365
Dec	0.303	**-8.990**	0.245	**-100.718**	0.292	**-5.382**	0.289	-5.036	0.342	-3.932	0.212	-1.654	0.085	-0.800	0.058	-0.370

Note: Bolds represent column wise highest and lowest values

The summary of monthly standard deviations for the eight representative grids is provided in Table 6.16. The most rapid changes in T_{min}, indicated by the highest TL (Trend Length), occur in October for the South Bengal grids UG2, UG4, UG15, and UG30. For the North Bengal grids UG20, UG28, and UG34, the maximum TL values are observed in May, while UG17, a central grid in West Bengal, shows the highest TL in September. The smallest TL values are observed in August for UG2 (north-western Purulia district), UG15 (mid-northern border of Hooghly district), and UG17 (the junction of Birbhum, Murshidabad, and Purba Bardhhaman districts). In July, the shortest TL is noted in two South Bengal grids (UG4 and UG30) and at UG20, located at the junction of Malda, Uttar Dinajpur, and Dakshin Dinajpur districts. The remaining northern grids UG28 and UG34 exhibit the lowest TL values in October. In terms of TS (Trend Slope), the longest values are recorded in December for three South Bengal grids, in November for UG17 and UG30, in July for UG20 (the junction of Malda, Uttar Dinajpur, and Dakshin Dinajpur districts), in April for the Kalim pong district grid, and in March for the Cooch Bihar grid. The lowest TS values occur in May for the southernmost grids (UG4 and UG30), the central grid (UG17), and the northernmost grids (UG28 and UG34). In February, UG2 and UG15 show the lowest TS. Finally, in June, the lowest TS is observed in UG20, the grid located in the mid-zone and north-zone of the region.

6.7 Monthly spatiotemporal analysis

Spatial analysis relates to the arrangement of objects in space, while temporal analysis pertains to the sequencing of events or moments in time (Rehman and Arif, 2024). In this context, spatial analysis refers to changes in minimum temperature concerning grid point locations. Conversely, temporal analysis varies with respect to seasons or months.

It is clearly observed from the spatiotemporal plot in Fig 6.15 that the 0.5° resolution data for all months are more precise than the 1° resolution data. This improvement in precision arises because the 0.5° resolution T_{min} data were derived through IDW interpolation of the course 1° resolution data. In simple terms, IDW interpolation uses the values from nearby points to estimate temperatures at a finer resolution. By interpolating the 1° resolution data, the 0.5° resolution data effectively provides a more detailed and refined picture of the spatial variation in T_{min}. This method improves the granularity and accuracy of the temperature estimates, making the finer resolution data appear more precise and informative.

From the monthly spatiotemporal analysis, it is very clear that January is the coldest month and June is the hottest month of the year. Though it is observed that, July is a little bit hotter than August in some specific locations, but it may be said that the mean minimum temperatures of July and August are almost the same over WB. The monthly temperature sequence from hottest to coldest of any year can be represented in the following way: June > July ≥ August > May > September > April > October > March > November > February > December > January.

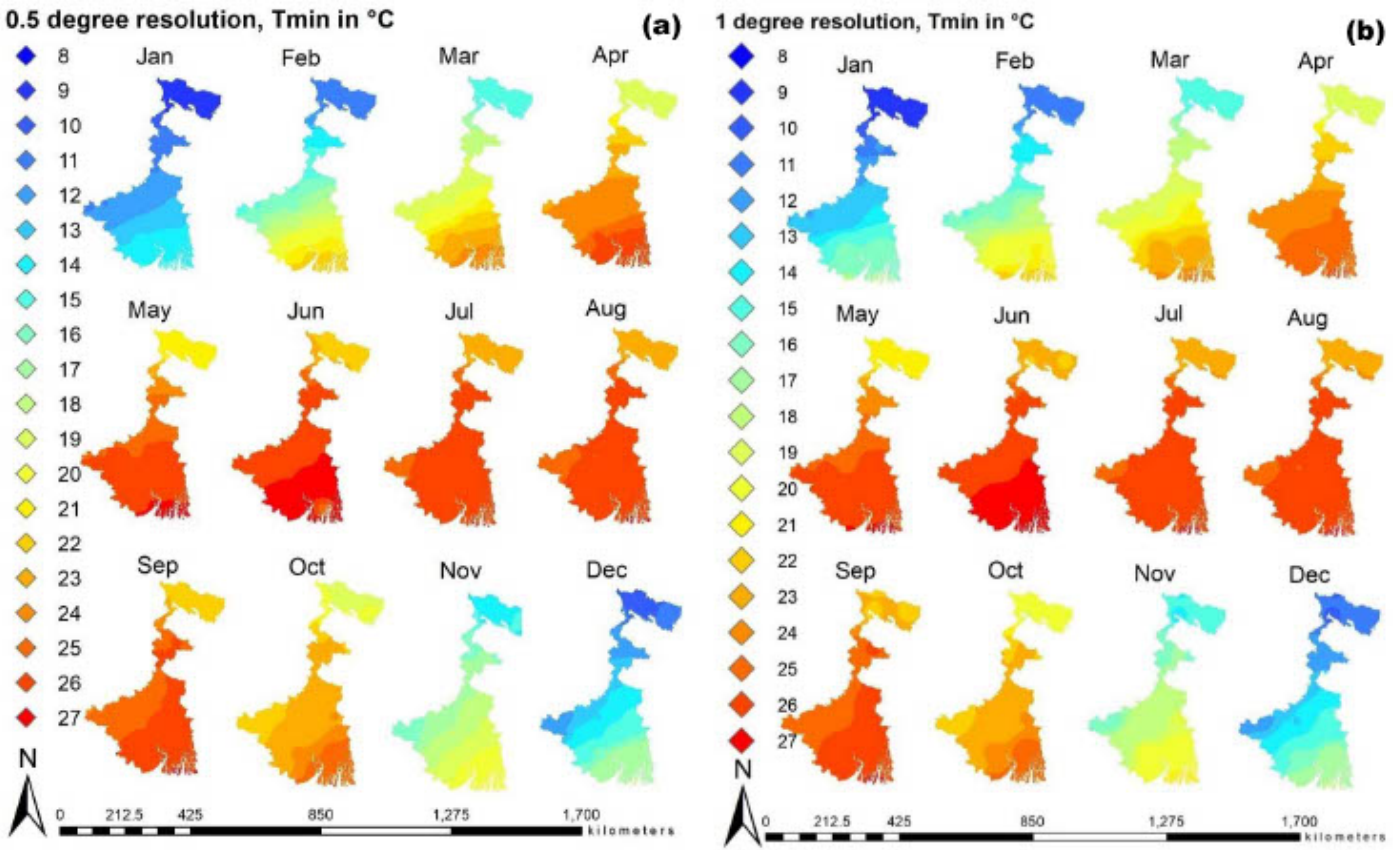


Fig. 6.15 Monthly spatiotemporal variation of average minimum temperature in West Bengal using gridded data at (a) 0.5° and (b) 1° resolutions, based on the 72-year mean (1951-2022)

6.8 Seasonal trend analysis

Division wise seasonal trend length and trend slope of all 56 grids are as follows in the tables where, TL represents the Trend Length (in °C) and TS represents the Trend Slope correspondingly, they both are IPTA statistics, same as before mentioned in monthly trend analysis.

Table 6.17 Representation of trend length (in °C) and trend slope (unitless) for seasonal mean and standard deviation across the Medinipur Division

Grids	IPTA Statistics	Seasonal Mean				Seasonal Standard deviation			
		Summer	Monsoon	Autumn	Winter	Summer	Monsoon	Autumn	Winter
KG1	TL	3.122	8.878	8.395	**14.148**	0.520	**0.775**	0.085	0.220
	TS	1.030	0.965	**1.051**	1.001	0.643	0.797	-0.024	**2.432**
KG2	TL	3.706	9.318	8.843	**14.453**	0.558	**0.787**	0.129	0.111
	TS	**1.060**	0.975	1.039	0.992	0.707	0.745	0.457	**1.616**
KG3	TL	2.341	7.080	7.908	**12.645**	0.483	**0.617**	0.115	0.248
	TS	1.033	0.968	**1.048**	1.005	0.809	0.761	0.899	**0.729**
KG4	TL	3.078	8.162	8.621	**13.701**	0.577	**0.663**	0.031	0.113
	TS	1.053	0.970	**1.054**	1.003	**0.863**	0.813	-0.291	0.303
KG5	TL	3.674	8.585	9.188	**14.097**	0.571	**0.687**	0.051	0.076
	TS	**1.072**	0.974	1.050	0.998	0.904	0.867	0.114	**1.355**
KG7	TL	2.203	6.405	8.003	**12.203**	0.555	**0.584**	0.109	0.159
	TS	1.031	0.965	**1.040**	1.001	**1.069**	0.860	0.645	0.223
KG8	TL	2.799	7.176	9.001	**13.376**	0.582	**0.602**	0.110	0.119
	TS	1.036	0.961	**1.043**	1.000	1.033	**1.067**	0.036	0.215
UG1	TL	3.395	8.736	8.761	**14.099**	0.560	**0.735**	0.068	0.114
	TS	**1.054**	0.971	1.048	0.998	0.777	0.797	0.353	**1.342**
UG2	TL	3.666	8.845	9.032	**14.209**	0.557	**0.719**	0.081	0.092
	TS	**1.059**	0.973	1.044	0.996	0.768	0.810	0.421	**1.952**
UG3	TL	3.437	8.561	8.890	**14.012**	0.569	**0.703**	0.047	0.088
	TS	**1.060**	0.972	1.049	0.999	0.835	0.822	0.481	**0.955**
UG4	TL	2.605	7.206	8.383	**12.981**	0.553	**0.620**	0.084	0.156

	TS	1.039	0.966	**1.046**	1.002	**0.947**	0.870	0.374	0.388
UG5	TL	2.944	7.714	8.710	**13.478**	0.572	**0.644**	0.051	0.120
	TS	1.047	0.967	**1.048**	1.001	**0.924**	0.889	0.026	0.365
UG6	TL	3.280	8.016	9.002	**13.735**	0.573	**0.654**	0.019	0.086
	TS	**1.052**	0.968	1.048	0.999	0.909	0.900	-0.876	**0.509**
UG7	TL	3.767	8.288	9.386	**13.905**	0.548	**0.628**	0.025	0.056
	TS	**1.046**	0.967	1.044	0.997	0.853	0.905	1.492	**1.298**
UG9	TL	2.584	7.079	8.445	**12.937**	0.559	**0.613**	0.090	0.149
	TS	1.038	0.965	**1.044**	1.002	**0.981**	0.904	0.334	0.340
UG10	TL	3.318	7.771	9.190	**13.640**	0.566	**0.624**	0.038	0.077
	TS	1.044	0.964	**1.045**	0.998	0.930	**0.962**	-0.384	0.469
UG13	TL	2.537	6.694	8.628	**12.782**	0.563	**0.587**	0.108	0.142
	TS	1.038	0.963	**1.039**	0.999	**1.078**	0.987	0.312	0.230

Note: Bold represents the highest values along the seasonal row

Table 6.18 Representation of trend length (in °C) and trend slope (unitless) for seasonal mean and standard deviation across the Presidency Division

Grids	IPTA Statistics	Seasonal Mean				Seasonal Standard deviation			
		Summer	Monsoon	Autumn	Winter	Summer	Monsoon	Autumn	Winter
KG13	TL	2.364	6.180	8.622	**12.436**	0.551	**0.574**	0.118	0.160
	TS	**1.053**	0.965	1.035	0.996	**1.222**	1.031	0.543	0.272
KG14	TL	2.811	6.611	9.263	**13.061**	**0.552**	0.531	0.124	0.106
	TS	1.033	0.956	**1.033**	0.993	1.103	**1.115**	0.147	0.040
KG15	TL	3.575	6.986	9.971	**13.379**	0.523	**0.534**	0.086	0.082
	TS	1.024	0.952	**1.036**	0.994	1.020	**1.153**	0.208	0.700
UG12	TL	2.472	6.596	8.542	**12.664**	0.560	**0.586**	0.109	0.147
	TS	**1.039**	0.963	1.039	0.999	**1.094**	0.975	0.377	0.235
UG14	TL	2.791	7.019	8.917	**13.142**	0.568	**0.591**	0.098	0.119

UG24	TS	1.038	0.962	**1.040**	0.998	**1.036**	1.020	0.135	0.229
	TL	1.837	5.670	8.803	**12.806**	0.390	**0.412**	0.113	0.135
UG25	TS	0.215	0.650	**1.037**	0.997	**0.285**	0.259	0.284	0.205
	TL	3.189	7.058	9.438	**13.304**	0.552	**0.564**	0.087	0.087
UG29	TS	1.032	0.957	**1.037**	0.995	1.031	**1.092**	0.066	0.307
	TL	2.532	6.455	8.782	**12.704**	0.558	**0.571**	0.116	0.141
UG30	TS	**1.043**	0.962	1.036	0.996	**1.145**	1.044	0.340	0.215
	TL	2.643	6.539	8.922	**12.816**	0.558	**0.567**	0.113	0.130
UG31	TS	**1.040**	0.961	1.036	0.996	**1.129**	1.065	0.275	0.201
	TL	2.885	6.715	9.204	**13.032**	0.556	**0.558**	0.108	0.109
	TS	1.034	0.958	**1.035**	0.995	1.092	**1.099**	0.173	0.201

Note: Bold represents the highest values along the seasonal row

Table 6.19 Representation of trend length (in °C) and trend slope (unitless) for seasonal mean and standard deviation across the Burdwan Division

Grids	IPTA Statistics	Seasonal Mean				Seasonal Standard deviation			
		Summer	Monsoon	Autumn	Winter	Summer	Monsoon	Autumn	Winter
KG6	TL	4.172	8.629	9.719	**14.175**	0.532	**0.608**	0.036	0.111
	TS	**1.043**	0.975	1.037	0.997	0.734	1.126	**4.026**	-3.184
KG9	TL	3.824	7.795	9.769	**13.738**	0.521	**0.561**	0.025	0.028
	TS	1.041	0.957	**1.042**	0.993	0.892	0.973	-3.938	**0.998**
KG10	TL	5.065	8.580	10.288	**13.800**	**0.479**	0.470	0.036	0.036
	TS	1.000	0.961	**1.025**	0.993	0.813	0.993	0.201	**-12.853**
UG8	TL	4.073	8.365	9.648	**13.938**	0.527	**0.589**	0.022	0.050
	TS	1.037	0.966	**1.039**	0.995	0.811	0.924	1.876	**3.842**
UG11	TL	4.210	8.293	9.805	**13.887**	0.516	**0.561**	0.020	0.041
	TS	1.029	0.963	**1.034**	0.993	0.810	0.944	3.076	**54.323**
UG15	TL	3.170	7.247	9.316	**13.389**	0.560	**0.585**	0.075	0.087
	TS	1.037	0.959	**1.040**	0.996	1.005	**1.055**	-0.007	0.322

UG16	TL	3.600	7.564	9.624	**13.584**	0.540	**0.574**	0.045	0.059
	TS	1.034	0.959	**1.040**	0.995	0.942	**1.028**	-0.226	0.620

Note: Bold represents the highest values along the seasonal row

Table 6.20 Representation of trend length (in °C) and trend slope (unitless) for seasonal mean and standard deviation across the Malda Division

Grids	IPTA Statistics	Seasonal Mean				Seasonal Standard deviation			
		Summer	Monsoon	Autumn	Winter	Summer	Monsoon	Autumn	Winter
KG11	TL	6.249	8.635	10.851	**13.236**	**0.438**	0.397	0.192	0.083
	TS	1.029	1.008	**1.032**	1.017	0.390	1.011	-0.324	**1.186**
KG16	TL	5.209	7.909	10.565	**13.264**	**0.451**	0.440	0.164	0.124
	TS	1.018	0.987	**1.024**	1.004	0.865	**1.084**	0.003	0.239
KG17	TL	6.586	8.700	10.905	**13.019**	**0.416**	0.345	0.147	0.056
	TS	**1.020**	1.012	1.026	1.019	0.557	0.939	0.079	**1.335**
UG17	TL	4.206	7.863	9.966	**13.622**	0.508	**0.529**	0.049	0.049
	TS	1.024	0.963	**1.034**	0.996	0.889	**1.020**	-0.223	0.766
UG18	TL	4.875	8.203	10.254	**13.580**	0.476	**0.482**	0.078	0.053
	TS	1.018	0.973	**1.029**	0.999	0.790	**1.020**	-0.206	0.841
UG19	TL	5.542	8.389	10.548	**13.395**	**0.448**	0.432	0.117	0.060
	TS	1.018	0.987	**1.027**	1.006	0.665	**1.017**	-0.171	0.891
UG20	TL	6.042	8.534	10.605	**13.096**	**0.437**	0.397	0.134	0.057
	TS	**1.019**	0.998	1.028	1.012	0.519	0.937	-0.188	**1.350**
UG21	TL	6.361	8.465	10.392	**12.495**	**0.431**	0.374	0.146	0.061
	TS	1.020	1.007	**1.027**	1.016	0.434	0.827	-0.125	**1.310**
UG26	TL	4.300	7.681	10.094	**13.473**	0.498	**0.508**	0.082	0.067
	TS	1.022	0.967	**1.032**	0.998	0.906	**1.065**	-0.078	0.496
UG27	TL	5.676	8.344	10.595	**13.262**	**0.444**	0.420	0.128	0.067
	TS	1.018	0.992	**1.027**	1.008	0.664	1.002	-0.102	**0.717**

Note: Bold represents the highest values along the seasonal row

Table 6.21 Representation of trend length (in °C) and trend slope (unitless) for seasonal mean and standard deviation across the Jalpaiguri Division

Grids	IPTA Statistics	Seasonal Mean				Seasonal Standard deviation			
		Summer	Monsoon	Autumn	Winter	Summer	Monsoon	Autumn	Winter
KG12	TL	6.461	8.214	9.834	**11.587**	**0.437**	0.381	0.126	0.052
	TS	1.012	1.004	**1.028**	1.020	0.337	0.625	-0.180	**1.210**
KG18	TL	6.600	8.212	9.675	**11.287**	**0.410**	0.345	0.139	0.069
	TS	**1.023**	1.017	1.020	1.016	0.406	0.719	0.064	**1.439**
KG19	TL	6.540	8.123	9.608	**11.191**	**0.402**	0.368	0.118	0.067
	TS	**1.018**	1.012	1.020	1.016	0.409	0.693	-0.097	**0.961**
KG20	TL	6.493	7.840	9.553	**10.900**	**0.420**	0.374	0.087	0.074
	TS	**1.020**	1.011	1.014	1.008	0.586	0.829	0.661	**-34.163**
KG21	TL	6.680	8.203	9.376	**10.899**	**0.389**	0.322	0.114	0.067
	TS	**1.030**	1.012	1.008	0.998	0.507	0.931	0.212	**-393.281**
UG22	TL	6.483	8.274	9.920	**11.712**	**0.424**	0.367	0.134	0.061
	TS	1.019	1.010	**1.024**	1.017	0.390	0.703	-0.074	**1.237**
UG23	TL	6.517	8.212	9.774	**11.469**	**0.419**	0.366	0.129	0.062
	TS	1.018	1.011	**1.023**	1.017	0.384	0.677	-0.063	**1.166**
UG28	TL	6.539	8.200	9.731	**11.391**	**0.413**	0.362	0.129	0.065
	TS	1.019	1.013	**1.022**	1.016	0.396	0.695	-0.036	**1.183**
UG32	TL	6.561	8.094	9.607	**11.140**	**0.407**	0.355	0.113	0.066
	TS	**1.022**	1.013	1.017	1.012	0.462	0.761	0.149	**2.439**
UG33	TL	6.567	8.116	9.601	**11.150**	**0.405**	0.354	0.115	0.065
	TS	**1.022**	1.013	1.017	1.011	0.453	0.758	0.114	**2.204**
UG34	TL	6.543	8.020	9.597	**11.075**	**0.411**	0.360	0.105	0.068
	TS	**1.022**	1.013	1.017	1.011	0.496	0.780	0.262	**3.773**
UG35	TL	6.527	8.089	9.537	**11.099**	**0.595**	0.282	0.164	0.236
	TS	**1.039**	1.011	1.018	1.001	0.309	**1.219**	0.130	-0.282

Note: Bold represents the highest value along the seasonal row

The highest integer values of Trend Length (TL) for all grids across the five divisions of Jalpaiguri, Malda, Bardhhaman, Medinipur, and Presidency are observed during winter and summer for the seasonal mean, as detailed in Tables 6.17 to 6.21. In the Medinipur division, the highest TL values for all 17 grids occur during the Monsoon season for seasonal standard deviation (std). Specifically, in Table 6.18, the maximum TL values for all grids are observed in Monsoon, except for KG14 (Bhangar town) in the Presidency division, where the peak is in summer. Similarly, for seasonal std in Table 6.19, the highest TL values for all grids occur in Monsoon, except for KG10 (Madhuban town of Dhanbad), where the peak is also in Summer. In the Malda division, the highest TL values for seasonal std are found in Summer for seven grids, while the remaining three grids UG17, UG18, and UG26 in the Murshidabad district have their highest values in Monsoon. Additionally, for seasonal std in Table 6.21, the highest TL values for all 12 grids of the Jalpaiguri division occur in Summer.

Trend Slope (TS) values exhibit more fluctuations (especially in the case of standard deviation), making the analysis of TL more straightforward than TS. Now, the detailed explanation of seasonal TS based on Tables 6.17 to 6.21 is as follows: The maximum TS values for seasonal mean are observed in Autumn for 10 grids in Table 6.17, with the remaining seven grids KG2, UG1, UG2 in Jharkhand, KG5, UG3 in Purulia district, UG6 in Kuldiha village, and UG7 in Patdoha village showing the highest values in Summer. The highest TS values for seasonal std in the Medinipur division are observed in Winter for nine grids, in Summer for six grids KG4, KG7, UG4, UG5, UG9, and UG13, and in Monsoon for the remaining two grids (KG8 in Shata Chak village and UG10 in Ashurali village). In the Presidency division, the maximum TS values for the seasonal mean are observed in autumn for six grids, while the remaining four grids (three above the Bay of Bengal and UG30 in Bangladesh) show the highest values in summer. In Table 6.18, the maximum TS values for seasonal std occur in Summer for six grids KG13, UG12, UG14, UG24, UG29, and UG30, while the remaining four grids KG14, KG15 in Dhubulia village, UG25 in Madanpur village, and UG31 in Kaliganj upazila show the highest values in the Monsoon.

In the Burdwan division, the highest TS values for all grids occur in autumn, except for KG6 (in Asta village), where the peak is in summer for the seasonal mean. For TS in seasonal std, the highest values are observed in Winter for four grids KG9 in Paduma village, KG10 in Madhuban town, UG8 in Semuldubi village, and UG11 in Raspur village, in Monsoon for two grids in Purba Bardhhaman district, and in Autumn for KG6. In Table 6.20, the highest TS values for all grids occur in autumn, except for Lahaganj village (KG17) and Chanchal village (UG20), where they peak in summer for the seasonal mean. In the Malda division, the highest TS values are observed in winter for five grids, while the remaining grids KG16 in Nundapur, UG17 in Khargram, UG18 in Ahiran, UG19 in English Bazar, and UG26 in Garibpur show the highest values in Monsoon. The TS values for all grids in Table 6.21 reach their maximum in winter, except for UG35, where it occurs in Monsoon for seasonal std. For the seasonal mean in the Jalpaiguri division, the highest TS values occur in Summer for grids KG18, KG19, KG20, KG21, UG32, UG33, UG34, and UG35, while the remaining four grids peak in Autumn.

6.9 Seasonal IPTA for representative boundary grids

The eight representative boundary grids, already mentioned in Fig 6.10 for the monthly analysis, have been chosen and selected for the discussion of the IPTA for the seasonal analysis as well.

6.9.1 Seasonal Mean

The minimum temperature does not exhibit a regular and stable pattern, and there is no distinct polygon visible in the graph for the four different southern district boundary grids in IPTA. It is observed that almost all months lie on or near the no-trend line in the IPTA graphs for these four grids. For UG2 and UG4, the pattern is similar, with no trend observed in summer and winter, while monsoon and autumn show an increasing trend. However, for UG15 and UG30, both IPTA graphs are consistent, with all four seasons falling within the increasing trend zone.

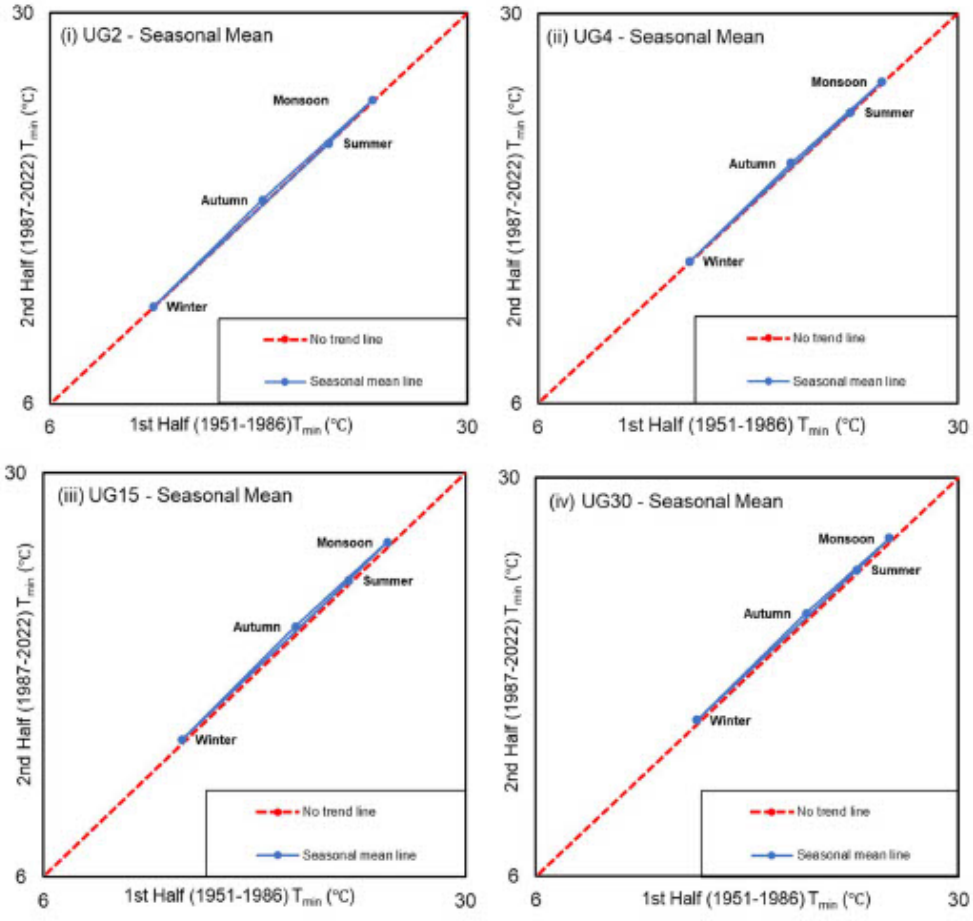


Fig. 6.16 IPTA graphs for the south zone of West Bengal, seasonal mean of minimum temperature records from some representative boundary grids (i) UG2, (ii) UG4, (iii) UG15, and (iv) UG30.

From Fig 6.16 and the analysis of the four grids, it is observed that UG2 is notably cooler than the other three grids. This is because the trends for the other three grids are shifted towards the upper-right corner, a pattern also evident in the monthly mean IPTA graphs for UG4, UG15, and UG30.

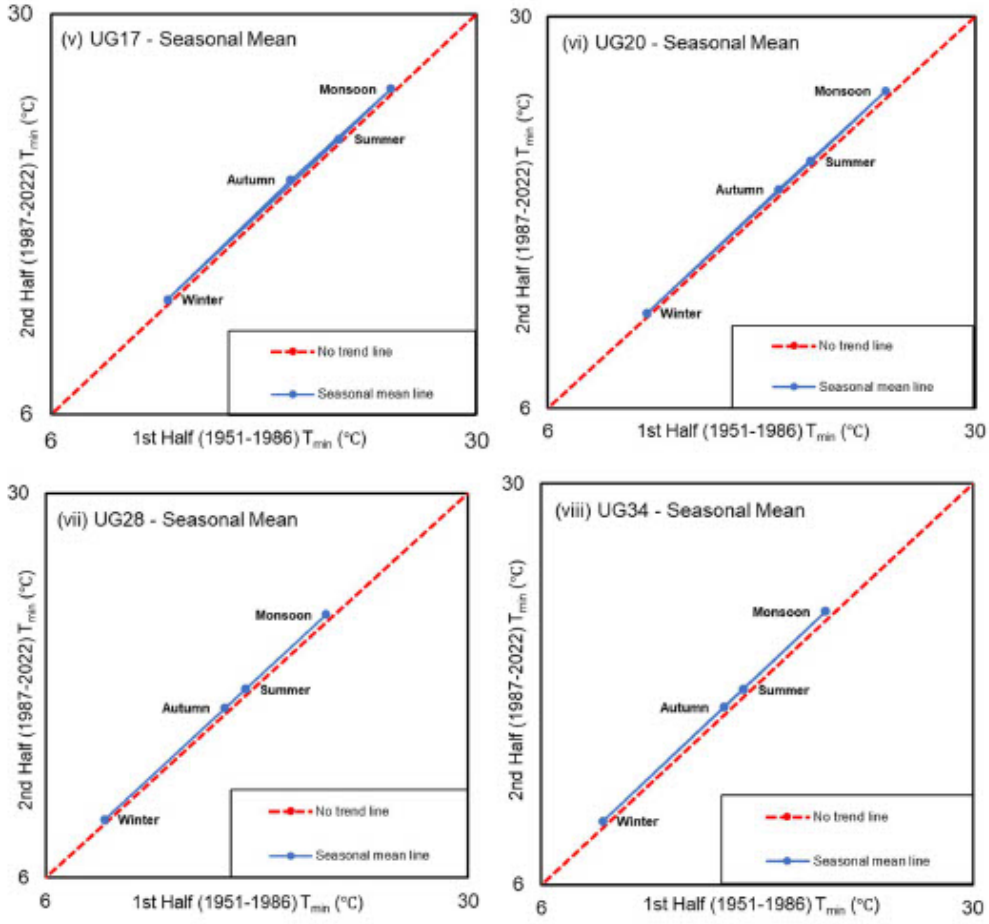


Fig. 6.17 IPTA graphs for the mid and north zone of West Bengal, seasonal mean of minimum temperature records from some representative boundary grids (v) UG17, (vi) UG20, (vii) UG28, and (viii) UG34.

Figure 6.17 shows that the four grids, primarily from the northern and middle zones of West Bengal, are very similar to the previously discussed grids in Fig 6.16. It is clear that the seasonal mean minimum temperature does not exhibit a stable form and no distinct polygon is visible; instead, the data generally follow a linear pattern. Almost all seasons lie above the no-trend line in the IPTA graphs for these four grids, indicating an increasing trend across all seasons (summer, monsoon, autumn, and winter). Additionally, UG17 and UG20, located in

the mid-zone of West Bengal, are hotter than the northern grids UG28 and UG34, which is why the graphs in Figs. 6.17(vii) and (viii) are shifted towards the lower-left corner.

6.9.2 Seasonal Standard deviation

It is observed that the IPTA seasonal standard deviation creates one or two polygons in the four grids from the southern zone of West Bengal shown in Fig. 6.18. All seasons lie below the trendless line, indicating a decreasing trend for these grids. Although all the grids are located in the southern zone of West Bengal, UG2 exhibits a slightly different trend in the seasonal standard deviation IPTA, as it creates two triangular polygons (i.e., the state of instability, inhomogeneity, and complexity, where the two different types of temperature present in this particular grid each year rather than a steady state), while the remaining three grids form similar single polygons which represents the regularity in terms of T_{min}.

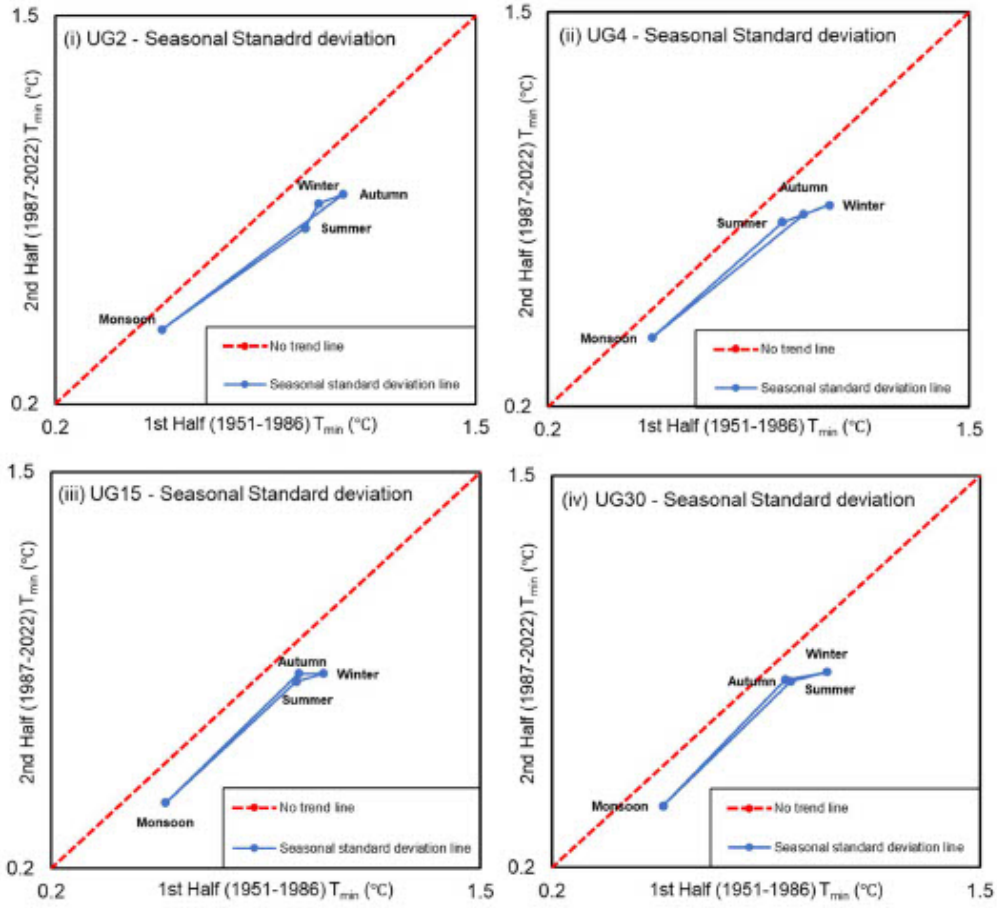


Fig. 6.18 IPTA graphs for the south zone of West Bengal, the seasonal standard deviation of minimum temperature records from some representative boundary grids (i) UG2, (ii) UG4, (iii) UG15, and (iv) UG30.

As usual, the monthly standard deviation of minimum temperature IPTA graphs is more complex than the seasonal standard deviation IPTA graphs. Although the four graphs in Fig. 6.19 are primarily from the northern and middle grids of West Bengal, they are quite similar to the graphs in Figure 6.18. Notably, UG28 and UG34 exhibit a somewhat exceptional pattern with an increasing trend in Monsoon, while all other seasons are in the decreasing trend area. In contrast, for UG17 and UG20, all four seasons are located in the decreasing trend zone, forming a single type of polygon.

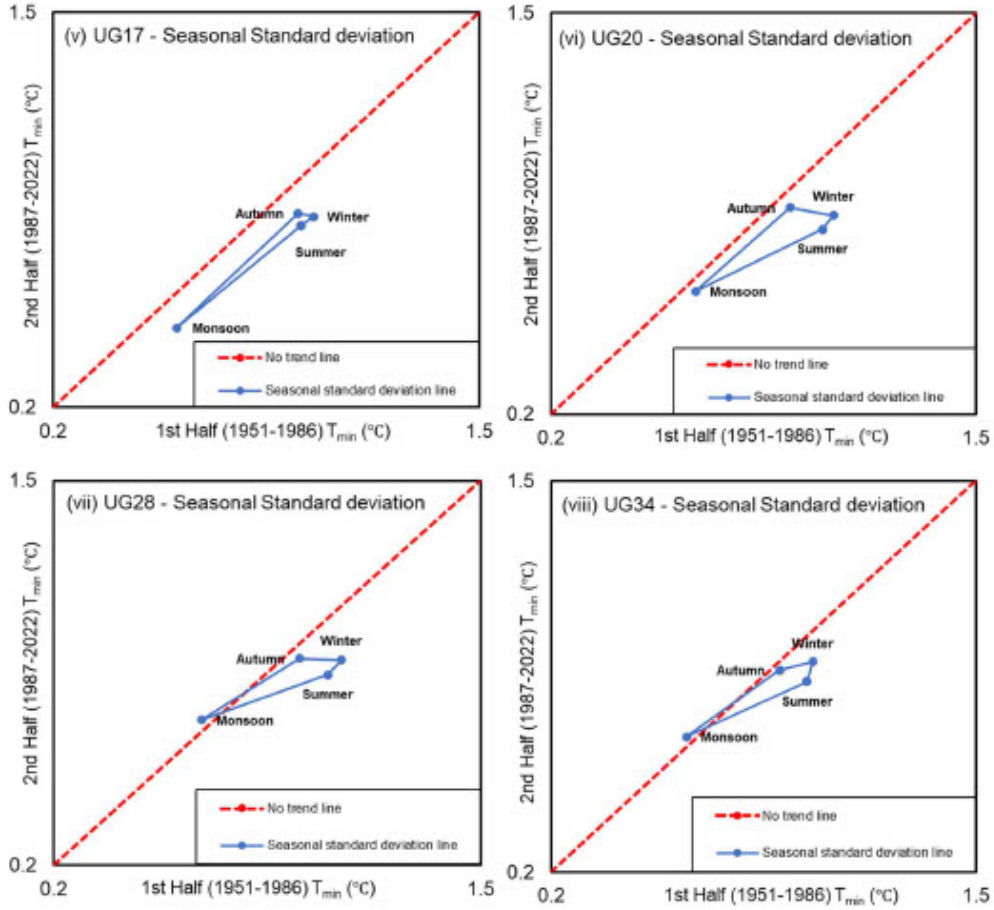


Fig. 6.19 IPTA graphs for the mid and north zone of West Bengal, the seasonal standard deviation of minimum temperature records from some representative boundary grids (v) UG17, (vi) UG20, (vii) UG28, and (viii) UG34.

Based on the previously plotted IPTA graphs for the eight representative boundary grids of seasonal mean and seasonal standard deviation, Table 6.22 has been developed to summarize the no trend, increasing trend, and decreasing trend using three specific sign conventions.

Table 6.22 Representation of seasonal mean and seasonal standard deviation IPTA trend

Grids	Seasonal Mean				Seasonal Standard Deviation			
	Summer	Monsoon	Autumn	Winter	Summer	Monsoon	Autumn	Winter
UG2	↔	↑	↑	↔	↓	↓	↓	↓
UG4	↔	↑	↑	↔	↓	↓	↓	↓
UG15	↑	↑	↑	↑	↓	↓	↓	↓
UG30	↑	↑	↑	↑	↓	↓	↓	↓
UG17	↑	↑	↑	↑	↓	↓	↓	↓
UG20	↑	↑	↑	↑	↓	↓	↓	↓
UG28	↑	↑	↑	↑	↓	↑	↓	↓
UG34	↑	↑	↑	↑	↓	↑	↓	↓

Note: ↔ represents no trend; ↑represents increasing trend; ↓ represents decreasing trend

It is observed that for both summer and winter, UG2 and UG4 exhibit no trends in seasonal mean. Conversely, in terms of seasonal standard deviation, UG28 and UG34 show increasing trends during Monsoon. Table 6.22, which is quite similar to the monthly trends, indicates that the maximum trends for the seasonal mean are generally increasing, while for seasonal standard deviation, the trends are mostly decreasing. As these grids represent various regions across West Bengal, the conclusion suggests that the average minimum temperature has generally increased over the past 36 years (1987-2022) compared to the period from 1951 to 1986. There is a likelihood of a seasonal increase in T_{min} each year.

Table 6.23 Trend length (in °C) and trend slope (unitless) of eight representative boundary grids for seasonal mean data

	South Zone								Mid and North Zone							
Grids	**UG2**		**UG4**		**UG15**		**UG30**		**UG17**		**UG20**		**UG28**		**UG34**	
Seasons	**TL**	**TS**	**TL**	**TS**	**TL**	**TS**	**TL**	**TS**	**TL**	**TS**	**TL**	**TS**	**TL**	**TS**	**TL**	**TS**
Summer	**3.666**	**1.059**	**2.605**	1.039	**3.170**	1.037	**2.643**	**1.040**	**4.206**	1.024	**6.042**	1.019	**6.539**	1.019	**6.543**	**1.022**
Monsoon	8.845	**0.973**	7.206	**0.966**	7.247	**0.959**	6.539	**0.961**	7.863	**0.963**	8.534	**0.998**	8.200	**1.013**	8.020	1.013
Autumn	9.032	1.044	8.383	**1.046**	9.316	**1.040**	8.922	1.036	9.966	**1.034**	10.605	**1.028**	9.731	**1.022**	9.597	1.017
Winter	**14.209**	0.996	**12.981**	1.002	**13.389**	0.996	**12.816**	0.996	**13.622**	0.996	**13.096**	1.012	**11.391**	1.016	**11.075**	**1.011**

Note: Bold represents column wise the highest and the lowest values

Table 6.24 Trend length (in °C) and trend slope (unitless) of eight representative boundary grids for seasonal standard deviation data

	South Zone								Mid and North Zone							
Grids	**UG2**		**UG4**		**UG15**		**UG30**		**UG17**		**UG20**		**UG28**		**UG34**	
Seasons	**TL**	**TS**	**TL**	**TS**	**TL**	**TS**	**TL**	**TS**	**TL**	**TS**	**TL**	**TS**	**TL**	**TS**	**TL**	**TS**
Summer	0.557	0.768	0.553	**0.947**	0.560	1.005	0.558	**1.129**	0.508	0.889	**0.437**	0.519	**0.413**	0.396	**0.411**	0.496
Monsoon	**0.719**	0.810	**0.620**	0.870	**0.585**	**1.055**	**0.567**	1.065	**0.529**	**1.020**	0.397	0.937	0.362	0.695	0.360	0.780
Autumn	**0.081**	**0.421**	**0.084**	**0.374**	**0.075**	**-0.007**	**0.113**	0.275	0.049	**-0.223**	0.134	**-0.188**	0.129	**-0.036**	0.105	**0.262**
Winter	0.092	**1.952**	0.156	0.388	0.087	0.322	0.130	**0.201**	**0.049**	0.766	**0.057**	**1.350**	**0.065**	**1.183**	**0.068**	**3.773**

Note: Bold represents column wise the highest and the lowest values

Table 6.23 presents a summary of the seasonal Trend Length (TL) and Trend Slope (TS) of the mean minimum temperature (T_{min}) across West Bengal. It reveals that the highest TL values for all grids occur in winter, while the lowest TL values are observed in summer. The TS does not follow a consistent pattern: UG2 (Purulia district), UG30 (South 24 Parganas), and UG34 (southeast of Cooch Bihar district) show their maximum TS in summer, whereas the remaining five grids have their highest TS in autumn. The lowest TS values are observed in the Monsoon season for all representative grids, except for the grid of Cooch Bihar (UG34), which has its lowest TS in winter.

Table 6.24 provides a summary of the seasonal standard deviation for the eight representative grids. The highest TL values are recorded for the grid of Malda district (UG20), mid-west of Kalim pong district (UG28), and southeast of Cooch Bihar district (UG34) in summer, while the maximum TL for the remaining five grids is observed during the Monsoon season. The lowest TL values are found in autumn for four grids in the southern zone and in winter for four grids in the mid-northern zone of West Bengal. The highest TS values are observed in summer for the southernmost boundary grids UG4 and UG30, in Monsoon for UG15 (southeast end of Purba Bardhhaman district) and UG17 (the central grid among the representative grids), and in winter for the remaining grids. Most of the lowest TS values occur in autumn for all grids except UG30 (South 24 Parganas), which has the lowest TS in winter.

6.10 Seasonal spatiotemporal analysis

The spatiotemporal analysis of minimum temperature (T_{min}) has been previously discussed in the context of monthly variations (Section 6.7). Here, the focus shifts to understanding how T_{min} changes with respect to grid point locations (spatial) and seasons (temporal).

For a more detailed comparison, Figures 6.20(a) and 6.20(b) present the seasonal T_{min} data based on 72 years of mean data. Figure 6.20(a) shows the T_{min} across 56 grids at a 0.5° resolution, while Figure 6.20(b) displays the T_{min} across 21 grids at a 1° resolution. Both figures illustrate the seasonal T_{min} for Summer (MAM), Monsoon (JJAS), Autumn (ON), and Winter (DJF).

As observed, the 0.5° resolution data in Figure 6.20(a) provides a more precise depiction of mean T_{min} variation compared to the 1° resolution data in Figure 6.20(b). This increased precision is due to the IDW interpolation of the 1° resolution data to obtain the 0.5° resolution T_{min} data.

The figures indicate that mean T_{min} ranges from 17°C to 26°C in summer, 22°C to 27°C in Monsoon, 16°C to 25°C in autumn, and 9°C to 16°C in winter. While summer is generally considered the hottest season, the high humidity during the monsoon can make it feel even hotter. The analysis confirms that winter is the coldest season, while monsoon is the hottest. The seasonal temperature sequence from hottest to coldest is summarized as: Monsoon > Summer > Autumn > Winter.

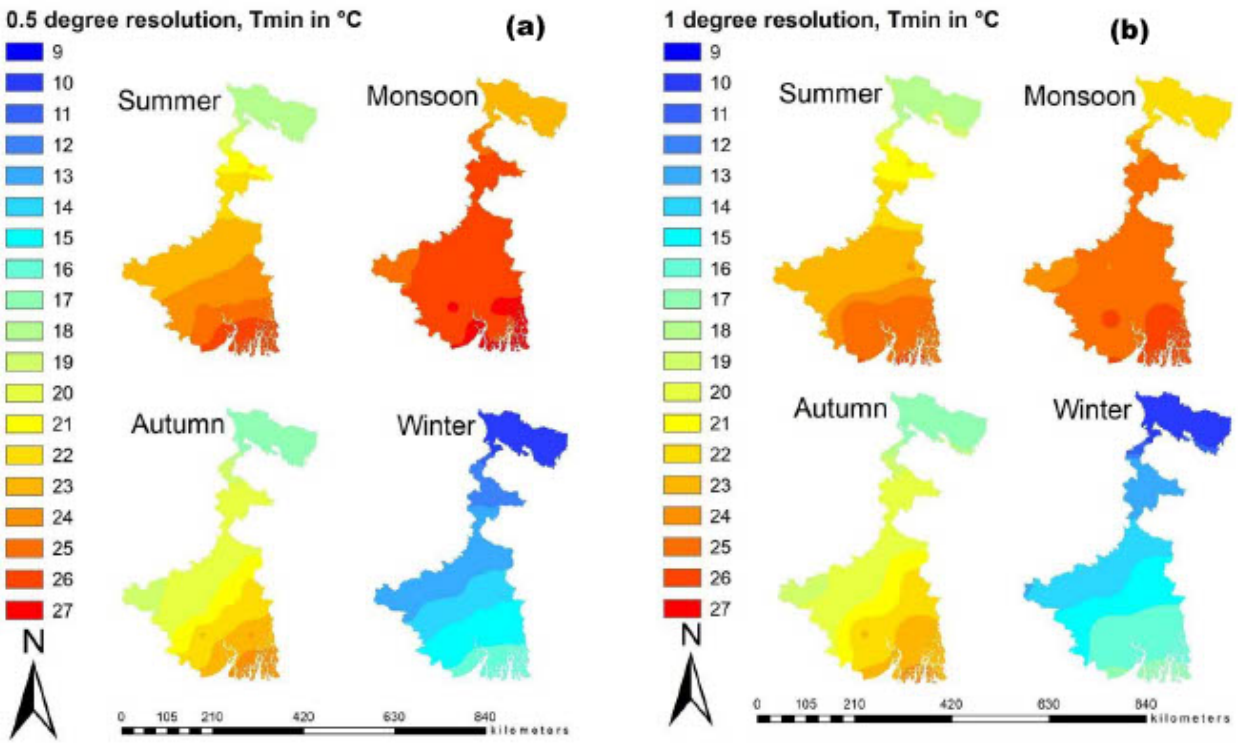


Fig. 6.20 Seasonal spatiotemporal variation of average minimum temperature in West Bengal **(a)** 0.5° and **(b)** 1° resolutions, based on the 72-year mean (1951-202

Chapter 7
CONCLUSIONS AND FUTURE RECOMMENDATIONS

7.1 Conclusions

The identification of trend elements is a crucial aspect of analyzing historical and projected time series data. In this study, trends in minimum temperature (T_{min}) were assessed for the entire state of West Bengal (WB) in India, with some grids from neighboring states or countries included for comparative purposes. This comparison involved two different resolutions: 0.5° and 1°, with the 0.5-degree resolution data obtained using the Inverse Distance Weighted (IDW) method. Trend analysis was performed using the non-parametric Innovative Polygon Trend Analysis (IPTA) method over a study period of 72 years (1951-2022). The analysis revealed both positive and negative trends in monthly and seasonal mean T_{min}, with some instances showing no significant trend. The conclusions drawn from this study are as follows:

- Despite the fact that the T_{min} data set of grids at 0.5 degrees resolution was extracted using the IDW approach, some rare climatological conditions may cause this data to be slightly inexact in all of the grids. Since IDW is one of the strongest methods for interpolating accessible, it has been deliberately utilized manually to reduce mistakes and improve consequences.
- During the 72-year T_{min} data analysis in MS-Excel, among all grids of West Bengal, the lowest T_{min} was identified on the date 05 January, 1955.
- Decadal analysis was primarily aimed at comparing 1° and 0.5° resolutions. Notable differences were observed in the middle southern region of West Bengal including parts of Medinipur, Burdwan, and the Presidency division, where variations were relatively minor. It was found that higher resolutions might yield more accurate results. A specific visualization for decadal analysis showed that the average T_{min} from 1951 to 1960 closely mirrored the mean T_{min} from 1961 to 1970. Similarly, mean T_{min} values for the decades 1971-1980 and 1981-1990 showed minimal variation. Differences between the subsequent three decades 1990-2000, 2001-2010, and 2011-2022 were nearly indistinguishable. Additionally, each decade displayed an average T_{min} of approximately 20°C from north to south across the state.
- Throughout the grids of West Bengal, the highest values of TL consistently occurred in the months of October and November, while the shortest values were observed in July and August. Seasonally, the highest TL was recorded in Winter, and the smallest TL was noted in Summer. However, a few grids exhibited unusual patterns according to the analysis of

standard deviation. This inconsistency indicates that the mean T_{min} may display non-isotropic behavior and complexity in certain grids.

- The length and slope of trends for monthly and seasonal mean T_{min} illustrate variations throughout the months. The maximum TL is observed as 8.21°C at grid point KG17 (located near Lahaganj village in Malda division) for monthly mean T_{min} and 14.012°C at UG3 (located near Hatnadih village in Medinipur division) for seasonal mean T_{min}. For the Trend Slope (TS), the highest positive value is +41.739 at KG8 (located near Shata Chak village in Paschim Medinipur district) and the lowest negative value is -98.69 at UG13 (located near Nandigram in Purba Medinipur district) for monthly mean T_{min}. The highest trend slope for the seasonal mean T_{min} is +1.072 at KG5 (located near Birkicha village in Purulia district).
- According to 72 years of IPTA results, nearly all grids in West Bengal exhibited an increasing trend in mean T_{min} across each month. However, several grids in the southern and central regions of the state showed a decreasing trend, and no trend was observed in North Bengal during January. In terms of seasonal means, all trends indicate an increase, except for the western grids of West Bengal, where no trend was observed in both summer and winter seasons.
- The 72-year spatiotemporal mean T_{min} data for the state revealed a slightly more refined variation at the 0.5° resolution compared to the 1° resolution. Given the minor difference observed, utilizing a higher resolution, such as 0.25°, may yield even more accurate findings for comparison.

7.2 Future Scopes

- It is recommended to continue the analysis by focusing on the maximum temperature (T_{max}) in addition to the minimum temperature (T_{min}) across West Bengal.
- Future research could benefit from applying Standardized Innovative Polygon Trend Analysis (S-IPTA) to study and analyze the trends of key meteorological parameters at the same locations.
- The recent analysis could be extended to other Indian states to predict temperature trends and enhance climatological research across the country.
- Converting the dataset to a higher resolution (e.g., 0.25° × 0.25°) and comparing it with the previously analyzed data could provide more detailed insights and potentially reveal finer-scale variations in temperature trends.

REFERENCES

Acar, E., Kankal, M., Akçay, F., and Şan, M. (2022). Innovative polygon trend analyses with star graph for rainfall and temperature data in agricultural regions of Turkey. *Environmental Earth Sciences*, Vol. 81, Issue 23, Art. No. 530. https://doi.org/10.1007/s12665-022-10646-9.

Achite, M., Ceribasi, G., Ceyhunlu, A. I., Wałęga, A., and Caloiero, T. (2021). The innovative polygon trend analysis (IPTA) as a simple qualitative method to detect changes in environment — example detecting trends of the total monthly precipitation in semiarid area. *Sustainability*, Vol. 13, Issue 22, Art. No. 12674. https://doi.org/10.3390/su132212674.

Administrative divisions of West Bengal - Wikipedia, Overview https://en.wikipedia.org/?title=Administrative _divisions of West Bengal & o l did =1139523251.

Aktas, B. (2020): Possible changes in some climate parameters and climate types in Konya depending on global warming. Kastamonu University. Institute of Science. Department of Sustainable Agriculture and Natural Plant Resources, Kastamonu, Turkey.

Almazroui, M., and Şen, Z. (2020). Trend analyses methodologies in hydro-meteorological records. *Earth Systems and Environment*, Vol. 4, pp. 713-738. https://doi.org/10.1007/s41748-020-00190-6.

Ceribasi, G., Ceyhunlu, A. I., and Ahmed, N. (2021). Analysis of temperature data by using innovative polygon trend analysis and trend polygon star concept methods: A Case Study for Susurluk Basin, Turkey. *Acta Geophysica*, Vol. 69, pp. 1949-1961. https://doi.org/10.1007/s11600-021-00632-3.

Choudhari, A. (2016): Spatial Trend Analysis of Temperature in Uttar Pradesh for Last Century. M.Tech. Dissertation Report, Department of Civil Engineering, Malaviya National Institute of Technology Jaipur.

Chowdari, K. K., Deb Barma, S., Bhat, N., Girisha, R., Gouda, K. C., and Mahesha, A. (2023). Trends of seasonal and annual rainfall of semi-arid districts of Karnataka, India: application of innovative trend analysis approach. *Theoretical and Applied Climatology*, Vol. 152, Issue 1, pp. 241-264. https://doi.org/10.1007/s00704-023-04400-9.

Coughlan de Perez, E., Arrighi, J., and Marunye, J. (2023). Challenging the universality of heatwave definitions: gridded temperature discrepancies across climate regions. *Climatic Change*, Vol. 176, Issue 12, Art. No. 167. https://doi.org/10.1007/s10584-023-03641-x.

Datta, P., and Das, S. (2019). Analysis of long-term seasonal and annual temperature trends in North Bengal, India. *Spatial Information Research*, Vol. 27, Issue 4, pp. 475-496. https://doi.org/10.1007/s41324-019-00250-8.

Dioha, M. O., & Kumar, A. (2020). Exploring greenhouse gas mitigation strategies for agriculture in Africa: the case of Nigeria. *Ambio*, Vol. 49, Issue 9, pp. 1549-1566. https://doi.org/10.1007/s13280-019-01293-9.

Director, H., and Bornn, L. (2015). Connecting point-level and gridded moments in the analysis of climate data. *Journal of Climate*, Vol. 28, Issue 9, pp. 3496-3510. https://doi.org/10.1175/JCLI-D-14-00571.1.

Esit, M. (2023). Investigation of innovative trend approaches (ITA with significance test and IPTA) comparing to the classical trend method of monthly and annual hydrometeorological variables: A Case Study of Ankara region, Turkey. *Journal of Water and Climate Change*, Vol. 14, Issue 1, pp. 305-329. https://doi.org/10.2166/wcc.2022.356.

Halder, P., Dey, R. K., and Mandal, S. (2023). Long-period trend analysis of annual and seasonal rainfall in West Bengal, India (1901–2020). *Theoretical and Applied Climatology*, Vol. 154, Issue 1, pp. 685-703. https://doi.org/10.1007/s00704-023-04577-z.

Hırca, T., Eryılmaz Türkkan, G., and Niazkar, M. (2022). Applications of innovative polygonal trend analyses to precipitation series of Eastern Black Sea Basin, Turkey. *Theoretical and Applied Climatology*, Vol. 147, Issue 1, pp. 651-667. https://doi.org/10.1007/s00704-021-03837-0.

Jain, S. K., and Kumar, V. (2012). Trend analysis of rainfall and temperature data for India. *Current Science*, pp. 37-49.

Karacosta, P., Pakalidou, N., Douka, M., and Karacostas, T. (2023). Innovative Polygon Trend Analysis (IPTA): A Case Study for Precipitation in Thessaloniki during the Last 50 Years (1971–2020). *Environmental Sciences Proceedings*, Vol. 26, Issue 1, Art. No. 161. https://doi.org/10.3390/ environsciproc2023026161.

Kendall MG (1975) Rank correlation methods. Griffin, London.

Khan, A., Chatterjee, S., and Bisai, D. (2015). On the long-term variability of temperature trends and changes in surface air temperature in Kolkata Weather Observatory, West Bengal, India. *Meteorology Hydrology and Water Management*, Vol. 3, Issue 2, pp. 9-16. https://doi.org/10.26491/mhwm/59336.

Khan, A., Chatterjee, S., and Bisai, D. (2017). Air temperature variability and trend analysis by non-parametric test for Kolkata observatory, West Bengal, India. *Indian Journal of Geo Marine Sciences*, Vol. 46, No. 5, pp. 966-971 http://nopr.niscpr.res.in/handle/123456789/41661.

Kundu, S. K., and Mondal, T. K. (2019). Analysis of long-term rainfall trends and change point in West Bengal, India. *Theoretical and Applied Climatology*, Vol. 138, pp. 1647-1666. https://doi.org/10.1007/s00704-019-02916-7.

Malik, A., Kumar, A., Guhathakurta, P., and Kisi, O. (2019). Spatial-temporal trend analysis of seasonal and annual rainfall (1966–2015) using innovative trend analysis method with significance test. *Arabian Journal of Geosciences*, Vol. 12, pp. 1-23. https://doi.org/10.1007/s12517-019-4454-5.

Mondal, A., Kundu, S., and Mukhopadhyay, A. (2012). Rainfall trend analysis by Mann-Kendall test: A case study of north-eastern part of Cuttack district, Orissa. *International Journal of Geology, Earth and Environmental Sciences*, Vol. 2, Issue 1, pp. 70-78.

NASA Science Editorial Team (2024). Warming seas may increase frequency of extreme storms. https://science.nasa.gov/earth/climate-change/warming-seas-may-increase-frequency-of-extreme-storms/.

National Geographic Society (2023). Climate Change. Encyclopedic Entry. National Geographic Headquarters, Washington, DC, USA. https://education.nationalgeographic.org/resource/climate-change/.

Nengzouzam, G., Hodam, S., Bandyopadhyay, A., and Bhadra, A. (2019). Spatial and temporal trends in high resolution gridded temperature data over India. *Asia-Pacific Journal of Atmospheric Sciences*, Vol. 55, pp. 761-772. https://doi.org/10.1007/s13143-019-00120-1.

Manishsiq, (2023): Climatology, Climatic Regions Classification, Factors Affecting Climate.... https://www.studyiq.com/articles/climatology/.

Mann HB (1945) Nonparametric tests against trend. *Econometrica* 13: pp. 245–259. https://doi.org/10.2307/1907187.

Pai, D. S., Rajeevan, M., Sreejith, O. P., Mukhopadhyay, B., and Satbha, N. S. (2014). Development of a new high spatial resolution (0.25× 0.25) long period (1901-2010) daily gridded rainfall data set over India and its comparison with existing data sets over the region. *Mausam*, Vol. 65, Issue 1, pp. 1-18. https://doi.org/10.54302/mausam.v65i1.851.

Patel, G., Das, R., and Das, S. (2023). Is the extreme temperature trend changed in last two decades compared to last seven decades? Case study from Eastern India. *Journal of Earth System Science*, Vol. 132, Issue 3, Art. No. 140. https://doi.org/10.1007/s12040-023-02158-2.

Patel, G., Das, S., and Das, R. (2024). Determine the best method for analysing long-term (120 years) annual and seasonal rainfall trends in four east India river basins. *Journal of Earth System Science*, Vol. 133, Issue 2, pp. 1-21. https://doi.org/10.1007/s12040-024-02282-7.

Piotrowicz, K., and Ciaranek, D. (2020). A selection of weather type classification systems and examples of their application. *Theoretical and Applied Climatology*, Vol. 140, pp. 719-730. https://doi.org/10.1007/s00704-020-03118-2.

Radhakrishnan, K., Sivaraman, I., Jena, S. K., Sarkar, S., and Adhikari, S. (2017). A climate trend analysis of temperature and rainfall in India. *Climate Change and Environmental Sustainability*, Vol. 5, Issue 2, pp. 146-153. https://doi.org/10.5958/2320-642X.2017.00014.

Radovic, V. and Iglesias, I. (2019). Extreme Weather Events: Definition, Classification and Guidelines towards Vulnerability Reduction and Adaptation Management. *Climate Action*, pp. 1-13. https://link.springer.com/referenceworkentry/10.1007/978-3-319-71063-1_68-1.

Rao, A. 2024, What do you mean by maximum and minimum temperature? *Education Revolution*. https://edurev.in/question/3375212/What-do-you-mean-by-maximum-and-minimum-temperature-.

Rehman, T. and Arif, U. (2024). Spatial vs. Temporal — What's the Difference?. *Ask Difference*. https://www.askdifference.com/spatial-vs-temporal/.

Rangarajan, S., Thattia, D., Subbiah, A., Cherukuri, A., Borah, T. A., and Joseph, J. K. (2016). Temperature trend analysis using nonparametric test: A Case Study of Coimbatore city. *Journal of Industrial Pollution Control*, Vol. 33, pp. 1393-1400.

Saboohi, R., Soltani, S., and Khodagholi, M. (2012). Trend analysis of temperature parameters in Iran. *Theoretical and Applied Climatology*, Vol. 109, pp. 529-547. https://doi.org/10.1007/s00704-012-0590-5.

Şan, M., Akçay, F., Linh, N. T. T., Kankal, M., and Pham, Q. B. (2021). Innovative and polygonal trend analyses applications for rainfall data in Vietnam. *Theoretical and Applied Climatology*, Vol. 144, pp. 809-822. https://doi.org/10.1007/s00704-021-03574-4.

Sen, Z. (2012). Innovative trend analysis methodology. *Journal of Hydrologic Engineering*, Vol. 17, Issue 9, pp. 1042-1046. https://doi.org/10.1061/(ASCE)HE.1943-5584.0000556.

Şen, Z. (2017). Innovative trend significance test and applications. *Theoretical and Applied Climatology*, Vol. 127, pp. 939-947. https://doi.org/10.1007/s00704-015-1681-x.

Sen, Z., Şişman, E., and Dabanli, I. (2019). Innovative polygon trend analysis (IPTA) and applications. *Journal of Hydrology*, Vol. 575, pp. 202-210. https://doi.org/10.1016/j.jhydrol.2019.05.028.

Sharma, V., and Ghosh, S. K. (2022). Temporal Trend Analysis of Climate Data by using Innovative Polygon Trend Analysis method for Hardwar, India. https://doi.org/10.21203/rs.3.rs-1762361/v1.

Shea, D. (2014). The Climate Data Guide: Trend Analysis. *National Center for Atmospheric Research Staff (Eds)*. https://climatedataguide.ucar.edu/climate-data-tools-and-analysis/trend-analysis.

Singh, L. K., Jha, M. K., and Pandey, M. (2023). Spatiotemporal Variability and Trends in the Rainfall and Temperature of a Sub-Tropical Region of Eastern India and Their Implications. *Pure and Applied Geophysics*, Vol. 180, Issue 3, pp. 1205-1223. https://doi.org/10.1007/s00024-023-03238-6.

Srivastava, A. K., Rajeevan, M., & Kshirsagar, S. R. (2009). Development of a high resolution daily gridded temperature data set (1969–2005) for the Indian region. *Atmospheric Science Letters*, Vol. 10, Issue 4, pp. 249-254. https://doi.org/10.1002/asl.232.

Thakur, K., Kumar, H., and Snehmani (2022). Framework for variability analysis of seasonal meteorological data. *Journal of Earth System Science*, Vol. 131, Issue 4, Art. No. 223. https://doi.org/10.1007/s12040-022-01963-5.

Tercek, M. T., Rodman, A., Woolfolk, S., Wilson, Z., Thoma, D., and Gross, J. (2021). Correctly applying lapse rates in ecological studies: comparing temperature observations and gridded data in Yellowstone. *Ecosphere*, Vol. 12, Issue 3, Art. No. e03451. https://doi.org/10.1002/ecs2.3451.

Wagholikar, N. K., Sinha Ray, K. C., Sen, P. N., and Kumar, P. P. (2014). Trends in seasonal temperatures over the Indian region. *Journal of Earth System Science*, Vol. 123, pp. 673-687. https://doi.org/10.1007/s12040-014-0433-0.

WPCB (2016). State of Environment Report-West Bengal. West Bengal Pollution Control Board (WPCB), W.B., India, https://www.wbpcb.gov.in/writereaddata/files/SOE_Report_2016_1.pdf.